RAFAELA VENANCIO FLORES

ELABORAÇÃO E CARACTERIZAÇÃO DE NANOESTRUTURAS E FILMES À BASE DE QUITOSANA E NANOCRISTAL DE CELULOSE PARA APLICAÇÃO EM ALIMENTOS

Tese apresentada à Universidade Federal de Viçosa, como parte das exigências do Programa de Pós-Graduação em Ciência e Tecnologia de Alimentos, para obtenção do título de *Doctor Scientiae*.

Orientadora: Nilda de Fátima Ferreira Soares

Coorientadores: Eduardo Basílio de Oliveira
Paulo César Stringheta

VIÇOSA - MINAS GERAIS
2022

Ficha catalográfica elaborada pela Biblioteca Central da Universidade Federal de Viçosa - Campus Viçosa

T
F634e
2022

Flores, Rafaela Venancio, 1992-
Elaboração e caracterização de nanoestruturas e filmes à base de quitosana e nanocristal de celulose para aplicação em alimentos / Rafaela Venancio Flores. – Viçosa, MG, 2022.
1 tese eletrônica (131 f.): il. (algumas color.).

Texto em português e inglês.
Orientador: Nilda de Fátima Ferreira Soares.
Tese (doutorado) - Universidade Federal de Viçosa, Departamento de Tecnologia de Alimentos, 2022.
Inclui bibliografia.
DOI: https://doi.org/10.47328/ufvbbt.2023.015
Modo de acesso: World Wide Web.

1. Nanotecnologia. 2. Alimentos - Embalagens. 3. Polímeros vegetais. 4. Quitosana. 5. Palmiteiro-juçara. I. Soares, Nilda de Fátima Ferreira, 1960-. II. Universidade Federal de Viçosa. Departamento de Tecnologia de Alimentos. Programa de Pós-Graduação em Ciência e Tecnologia de Alimentos. III. Título.

CDD 22. ed. 664.09

RAFAELA VENANCIO FLORES

ELABORAÇÃO E CARACTERIZAÇÃO DE NANOESTRUTURAS E FILMES À BASE DE QUITOSANA E NANOCRISTAL DE CELULOSE PARA APLICAÇÃO EM ALIMENTOS

Tese apresentada à Universidade Federal de Viçosa, como parte das exigências do Programa de Pós-Graduação em Ciência e Tecnologia de Alimentos, para obtenção do título de *Doctor Scientiae*.

APROVADA: 24 de agosto de 2022.

Assentimento:

Documento assinado digitalmente
gov.br
RAFAELA VENANCIO FLORES
Data: 13/01/2023 17:55:36-0300
Verifique em https://verificador.iti.br

Rafaela Venancio Flores
Autora

Documento assinado digitalmente
gov.br
NILDA DE FATIMA FERREIRA SOARES
Data: 15/01/2023 22:53:25-0300
Verifique em https://verificador.iti.br

Nilda de Fátima Ferreira Soares
Orientadora

Aos meus pais, José Norberto e Terezinha e todos os amigos e amigas que contribuíram nessa caminhada.

AGRADECIMENTOS

A Deus, por seu amor infinito e misericordioso. Obrigada por me sustentar até aqui.

Aos meus pais, por todo incentivo, orações incessantes e suporte.

Aos meus familiares, por me incentivarem e sempre acreditarem em mim.

Às minhas amigas da república, Amanda, Letícia, Maria e Mariana, obrigada pelos momentos compartilhados, por serem meu suporte na cidade de Viçosa e fazerem os meus dias ainda melhores. Amo vocês e guardo cada momento que vivemos dentro do meu coração.

Às grandes amigas e amigos, Katia, Kely, Michele, Monique, Mila, Bruna, Danielle, Taila, Raquel, Nelson, Lucas, Pedro vocês são simplesmente fantásticos! Não seria nada sem o carinho, a amizade e parceria de vocês.

Aos colegas de laboratório, gratidão por todo conhecimento compartilhado.

Ao Fernando, técnico do Laboratótio de Embalagens – DTA, obrigada por todo suporte e tornar nossos dias mais leves e divertidos.

Aos estagiários do LABEM, em especial à Mariane, Laura, Gabriela e Wilton, gratidão pela parceria, ajuda e comprometimento durante a realização dos experimentos.

Aos amigos dos laboratórios LOP/LEMA e LACBIO, minha eterna gratidão por toda ajuda, pelos conhecimentos compartilhados e momentos vividos. Com certeza minha caminhada foi muito mais leve com vocês.

À professora Nilda, obrigada por abrir as portas do LABEM e dar o suporte necessário.

Ao professor Eduardo, minha eterna gratidão por todo conhecimento compartilhado, por estimular meu crescimento enquanto pesquisadora, pelas reuniões que na verdade pareciam conversas entre colegas de profissão e de vida. Você exerceu lindamente seu papel como professor e coorientador.

Ao professor Stringheta, gratidão! Você sempre foi meu ídolo e pude comprovar no momento em que te conheci. Obrigada por todo suporte em seu laboratório, acolhimento enquanto coorientador, excelentes conversas e trocas intermináveis de conhecimento.

Ao professor Wagner Otoni, obrigada por ceder seu laboratório com tanto carinho.

À Universidade Federal de Viçosa, pela oportunidade de realizar a pós-graduação.

À Coordenação de Aperfeiçoamento de Pessoal de Nível Superior (CAPES), pela concessão da bolsa de estudos.

O presente trabalho foi realizado com apoio da Coordenação de Aperfeiçoamento de Pessoal de Nível Superior – Brasil (CAPES) – Código de Financiamento 001.

RESUMO

FLORES, Rafaela Venancio, D.Sc., Universidade Federal de Viçosa, agosto de 2022. **Elaboração e caracterização de nanoestruturas e filmes à base de quitosana e nanocristal de celulose para aplicação em alimentos**. Orientadora: Nilda de Fátima Ferreira Soares. Coorientadores: Eduardo Basílio de Oliveira e Paulo César Stringheta.

A ciência de materiais aplicada à área de alimentos tem ganhado posição de destaque nos últimos anos. Materiais à base de polímeros naturais, sustentáveis e biodegradáveis têm sido o foco de pesquisas nos setores de embalagens e encapsulamento de compostos bioativos. Dentre os polímeros estudados, celulose e quitosana se destacam por serem abundantes e por apresentarem diversas aplicações. Nesse sentido, este trabalho visou contextualizar e apontar os principais desafios e avanços a respeito do desenvolvimento de nanocomplexos e filmes à base de quitosana e derivados de celulose, em especial o nanocristal de celulose (CNC), além de avaliar as estruturas desenvolvidas quanto a suas propriedades estruturais, térmicas e físico-químicas. Primeiramente, desenvolveu-se e otimizou-se nanocomplexos de quitosana/CNC por meio do design Box-Behnken. As variáveis envolvidas foram pH_{CNC}, concentração de NaCl ([NaCl]) e proporção molar de quitosana:CNC. Nanocomplexos com diâmetro médio < 200 nm e potencial zeta próximo a +40 mV foram obtidos. Além disso, elevados rendimentos de complexação (~8%) foram obtidos em condições envolvendo maior valor de pH e menores [NaCl] ($p < 0.05$). Análises de XRD e TGA/DTG mostraram uma maior resistência térmica dos nanocomplexos e modificações de cristalinidade, em comparação com a quitosana. A ausência de alterações microscópicas indicou estabilidade térmica para o nanocomplexo CH:CNC = 3:1, armazenado durante 30 dias, a 7 ºC e 25 ºC. Em um segundo estudo, uma blenda polimérica ativa foi desenvolvida. Nesse estudo, objetivou-se avaliar a influência do tipo de ácido (lático e propiônico) usado para dispersar a quitosana e de diferentes concentrações de CNC em filmes de quitosana/PVA adicionados de extrato de Juçara. A avaliação dos espectros FTIR mostraram uma forte influência do tipo de ácido na estrutura dos filmes, o que influenciou a cor e a atividade antioxidante dos mesmos, sendo que aqueles produzidos com ácido propiônico apresentaram coloração roxa, enquanto aqueles com ácido lático apresentaram coloração avermelhada e maior atividade antioxidante (95%). A adição de CNC aos filmes aumentou o módulo de Young e reduziu a resistência à tração e alongamento na ruptura dos mesmos, sendo que filmes formulados com ácido lático apresentaram maior alongamento na ruptura (236%) e menor módulo elástico (30 Mpa), comparando com aqueles com ácido propiônico (171.4% e

46,6 MPa, respectivamente). Os estudos conduzidos evidenciaram o potencial de aplicação dos materiais à base de quitosana e nanocelulose e como estes podem ser funcionalizados e aplicados na área de alimentos. Novas perspectivas foram criadas para o desenvolvimento de produtos, mostrando que propriedades desejadas e únicas são alcançadas quando os fatores intrínsecos e extrínsecos que influenciam as interações, propriedades e funções dos materiais são exploradas.

Palavras-chave: Nanocomplexos. Box-behnken design. Embalagens. Filmes ativos. Extrato de Juçara.

ABSTRACT

FLORES, Rafaela Venancio, D.Sc., Universidade Federal de Viçosa, August, 2022. **Study of structural and physico-chemical properties of chitosan/cellulose nanocrystal-based materials for food applications**. Adviser: Nilda de Fátima Ferreira Soares. Co-advisers: Eduardo Basilio de Oliveira and Paulo César Stringheta.

The science of materials applied to the food area has gained a prominent position in recent years. Natural, sustainable and biodegradable polymer-based materials have been the focus of much research in the packaging sector and in the encapsulation of bioactive compounds. Among the polymers studied, cellulose and chitosan stand out because they are abundant and have several applications. In this sense, this work aimed to contextualize and indicate the main challenges and advances regarding the development of nanocomplexes and films based on chitosan and cellulose derivatives, especially cellulose nanocrystal (CNC), and to evaluate the developed structures regarding their structural, thermal, and physicochemical properties. First, chitosan/CNC nanocomplexes were developed and optimized by means of Box-Behnken design involving the variables pH_{CNC}, NaCl concentration ([NaCl]) and chitosan:CNC molar proportion. Nanocomplexes with average size < 200 nm and zeta potential near +40 mV were obtained. Furthermore, high complexation yields (~8%) were obtained at higher pH values and lower [NaCl] ($p < 0.05$). XRD and TGA/DTG analysis showed higher thermal resistance of the nanocomplexes and crystallinity modifications compared to chitosan. The absence of microscopic changes indicated thermal stability for the CH:CNC = 3:1 nanocomplex stored for 30 days at 7 °C and 25 °C. In a second step, an active polymeric blend was developed. In this study, the objective was to evaluate the influence of the type of acid (lactic and propionic) used to disperse the chitosan and of different concentrations of CNC on chitosan/PVA films added with Jussara extract. Evaluation of the FTIR spectra showed a strong influence of the type of acid on the structure of the films, which influenced the color and antioxidant activity of the films, with those produced with propionic acid showing a purple coloration while those with lactic acid showed a reddish color and higher antioxidant activity (95%). Addition of CNC to the films increased Young's modulus and reduced the tensile strength and elongation at break of the films, and films formulated with lactic acid showed higher elongation at break (236 %) and lower elastic modulus (30 MPa compared to those with propionic acid (171.4% and 46.6 MPa, respectively). The studies conducted showed the potential application of materials based on chitosan and nanocellulose and how these can be functionalized and applied in the food area.

New perspectives have been created for product development, showing that desired and unique properties are achieved when the intrinsic and extrinsic factors that influence the interactions, properties and functions of materials are explored.

Keywords: Nanocomplexes. Box-behnken design. Packaging. Active films. Jussara extract.

SUMÁRIO

INTRODUÇÃO GERAL

Nos últimos anos, a busca por alternativas aos recursos fósseis e redução de custos de extração e processamento tem estimulado um grande interesse por alternativas renováveis e sustentáveis que substituam o petróleo como fonte de produtos químicos, materiais e combustíveis. Dentro dessa estratégia, os polissacarídeos são candidatos vitais devido à sua natureza renovável e reciclável e caráter biodegradável, juntamente com o fato de representarem a fração mais abundante da biomassa (Fernandes et al, 2011). A celulose e a quitina são os polissacarídeos naturais mais difundidos e têm sido amplamente explorados em diversas aplicações.

Quitosana é um polissacarídeo derivado da quitina por um processo de desacetilação parcial, o que a torna um copolímero constituído de unidades N-acetil-D-glicosamina e D-glicosamina unidas por ligações β-1,4. Está presente principalmente na parede celular de fungos e no exoesqueleto de diversos crustáceos e insetos, além de ser o segundo polímero mais abundante no mundo (Cheng, Wang, & Weng, 2015). Suas propriedades biológicas e físico-químicas dependem de sua pureza, grau de desacetilação, massa molar e viscosidade, conferindo diferentes aplicações ao polímero. Em sua estrutura, quitosana apresenta grupamentos amino e hidroxila, capazes de interagir com outras moléculas.

As propriedades físico-químicas e a carga adquirida pelas moléculas de quitosana em dispersões aquosas são ditadas pelo pH e pela força iônica do meio (Soares et al., 2019; Amorim et al., 2016). Uma vez que o valor de pKa dos grupamentos amino da quitosana é 6,3, em valores de pH maiores, esses grupamentos tornam-se desprotonados e o polímero perde grande parte de sua carga e solubilidade. Em menores valores de pH, os grupamentos amino tornam-se protonados e a molécula de quitosana adquire carga positiva, tornando-se um polieletrólito catiônico solúvel em água (Soares et al., 2019; Hembram et al., 2016).

Pelo fato dos ácidos estarem envolvidos em grande parte do processamento da quitosana, incluindo sua dispersão em meios aquosos, os efeitos desse componente na estrutura e propriedades dos materiais de quitosana têm sido extensivamente estudados (Zhang et al., 2022; Pavoni, Luchese, & Tessaro, 2019; Soares et al., 2019; Kim et al., 2006). A busca por métodos de processamento eficientes para personalizar produtos de quitosana requer uma compreensão completa dos fatores que interferem em suas propriedades técnico-funcionais. (Chen et al., 2015)

Quanto aos materiais a base de celulose, os nanocristais de celulose (CNC) tomaram posição de destaque, sendo estruturas cristalinas compactas isoladas a partir de fibras de

celulose e que podem ser obtidos por hidrólise ácida com ácido sulfúrico. Os CNC apresentam-se na forma de hastes ou de filamentos alongados e emaranhados, e possuem dimensões que variam de 5 a 25 nm de diâmetro e de 100 a 500 nm de comprimento (Wang & Roman, 2011). Durante o processo de extração dos nanocristais de celulose, o ácido sulfúrico é capaz de clivar as ligações glicosídicas das regiões amorfas, mantendo apenas os domínios cristalinos (Abdul Khalil et al., 2016). Após a etapa de hidrólise ácida, a superfície dos nanocristais adquire grupamentos sulfonato que apresentam carga negativa em valores de pH acima de seu valor de pKa = 2,6 (Abo-Elseoud et al., 2018; Wang & Roman, 2011).

Muitos materiais a base de quitosana e CNC tem sido desenvolvidos, principalmente aqueles direcionados a sistemas de liberação controlada e embalagens, uma vez que nessas áreas a busca por materiais com propriedades únicas, sustentáveis e agregados a alta tecnologia vem crescendo aceleradamente.

Dentro do campo de sistemas de liberação controlada, nanopartículas de quitosana desenvolvidas com tripolifosfato de sódio são os sistemas de liberação mais comuns e estudados a base de quitosana, contudo são considerados sistemas metaestáveis (Wang, Jung, & Zhao, 2017) sendo muito susceptíveis ao grau de ionização da quitosana, ao pH do meio de reação, concentração de polieletrólitos, distribuição de grupos iônicos, peso molecular, razão de mistura, pH, força iônica, temperatura (Luo & Wang, 2014). Limitações também são encontradas em filmes de quitosana. Muitos pesquisadores relatam, por exemplo, baixa resistência mecânica e alta solubilidade e permeabilidade ao valor de água (Zhang et al., 2022; Chen et al., 2015; Bonilla et al., 2014; Caner, Vergano, & Wiles, 1998).

Nesse sentido, usar estratégias com nanopreenchedores, como o CNC demonstra uma alternativa viável e sustentável (Mu et al., 2019; Ali & Ahmed, 2018; Sunasee, Hemraz, & Ckless, 2016). Nanocompósitos de quitosana geralmente se referem ao polímero de quitosana contendo nano-preenchimentos com um tamanho médio de partícula inferior a 100 nm. Esses nano-preenchedores são capazes de melhorar diversas propriedades relativas tanto ao polímero quanto às nanopartículas (Ali e Ahmed, 2018).

Com as estratégias supracitadas, é possível funcionalizar os materiais com agentes bioativos, conferindo a eles propriedades antioxidantes, antimicrobianas e antinflamatórias para aplicação nas áreas farmacêutica, biomédica e de alimentos, e até mesmo em outras áreas, incluindo as ciências agronômicas e veterinária. Dentre os compostos bioativos, o grupo de compostos fenólicos, em especial as antocianinas, tem demonstrado grandes resultados tanto na

saúde humana como no desenvolvimento de embalagens ativas e biosensores (Freitas et al., 2020; Ma et al., 2018).

Antocianinas estão presente em frutos pequenos e polposos e alguns vegetais e legumes, como amoras, morangos, jabuticaba, jamelão, berinjela, repolho roxo, açaí e Juçara, sendo responsável pela coloração vermelha – arroxeada desses alimentos. Em sua estrutura, a antocianina apresenta o núcleo flavilium, que em meio ácido adquire carga residual positiva, que é estabilizada por ressonância (Yousuf, Gul, Wani, & Singh, 2016). Essa deficiência de elétrons presente na estrutura básica das antocianinas faz com que elas sejam altamente reativas, motivo pelo qual são encontradas na forma glicosilada na natureza (Santos-Buelga & González-Paramás, 2018). A partir disso, é fácil perceber a influência do pH, temperatura e outros fatores físicos na estabilidade e reatividade da molécula, o que permite uma gama de aplicações quando estratégias corretas são aplicadas.

Levando em consideração a influência de fatores físico-químicos no desenvolvimento de materiais a base de polieletrólitos e como estes ditam o sucesso no momento de sua aplicação, neste trabalho, objetivou-se esclarecer, dar suporte e direcionar pesquisas com materiais a base de quitosana por meio de uma revisão de literatura em que são expostos, principalmente, os principais pontos a serem levados em consideração ao desenvolver nanomateriais. Em seguida, com intuito de aplicar e validar esses fundamentos, no segundo capítulo objetivou-se otimizar e estudar a estabilidade e as propriedades estruturais e físico-químicas de nanopartículas de quitosana/CNC ao levar em consideração variações no pH das dispersões de CNC, concentração de NaCl das dispersões poliméricas e proporção molar entre essas dispersões. Mais adiante, no terceiro capítulo, objetivou-se avaliar a influência do tipo de ácido (propiônico e lático) usado no preparo de dispersões de quitosana e das concentrações de CNC nas propriedades mecânicas, antioxidantes, térmicas e estruturais de filmes de quitosana/PVA adicionados de extrato de Juçara.

Artigo 1*

* Formatado de acordo com as diretrizes da revista *Research, Society and Development*

Recent advances and challenges on chitosan-based nanostructures by polyelectrolyte complexation and ionic gelation for anthocyanins stabilization

Avanços e recentes desafios sobre nanoestruturas à base de quitosana preparadas por complexação polieletrolítica e gelatinização iônica para estabilização de antocianinas

Avances y desafíos recientes en nanoestructuras a base de quitosano preparadas por complejación polielectrolítica y gelatinización iónica para la estabilización de antocianinas

Received: 07/18/2022 | Reviewed: 07/26/2022 | Accept: 07/27/2022 | Published: 05/08/2022

Rafaela Venancio Flores
https://orcid.org/0000-0002-5498-336X
University Federal of Viçosa, Brazil
E-mail: rafavenacio2@gmail.com
Rafael Resende Assis Silva
https://orcid.org/0000-0001-6112-8727
University Federal of São Carlos, Brazil
E-mail: rafaelmega@yahoo.com.br
Taíla Veloso de Oliveira
https://orcid.org/0000-0001-5444-9530
University Federal of Viçosa, Brazil
E-mail: taila.oliveira@ufv.br
Eduardo Basílio de Oliveira
https://orcid.org/0000-0002-2329-2507
University Federal of Viçosa, Brazil
E-mail: eduardo.basilio@ufv.br
Paulo César Stringheta
https://orcid.org/0000-0002-1229-7038
University Federal of Viçosa, Brazil
E-mail: paulocesar@ufv.br
Nilda de Fátima Ferreira Soares
https://orcid.org/0000-0001-9506-6130
University Federal of Viçosa, Brazil
E-mail: nfsoares@ufv.br

Abstract

Anthocyanins are water-soluble polyphenols responsible for the color of many fruits, flowers, and vegetables. In addition to natural dyes, anthocyanins are also related to the prevention of several chronic diseases. However, anthocyanins are extremely sensitive to variations in pH,

temperature, light, enzymes, and other environment variables, being necessary to employ artifices and technologies to expand their application in both the food and pharmaceutical sectors. In this context, biopolymeric nanoparticles can be used to protect and intensify the functions conferred to the anthocyanins. Among the techniques used, polyelectrolytic complexation (PC) and ionic gelation (IG) stands out due to convenience, speed, low cost, and possibility of using a versatile, biocompatible and natural polymer such as chitosan. Therefore, scoring and understanding the main factors that affect the stability of chitosan-based nanoparticles produced by PC and IG, and knowing the strategies that can be adopted to overcome these problems ~~is~~ extremely important. Thus, this review aims to provide an overview of anthocyanins and biopolymeric nanoparticles with an emphasis on PC and IG techniques. The main challenges that need to be faced when anthocyanins are incorporated into these nanoparticles will be scored, mainly when chitosan is used as a polymeric base. Also, some directions will be given to those who intend to develop new projects focusing on the stabilization of anthocyanins.
Keywords: Encapsulation; Biopolymeric nanoparticle; Nanocomplexes, Biopolymers.

Resumo

Antocianinas são polifenóis solúveis em água, responsáveis pela coloração de diversas frutas, flores e vegetais. Além de corantes naturais, antocianinas também estão relacionadas a prevenção de diversas doenças crônicas. Contudo, antocianinas são extremamente sensíveis a variações de ph, temperatura, luz, enzimas e outras variáveis do meio em que se encontram, sendo necessário empregar artifícios e tecnologias para expandir sua aplicação tanto no setor de alimentos como farmacêutico. Nesse contexto, nanopartículas biopoliméricas podem ser usadas para proteger antocianinas e até mesmo intensificar as funções conferidas a elas. Dentre as técnicas usadas, complexação polieletrolítica (PC) e gelatinização iônica (IG) tomam posição de destaque devido a praticidade, rapidez, baixo custo e possibilidade de uso de polímeros versáteis, biocompatíveis e naturais, como a quitosana. Desse modo, pontuar e entender os principais fatores que afetam a estabilidade das nanopartículas à base de quitosana produzidas por PC e IG, e conhecer as estratégias que podem ser adotadas para contornar esses problemas são de extrema importância. Diante do exposto, essa revisão tem como objetivo fornecer uma visão geral sobre antocianinas e nanopartículas biopoliméricas com ênfase nas técnicas de PC e IG, identificando os principais desafios que precisam ser enfrentados ao incorporar

antocianina3s nessas nanopartículas produzidas em base de quitosana, e direcionar o desenvolvimento de novos projetos com foco na estabilização de antocianinas.
Palavras-chave: Encapsulamento; Nanopartículas biopoliméricas; Nanocomplexos; Biopolímeros.

Resumen

Antocianinas son polifenoles solubles en agua, responsables por la coloración de diversas frutas, flores y verduras. Además de los colorantes naturales, las antocianinas también están relacionadas con la prevención de varias enfermedades crónicas. Sin embargo, las antocianinas son muy sensibles a las variaciones de pH, temperatura, luz, enzimas y otras variables del medio en el que se encuentran, por lo que es necesario emplear artificios y tecnologías para ampliar su aplicación tanto en el sector alimentario como en el farmacéutico. En este contexto, las nanopartículas biopoliméricas pueden ser utilizadas para proteger las antocianinas e incluso potenciar las funciones que les confieren. Entre las técnicas utilizadas, la complejación polielectrolítica (PC) y la gelatinización iónica (IG) ocupan un lugar destacado por su practicidad, rapidez, bajo costo y la posibilidad de utilizar polímeros versátiles, biocompatibles y naturales, como el quitosano. Por lo tanto, calificar y comprender los principales factores que afectan la estabilidad de las nanopartículas a base de quitosano producidas por PC e IG, y conocer las estrategias que se pueden adoptar para superar estos problemas es extremadamente importante. Dado lo anterior, esta revisión tiene como objetivo proporcionar una visión general de las antocianinas y las nanopartículas biopoliméricas con énfasis en las técnicas de PC e IG, señalar los principales desafíos que deben afrontarse al incorporar antocianinas a estas nanopartículas cuando se utiliza quitosano como base polimérica; y dar dirección a quienes pretenden desarrollar nuevos proyectos enfocados en la estabilización de antocianinas.
Palabras clave: Encapsulación; Nanopartículas biopoliméricas; Nanocomplejos; Biopolímeros.

1. Introduction

Anthocyanins make up the largest group of water-soluble pigments in the plant kingdom and fall into the class of polyphenols, a subgroup of flavonoids, responsible for the color of various fruits, flowers, and vegetables (Akhavan & Jafari, 2017). There are more than 700 anthocyanin structures identified, which offer a range of colorings that could be explored, ranging

from orange to red and purple to blue, according to the environment in which it is found (Iosub et., al, 2012).

The food and pharmaceutical industries are very interested in this natural pigment, due to its attractive color and health benefits (Lee & Choung, 2011). Additionally, there is a growing demand for the use of natural products due to the toxic effects caused by synthetic products, including dyes (Khoo, Azlan, Tang, & Lim, 2017). Besides being used as a natural dye (Chi et al., 2019), anthocyanins also play a role as an antioxidant in foods and beverages (He et al., 2017), and even as modulators of intestinal microflora. This helps prevent and even treat candidiasis and chronic diseases, such as diabetes (Suket, Srisook, & Hrimpeng, 2014; Morais, de Rosso, Estadella, & Pisani, 2016). Other applications of anthocyanins are related to performance in inflammatory conditions in the body, including the prevention of cardiovascular diseases (Reis et al., 2016), and cancer prevention (Jeong, Bae, Park, & Na, 2016).

Despite the excellent properties conferred to anthocyanins, the application is still limited due to its instability under processing and storage conditions, such as heat, high pH, and exposure to light and oxygen, which induces the degradation of the anthocyanin structure to colorless phenolic acids and aldehydes (Wang, Zhung, Zhao, 2017). Low bioavailability and rapid elimination from the body are also other limitations of anthocyanins (Peixoto et al., 2016; Kay et al., 2017; Wang, Jung, & Zhao, 2017).

In an attempt to circumvent these problems, new strategies have been adopted, such as encapsulation with biopolymer nanoparticles, especially those developed by complexation polyelectrolytic (PC) and ionic gelation (IG) techniques. Through these techniques, it is possible to produce nanoparticles simply and free of toxic solvents using biodegradable polymers (Wu et al., 2020).

Chitosan stands out in PC and IG techniques because it is a cationic, versatile, natural, and biodegradable polymer (Mohammed, Syeda, Wasan, & Wasan, 2017). In an aqueous medium (pH <6.5), the chitosans' amino groups are protonated and capable of forming complexes, hydrogels, or particles with natural anionic polymers and salts' polyanions GRAS (Generally Recognize as Safe), such as sodium tripolyphosphate (Zhao et al., 2011).

The formation of these different nanostructures facilitates the incorporation of anthocyanins. From there, it is possible to expand the application of anthocyanins, overcome the challenges of the pharmaceutical and food process, to produce packaging for food, beverages, and orodispersible films, among others.

Despite the great interest in PC and IG techniques, there are still points that deserve attention and need further study and discussion, such as the structure-property-function relationships of polymers with the active compound, intrinsic and extrinsic properties of the materials used in the development of nanostructures, and compatibility of these nanostructures with the matrix to which it will be added. In this review, the structural properties of anthocyanins and their limitations are addressed together with an overview of biopolymeric nanoparticles. The challenges and strategies for anthocyanin nanoencapsulation are also described using two relatively simple techniques: polyelectrolytic complexation and ionic gelatinization.

2. Methodology

A narrative and qualitative review was conducted, and searches for scientific articles were performed using the *U.S. National Library of Medicine and the National Institutes of Health* (PubMed), *Scopus*, *Web of Science* and *Google Scholar* databases. The searches were limited to articles published in the last 10 years using the keywords "biopolymeric nanoparticles", "chitosan, nanoparticles", "anthocyanin", "complexation", "nanocomplexes", "chitosan polyelectrolyte complexes", "anthocyanins microencapsulation", "anthocyanins nanoencapsulation", and "ionic gelatinization" combined with each other through the Boolean operators "AND" or "OR". The exclusion criteria adopted included particle sizes greater than 500 nm, nanocomplexation studies without the use of chitosan, nanoencapsulation studies with bioactive compounds different from those sources of anthocyanin. The reference lists of selected articles were also manually analyzed to identify other relevant studies that could be included in this review.

3. Anthocyanins

3.1 Definition, food source and consumption

Anthocyanins (from Greek *Anthos*, a "flower", and *kyanos* "dark blue color") are polyphenolic pigments of the flavonoid class, widely available in various parts of vascular plant materials. Anthocyanins are the main elements responsible for the variety of colors found in flowers and fruits (Akhavan & Jafari, 2017). These pigments are the only polyphenolic compounds capable of absorbing light both in the ultraviolet region and in the entire visible range (Brouillard, Chassaing, Isorez, Kueny-Stotz, & Figueiredo, 2010), which makes them responsible for the red, blue, and purple colors of flowers such as red hibiscus, blue rosemary, and lavender, respectively (Khoo et al., 2017).

Fruits and vegetables, such as blueberry, juçara, açaí, grape, cranberry, red carrot, and red cabbage are known and consumed worldwide, and the colors of each one come from anthocyanins. (Yousuf, Gul, Wani, & Singh, 2016; Ko, Lee, Sop Nam, & Gyu Lee, 2017). The daily consumption of anthocyanins is high (~200 mg/per capita/day), especially when you have a diet rich in colorful fruits and vegetables. (Bueno et al., 2012).

There is still no consensus on the daily amount of anthocyanins to be ingested. However, in 2013 the Chinese Nutrition Society established a daily consumption of 50 mg / per capita/day, while the FAO / WHO Committee of experts proposed consumption of 2.5 mg/kg human body weight/day for the extract of the peel grape, but not for anthocyanins in general (Wallace & Giusti, 2015).

In addition to color ability, anthocyanins also have other properties, such as antioxidant, anticancer, and anti-inflammatory (Bueno et al., 2012). This makes the aforementioned foods potentially functional, due to the fact that they are associated with reduced risk of diseases (Khoo et al., 2017), such as atherosclerosis, cardiovascular diseases, diabetes, and other chronic diseases (Kay et al., 2017). Therefore, consuming foods rich in anthocyanins can contribute to consumer health and satisfaction, since foods that are anthocyanin sources are associated with better performance of the body's biological functions (Singh et al., 2020).

3.2 Chemical structure

Anthocyanins are glycosylated forms of anthocyanidins, *flavylium* cation deriving from (2-fenilbenzopilrilium) linked only to hydroxyl and methoxyl groups. (Bueno et al., 2012). Anthocyanidins, also known as aglycone (Figure 1), are the basic structure of anthocyanins. They have a 15-carbon skeleton, containing two aromatic rings (A and B) separated by an oxygenated heterocyclic ring (C) (Castañeda-Ovando, de Lourdes, Páez-Hernández, Rodríguez, & Galán-Vidal, 2009; Bueno et al., 2012; Tarone, Cazarin, & Junior, 2020).

Due to the existence of conjugated double bonds, the positive residual charge that the *flavilium* nucleus presents in an acid medium is relocated throughout the cycle, being stabilized by resonance. The electron deficiency of the *flavilium* cation makes the free aglycones highly reactive, which do not occur naturally (Srivastava & Vankar, 2010), explaining the glycosylated form with sugars that increase the stability of the molecule. There are more than 30 anthocyanidins identified in nature, differing in the number and position of the hydroxyl groups and, or methoxyl in the carbon structure. The presence of reactive hydroxyls favors the formation of covalent bonds with different sugars, such as glucose, rhamnose, galactose, xylose, and

arabinose; however, glucose is the most found in anthocyanins (Santos-Buelga & González-Paramás, 2018; Tarone, Cazarin, & Junior, 2020).

Fig.1. Structural representation of anthocyanidin

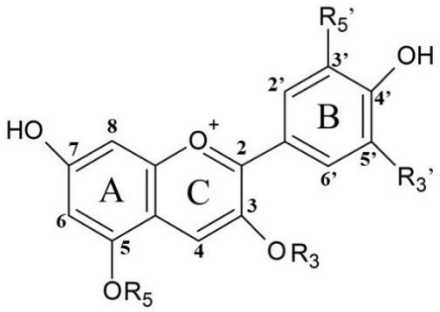

Font: Own authorship (2022)

Aliphatic, hydroxybenzoic, or hydroxycinnamic acids may substitute the sugars. The most usual are malonic, acetic, p-coumaric, and caffeic acids (Santos-Buelga & González-Paramás, 2018). Koley et al. (2014) demonstrated that acylated anthocyanins are more stable to heating, light, and external environment than non-acylated ones. Six anthocyanidin structures are commonly found in nature (Figure 2), including cyanidin, delphinidin, pelargonidin, peonidin, malvidin, and petunidin in which the last three have methoxy groups as substitutes in their B rings. Together, these six anthocyanidins represent about 90% of all anthocyanins identified so far (Bueno et al., 2012).

So far, they have been described more than 700 anthocyanins from natural sources (Santos-Buelga & González-Paramás, 2018). In addition to the variations that occur in the previously mentioned anthocyanidins, anthocyanins have structures, properties, and functions affected by the physical-chemical environment in which they are inserted (Yousuf et al., 2016; Tarone, Cazarin, & Junior, 2020). In aqueous solution, for example, anthocyanins have different chemical structures in equilibrium. These structures depend on the type of reaction (hydration, tautomerization, proton transfer) of the flavilium cation at certain pH values and conditions of the medium in which it is present (Figure 3) (Santos-Buelga & González-Paramás, 2018; Bueno et al., 2012).

Fig. 2. Structures of the main anthocyanidins found in the nature.

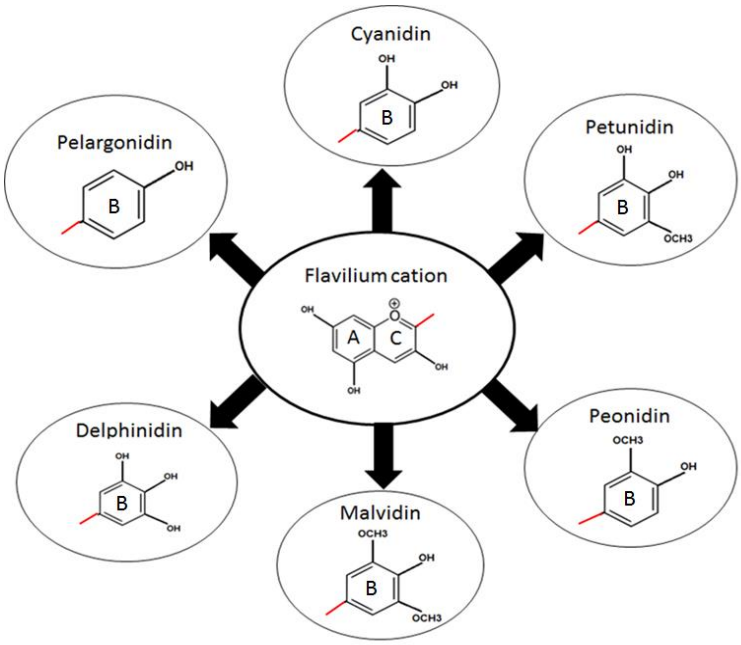

Font: Own authorship (2022)

When pH values are between 1 and 3, anthocyanins exhibits an intense red color due to the predominance of the structure in the form of the flavilium cation (AH^+). However, when the pH increases to values of 4 - 6, two reactions can occur as the same time: I) Deprotonation and formation of the purple/blue quinoid base and, II) C2 hydration of the flavilium cation as well as the appearance of the carbinol pseudo base (colorless hemiketal shape). The hemiketal shape undergoes the opening of ring C by tautomerization and gives rise to cis-chalcone. Trans-chalcone also makes up the medium when cis-chalcone is isomerized (Santos-Buelga & González-Paramás, 2018; Pina, Melo, Laia, Parola, & Lima, 2012). In this way, with an increase in pH to values between 7 and 8, rapid deprotonation occurs, which results in the predominant formation of the blue colored quinoid base (A) (Pina et al., 2012; Bueno 2012).

According to Babaloo & Jamei (2017), the anthocyanin colorimetric change as a function of pH reduces the conjugated double bonds, which causes the displacement of maximum absorption values to shorter wavelengths. A phenomenon known as hypsochromic displacement.

Fig. 3. Main structures of anthocyanin in pH-dependent equilibrium in aqueous solution.

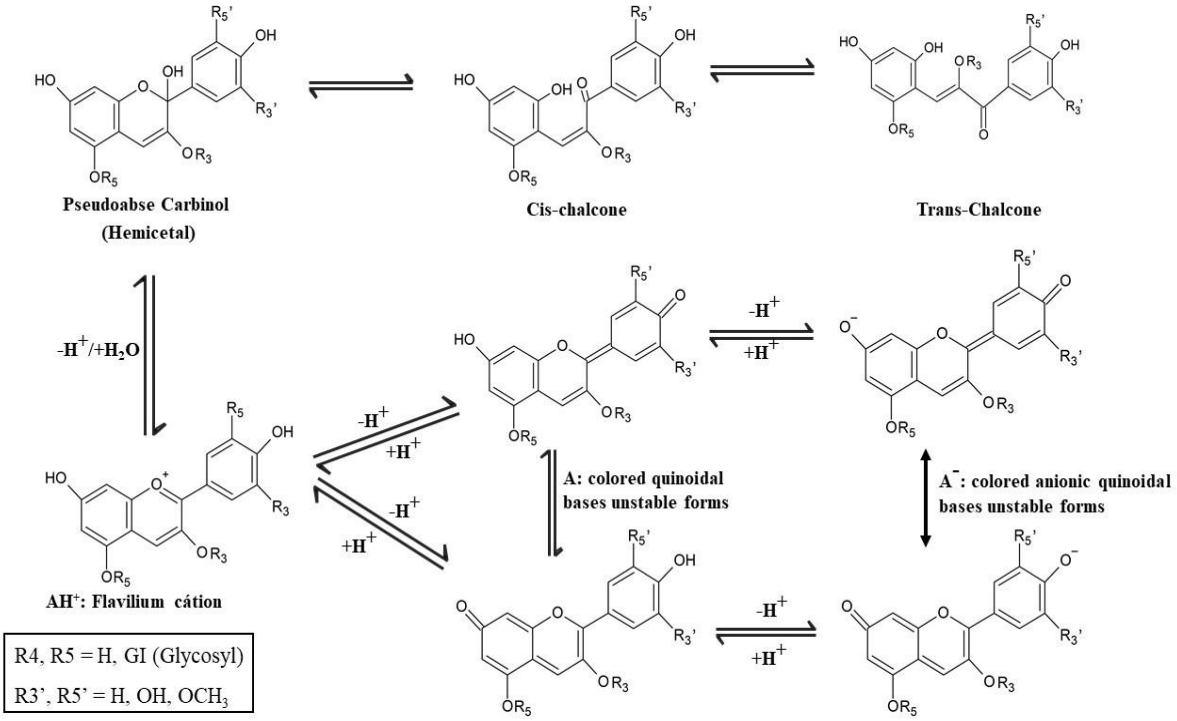

Font: Adapted from Brouillard, Chassaing, Isorez, Kueny-Stotz, & Figueiredo (2010).

3.3 Stability

Elevated temperatures, oxygen, and light are some factors that promote changes in the chemical structure and influence the anthocyanins' stability, which can result in loss of the total anthocyanin content and reduction in its antioxidant capacity (Khoo et al., 2017). On oxygen presence and high temperatures exposure, the anthocyanins degradation is intensified. In this case, hydrolysis of the 3-glycosidic bond occurs, with consequent release of the aglycone and hydrolytic opening of the C ring (Sipahli, Mohanlall, & Mellem, 2017). This process favors the formation of chalcones, which degrade to dark insoluble compounds of polyphenolic nature (Roobha et al., 2011; Bobbio, & Bobbio, 2003).

Exposure to light also accelerates anthocyanin degradation through a photooxidative mechanism, often described by first-order, low-activation degradation kinetics (Askar, Al-sawad, & Khalaf, 2015). This process is influenced by the medium pH, temperature, and exposure time (Karaoglan, Keklik, & Isıklı, 2019).

The pH has a direct interference in the chemical structure of anthocyanin and, consequently, in its stability, which implies changes in bioavailability, coloring power, and capabilities of antioxidant, anticancer, and anti-inflammatory (Cahyana & Gordon, 2013; Santos-Buelga & González-Paramás, 2018; Zapata et al., 2019).

Jiang et al. (2019) evaluated the effect of thermal processing at 90ºC and pH values of 3 to 7 in purple sweet potato extract. The authors found that anthocyanins degradation occurred through a first-order reaction, regardless of the pH value. The half-lives at pH values 3, 5, and 7 were 10.27, 12.42, and 4.66 h, respectively. Additionally, there were changes in the color of the extract varying with the heating time and change in the pH values, with higher values of these variables resulting in color losses and consequent appearance of brown pigments in the extracts from 5 to 7 pH values. In their study, Atnip et al. (2017) demonstrated that anthocyanins in a medium with pH around 5 interact less with gastrointestinal tract cells, especially gastric epithelial cells (NCI-N87), than in the culture media at pH 3 and 7.4. The authors justify this fact due to the predominance of chalcones in the medium, hydrated structures and with the opening of the C ring, showing that the transport of anthocyanins in the mentioned cells is preferable for those structures with closed C rings (cation flavilium and pseudo base carbinol).

One way to stabilize and even increase the color intensity of anthocyanins is through copigmentation. Mazza & Brouillard (1987) showed that the increased concentration of anthocyanin and the proportion between co-pigments and anthocyanin promotes a greater copigmentation effect. In general, compounds that perform copigmentation alone are not colored. When mixed with anthocyanins in a solution, there is a non-covalent molecular interaction between these two components. This interaction can generate the hyperchromic effect (increased absorption intensity) and/or the bathochromic change (displacement of the maximum absorption band for longer wavelengths) in the UV-Vis spectrum as previously mentioned (Santos-Buelga & González-Paramás, 2018; Khoo et al., 2017; Bimpilas et al., 2016; Castañeda-Ovando et al., 2009; Mazza & Brouillard, 1987).

The use of copigments is very common in the food industry to increase the stability of anthocyanins in juices, jellies, concentrates, and fruit extracts, as well as to intensify the color of foods and beverages in the presence of anthocyanins. Some copigments studied include sinapic acid (Terefe et al., 2019; Ko et al., 2017); phenolic acids, such as ferulic, caffeic, gallic acid (Qian et al., 2017), tannic, benzoic (Babaloo & Jaime, 2018); and sugars, such as honey and maltose syrup (Ertan, Turkyilmaz, Ozkan, 2018).

Despite the efforts made to improve the stability of anthocyanins to expand their applications, the use of copigments is not sufficient for this. Many structures of copigmented anthocyanins remain satisfactorily stable only at low pH values (Babaloo & Jaime, 2018), which makes it difficult to use these compounds as dyes in foods with pH> 4.0.

Another factor observed is that copigmentation may not affect heat-treated foods, as is the case with strawberry purees treated at 88°C / 2 minutes in the presence of sinapic acid (Terefe et al, 2019). In addition, copigmentation alters the original structure of anthocyanin (Chen & Inbaraj, 2019; Bimpilas et al., 2016), which can interfere with bioavailability and absorption into the bloodstream (Khoo et al, 2017).

In this context, based on facts and recent literatures, the use of biopolymeric nanoparticles has aroused the interest of many research groups due to the favorable properties of these nanostructures, such as good biocompatibility, simple design, easy preparation, and diversity of the structures (Meka et al., 2017). These properties make it possible to deliver bioactive compounds directly to the intended site of action. In this way, the stability and even the functionality of anthocyanins can be improved through encapsulation in biopolymeric nanoparticles.

4. Nanotechnology and anthocyanin stabilization

Nanotechnology is the area of science dedicated to the study, creation, and application of materials on a nano size. It has contributed to the technological development of chemistry, biology, physics, materials science, and engineering. Concerning the dimensions, the precise size that the authors considered a nanoparticle is still an issue under debate (Joye & McClements, 2014). For some scientists a nanoparticle should be ≤ 100 nm in diameter (Tong et al., 2020; Fathi et al., 2014), while for others, the sizes should be up to 500 nm (Tan, Selig, & Abbaspourrad, 2018; Wang, Yang, Ju, Udenigwe, & He, 2018; He et al., 2017).

It`s known that the use of the concept of nanotechnology is valid when materials produced at the nanoscale have surface properties superior to the same material in its original size or on the microscale. However, such properties are not always associated only with particle size (Joye & McClements, 2014). Optical, mechanical, biological, physical-chemical, and morphological properties, including size, are also extremely dependent on the type of wall material used (Bazana, Codevilla, & de Menezes, 2019). Therefore, excellent properties can also be found in particles with sizes between 100 and 500 nm (Ko et al., 2017; Joye & McClements, 2014). Among the nanostructures with these properties, those directed to bioactive compounds nanoencapsulation have been highlighted in the biomedical, food and material sciences areas.

In the pharmaceutical and food industries, nanoencapsulation is preferably used for compounds that need to be released in a controlled, continuous manner and at a specific location in the human organism or food (Robert & Fredes, 2015). Still, the use of nanoencapsulation in the food sector can also maintain or enhance, for a longer period, the interest properties of the active

compound in a product, such as the antioxidant, antimicrobial, color capacity, and antifungal activity (Pola et al., 2019; He et al., 2017; Comin et al., 2016). Packaging and polymers area, in general, also benefits from this technology, which can be used to increase the mechanical resistance and thermal properties of different types of materials, as well as to improve their gas and water vapor barrier properties (Espitia et al., 2013).

According to Jafari (2017), nanoparticles can be classified into five groups: lipid-based nanoparticles (nanoemulsions, solid lipid nanoparticles, liposomes, nanostructured lipid carriers), polymeric nanoparticles (ionic gelatinization, coacervation, emulsification - solvent evaporation, polyelectrolytic complexation), miscellaneous nanoparticles (nanocrystals, nanostructured surfactants, inorganic nanoparticles), nanoparticles produced by special equipment (electrospraying/electrospinning, nanospray-dryer, nanofluidization), and naturally produced nanoparticles (caseins, cyclodextrins, nanostructured amyloses).

Several techniques have been used in anthocyanin nanoencapsulation to obtain smaller sizes, higher encapsulation efficiency, and greater therapeutic activity or coloring power. Table 1 presents several studies that evaluated the incorporation of anthocyanins in nanostructured systems in the last 10 years. Among the techniques employed, lipid-based nanoparticles, nanoparticles produced by special equipment, and polymeric nanoparticles are frequently used.

Despite being well studied, many lipid-based formulations are added to surfactants in relatively high amounts. This fact limits the application of these nanomaterials in some products for food and pharmaceutical purposes due to economic, legal, or sensory problems (Joye, Davidov-Pardo, & McClements, 2014). Besides, lipid-based nanomaterials are also more prone to oxidation and physical instability, as in the case of liposomes (Bryła, Lewandowicz & Juzwa, 2015; Joye, Davidov-Pardo, & McClements, 2014).

Ravanfar, Tamaddon, Niakousari, & Moein (2016) tried to nano encapsulate the anthocyanins in solid lipid nanoparticles using the microemulsion dilution method. First of all, a factor screening was performed with the Placket-Burman model, followed by an optimization of the encapsulation efficiency (EE%) and size (nm) responses by the Box-Behnken response surface methodology. Nanoparticles' average size was 479 nm with EE = 93.8%. However, 50% surfactant was required in the formulation concerning the lipid phase. The authors' conclusion regarding the surfactant content was as the higher the concentration, the smaller the particle size, and the higher the EE%.

Regarding the nanoparticles produced by special equipment, there are still difficulties in the construction, operation, and maintenance of this equipment due to the complexity they

demand and the high cost involved (Tarone, Cazarin, & Junior, 2020). Besides, there are techniques within this class of nanoparticles that require the use of solvents and presenting difficulties in monitoring the size of the formed particle, such as the supercritical fluid technique. Additional difficulties can also be found in sophisticated techniques, e.g. electrospinning and electrospraying can present low performance and slow process, while nanospray-dryer and freeze-dryer can produce high particle porosity (Tarone, Cazarin, & Junior, 2020; Arpagaus, Collenberg, Rütti, Assadpour, & Jafari, 2017; Gu, Linehan & Tseng, 2015).

In this context, biopolymeric nanoparticles have interesting properties to nanoencapsulation anthocyanins extending their use in the pharmaceutical and food areas. Aside from the similar properties that the bio polymeric nanoparticles have with those produced with synthetic polymers, they also exhibit non-toxicity, biocompatibility, biodegradability, widely available, low cost, and possibiliting their use in food processing (Luo & Wang, 2014). Furthermore, it is possible to produce biopolymeric nanoparticles with high encapsulation efficiency, absence of pores, safe (many are produced free of organic solvents and with polymers recognized as GRAS), and with bioadhesive properties (Sharif, Khoshnoudi-Nia, & Jafari, 2020; Akhavan, & Jafari, 2017).

Depending on the preparation method, the biopolymer nanoparticles can be obtained as nanocapsules (vesicular system in which the bioactive compound is located inside a cavity, which consists of an internal liquid core surrounded by a polymeric membrane) or nanospheres (the bioactive compound found physically and uniformly dispersed throughout the matrix) (Esfanjani & Jafari, 2016). In general, the shape of biopolymeric nanoparticles is spherical, but they can also appear as spheroids, ellipsoids, agglomerates, disc-shaped, or needle-like when methods of macroscopic rupture, extrusion, or gel molding are used (Wen, Gailani, & Yin, 2018).

Several properties and functions conferred to biopolymeric nanoparticles come from the diversity of existing biopolymers, including polysaccharides (chitosan, gums, cellulose and their derivatives, pectin, starch) and proteins (zein, B-lactoglobulin, soy protein isolate, whey protein) (Esfanjani & Jafari, 2016).

Table 1. Summary of recent work involving anthocyanin nanoencapsulation

System	Technique	Composition of wall material	Anthocyanin sources	EE Size PDI Zeta potential	Study variables	Source
Lipid-based nanoparticles	**Solid lipid nanoparticle**	Palmitic acid Span 85 Egg lecithin	Red cabbage powder extract	20.45 - 94.43% 0.414 - 59.482µm - -	**Placket-Burman**: % primary aqueous phase volume in the lipid phase / % lipid / homogenization rate / % Pluronic F127 in the secondary aqueous phase / % total surfactant / lecithin:span 85 ratio / homogenization time (minafter total lipid dispersion in the secondary aqueous phase / T[a] secondary aqueous phase / injection rate of the lipid phase into the aqueous phase / volume ratio of lipid phase to secondary water phase / co-surfactant type (ethanol, isobutanol) over EE%, size and SPAN index. **Box–Behnken**: EE%; size	Ravanfar, Tamaddon, Niakousari, & Moein, (2016)
	Pickering emulsion	Soy protein isolate Soy oil	Black rice extract	90.02 – 94.18% 186 - 675 nm - (-14) - (-18) mV	Size, zeta potential, Surface hydrophobicity, antioxidant capacity, oxidative stability, released free fatty acids, CLSM, Cryo-SEM, Creaming index	Ju et al. (2020)
	Double emulsion / Niosome	**double-emulsion**: polycaprolactone tween 20 **Niosome**: cholesterol Tween 20	Black carrot extract	**double-emulsion:** 40% 252.4 - 1003 nm - **Niosome**: 130-333.5 130-333.5 nm -	**Double-emulsion:** feeding time, T[a], mixing speed, PCL, [anthocyanin], %Tween 20 **Niosomes:** Cholesterol, Tween 20, anthocyanin amounts, feeding time, ultrasonication, ultrasonic probe and T[a]	Fidan-Yardimci et al. (2019)
	Liposome	soy lecithin	Black carrot extract	40 - 66% Day 0: 42.2 - 46.8 nm; Day 21: 41.0 - 50.8 nm; Day 0: 0.269 - 0.352; Day 21: 0.301 - 0.429; Day 0: 21.3 - 26.3 mV; Day 21: 26.3 - 28.6 mV	size, PDI, zeta potencial, EE%, phenolic content, antioxidant activity, anthocyanin content, color, lipid oxidation (hexanal content)	Guldiken, Gibis, Boyacioglu, Capanoglu, & Weiss, (2018)

	Liposome	Soy lecithin; cholesterol	Bilberry	50.6% 159 nm 0.244 -40.2 mV	Size, zeta potential, PDI, EE%; TEM; *in vitro* gastrointestinal drug release; FTIR	Zhao, Temelli, & Chen (2017)
Miscellaneous Nanoparticles	**Bicontinuous microemulsion**	Tween 80/ span 80, isopropyl palmitate, ethanol	blueberry	- 70 nm - 40.2 mV	HLB value; Km value; TEM; size; viscosity; anthocyanin content; light, T[a], NaCl, sucrose, and glucose stability	Chen, Ma, Yao, Zhang, & Zhao (2018)
Biopolymer nanoparticles	**Copigmentation + Polyelectrolite complex**	chondroitin sulfate / chitosan /cathechin	Blueberry extract	~ 60 – 70% -	Size, zeta potential, color, FTIR, CE%, EE%, Stability (ascorbic acid, T[a], auto-oxidation)	Tan, Celli, Selig, & Abbaspourrad, (2018)
	Emulsification-solvent evaporation	PLGA/PEG	-	60% 120–165nm 0.4 12mV	EE%; TEM; size, zeta potential; FTIR; In vitro drug release; cell culture, cytotoxicity; in vitro oxidative stress; ApoTox-Glo triplex assay	Amin, Shah, Badshah, Khan, & Kim (2017)
	Ionic gelation + Polyelectrolite complex	Chitosan / sodium alginate	blackrice extract	56.34 - 68.92% 35.5-635 nm - -	EE%; size, SEM, FTIR, antioxidant capacity	Bulatao, Samin, Salazar, & Monserate, (2016)
	Polyelectrolyte complex	Chitosan / Arabic gum	acai berry	- 230 - 260 nm 0.21 - 0.29 -	antioxidant capacity, size, PDI, stability (pH 4 and 7)	Shim, Lee, Nam, & Lee (2016)
	Copigmentation + Polyelectrolite complex	chitosan (CS)/ chondroitin sulfate	blueberry powder extract	~ 60 – 85% ~ 200 - 600nm - ~18 - 33 mV	copigment type; size, zeta potential, color, FTIR, EE%, ascorbic acid stability	Tan, Celli, & Abbaspourrad (2018)
	Polyelectrolyte complex	Chitosan hydrochloride/ Carboxymethyl chitosan/ β-lactoglobulin	Anthocyanins mixture (25% of purity)	41.3 - 70.8% 88.3 - 144.1 nm - -	%ATN retention, size, EE%, zeta potential, *in vitro* releasing test, *in vitro* digestion	Ge et al. (2019)
	Polyelectrolyte complex	chitosan + Sodium tripoliphosphate (TPP)	Blueberry extract	94.02% (NCC) – 32.54% (TPP) 64.8 nm (NCC) – 33887 nm (TPP) -	size; %Yield; EE%, phenolics content, antioxidant activity, anthocyanin distribuition; In vitro releasing test; FTIR; FE-SEM	Wang, Jung, Zhao (2017)

		/ cellulose nanocrystal (CNC)				
	Polyelectrolyte complex	chitosan/ chondroitin sulfate	black rice extract	~ 87% 350.1 nm 42.55 0.158 42.55 mV	size; zeta potential; PDI; loading efficiency%; TEM; AFM; FTIR, thermogravimetric analysis; cell culture; cell viability; cell apoptosis	Liang, Zhang & Jing (2019)
	Polyelectrolyte complex	carboxymethyl chitosan/chitosan hydrochloride	Blueberry extract	38.2 - 64,2% 211 - 751 nm - -	EE%; size, *in vitro* digestion; anthocyanin content; stability in a beverage system model;	He et al. (2017)
	Polyelectrolyte complex	carboxymethyl chitosan / chitosan hydrochloride	Blueberry extract	16.2 - 44.0% 178.1 - 273.6 - nm 0.315 - 0.571 15.3 - 27.8 mV	anthocyanin content; size; zeta potential; EE%; thermal properties; FTIR, TEM; storage stability (light, pH, T^a, ascorbic acid)	Ge, Yue, Chi, Liang, & Gao, (2018)
Nanoparticles produced by special equipments	**uniaxial and coaxial eletospinning**	Gelatin / Lactoalbumin	sour cherry concentrate	89.7 and 91.3% (phenolic acids); 70.3 and 77.8% (flavonoids); (-3.19) – (-16.6) - -16.6 to -3.19 mV	SEM; zeta potential; contact angle; phenolics content; flavonoids content; anthocyanins content; antioxidant capacity; EE%; *in vitro* digestion;	Isik; Altay; Capanoglu (2018)
	eletrospraying	chitosan / gelatin	black carrot extract	75.6 - 76.9% ~100 nm - ~1.5µm - -	SEM; FTIR; EE%; *in vitro* drug release in ethanol 10 % and acetic acid 3%	Isik, Altay, & Capanoglu (2018)
	electrospinning	Zein	Red Cabbage	- 444 - 510 nm - -	size; color; SEM; FTIR; contact angle	Prietto et al. (2018)
Naturally produced nanoparticles	**inclusion complex**	cycloamylose / β-cyclodextrin	Black rice extract	-	FTIR, antioxidant capacity, stability (thermal, color)	Jung, Joo, Rho, & Kim (2020)

Font: Own authorship (2022)

Abbreviations: EE%, encapsulation efficiency; PDI, polydispersity index; T^a, temperature; CLSM, Confocal laser scanning microscopy; SEM, scanning electronic microscopy; PCL, polycaprolactone; PLGA/PEG, poly(lactic-co-glycolic acid)/ Polyethylene glycol; TEM, Transmission electron microscopy; FTIR, Fourier transform infrared; HLB, hydrophilic-lipophilic balance; CE%, capacity encapsulation.

The use of biopolymers enables the occurrence of different interactions during the formation of nanoparticles, such as electrostatic attractions, hydrogen bonds, and hydrophobic interactions (Pisoschi et al, 2018; Arroyo-Maya & McClements, 2015). Thus, biopolymeric nanoparticles can prevent the hydration of anthocyanins, maintain the flavylium cations, and improves the stability of these molecules in media considered “unsuitable” for them through associations with biopolymers (He et al., 2017).

Among the polymers used in the production of nanoparticles, chitosan is a linear polysaccharide obtained from the deacetylation of chitin and composed of randomly distributed β-(1-4) -linked D-glucosamine residues and N-acetyl-D-glucosamine units (Figure 4) (Wu et al., 2020; Ali & Ahmed, 2018). Chitosan is the second most abundant polymer in the world, behind only cellulose, and stands out because it is derived from a non-toxic natural source. Furthermore, chitosan is a versatile, biodegradable, biocompatible polymer, and has excellent functional properties, such as bio adhesiveness and anti-tumor activity (Mohammed et al., 2017; Ali & Ahmed, 2018).

Chitosan's versatility is due to the presence of active amino groups in its structure. This allows chitosan to be soluble and to have a positive charge in aqueous acidic media, which makes it capable of carrying out various interactions with other compounds of interest in the food and pharmaceutical industry (Ali & Ahmed, 2018; Zhao et al., 2011). In pH values <6.5, the amino groups located on the C2 position of the repeating-glucopyranose units of chitosan become protonated. Therefore, these groups can interact electrostatically with polyanions to form complexes and hydrogels (Hamman, 2010; Zhao et al., 2011).

Fig 4. Chitosan chemical structure

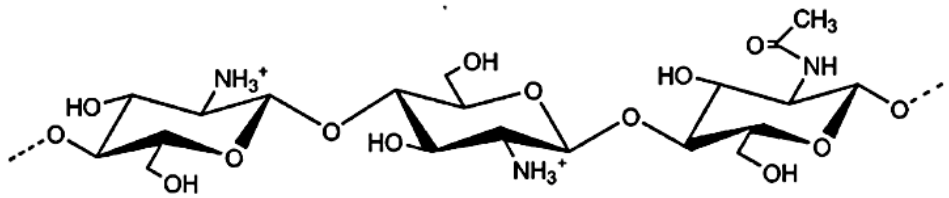

Font: Adapted from <https://www.crq4.org.br/quimica_viva__a_quimica_das_quitosanas>

Chitosan is particularly useful for producing biopolymer nanoparticles based on electrostatic interactions. In addition, chitosan can be found with different molecular weights and acetylation degrees, which enable greater control of particle characteristics (Joye & McClements, 2014). Among the methods for preparing chitosan nanoparticles, IG and PC are

the most used, since they do not require sophisticated equipment and present simple, fast and inexpensive methodologies.

Ionic gelatinization consists of the ionic interaction between the positive charges of chitosan's amino groups and the negative groups of polyanions, such as sodium tripolyphosphate (Sreekumar; Goycoolea; Moerschbacher & Rivera-Rodriguez, 2018), pyrophosphate (Cai & Lapitsky, 2014), glutaraldehyde (Asiri, Khan & Bozkurt, 2018), genipin (Pujana, Pérez-Álvarez, Iturbe & Katime, 2013), among others. Among polyions studied to date, sodium tripolyphosphate (TPP) is the most used in the chitosan cross-linking, because it presents low toxicity and formation of nanoparticles with desirable sizes and shapes (Sreekumar et al., 2018; Fan et al., 2012).

Polyelectrolytic complexation involves the formation of interpolymer complexes through non-covalent interactions (electrostatic interactions, hydrophobic interactions, hydrogen bonding, and Van der Waals interactions) between polymers with opposite charges. Electrostatic interactions mainly arise from an increase in entropy due to the release of low-molecular-weight counterions (Shovsky, Varga, Makuška, & Claesson, 2009). These interactions promote the formation of a three-dimensional network and particles with different sizes, depending on the polymers used, can be formed (Wu et al., 2020; Meka et al., 2017). This process is safe, ecological, simple to perform, free of chemical cross-linking agents and organic solvents, and requires little energy. (Wu et al., 2020).

4.1 Production of chitosan nanoparticles

In a stable colloidal system, the particles remain in suspension and resist aggregation or flocculation. This stability depends on the balance between repulsive and attractive forces inherent to the surface charges of the particles and the Brownian motion contained in the system (De Robertis, Bonferoni, Elviri, Sandri, Caramella, & Bettini, 2014). If there is little or no repulsive force, destabilizing mechanisms such as flocculation or aggregation may occur. Once destabilized, the particles in the colloidal system interact with each other and form aggregates that precipitate by gravity (Meka et al., 2017).

For the production of nanoparticles using PC and IG, the most common method is extrusion/drip with a syringe (Figure 4) (Wu et al., 2020; Bulatao et al., 2017; Meka et al., 2017; Patil et al., 2010). In this method, the crosslinking agent (IG method) or the negatively charged polymer dispersion (PC method) is added through a manual or automatic drip to another dispersion, which is kept under constant agitation (Patil et al., 2010).

Some research points to the effect of the order of addition/titration on the formation of polyelectrolytic complexes and their influence on the average size, zeta potential, and morphology of the particles formed, showing that in the same molar or mass ratio, different complexes are formed due to this effect (Wang, Jung & Zhao, 2017; Wang, Qian & Roman, 2011). However, it is worth remembering that an excess of positive charges leads to the formation of nanoparticles instead of aggregates and macrogels, which does not occur when there is an excess of polyanion charges. In the latter case, more unstable aggregates and complexes are formed (Costalat, Alcouffe, David, & Delair, 2015; Wang & Roman, 2011).

Some parameters can be controlled to achieve the desired particle size. Some of them are: the rate of addition of the dispersion to be dripped, pH and ionic strength of the dispersions, agitation speed, direction of the titration, and molar and mass ratio between the polymers or polymer-polyanion (Yuan & Huang, 2019; Sreekumar; Goycoolea; Moerschbacher & Rivera-Rodriguez, 2018; Ramasamy et al., 2013; Wang; Qian & Roman, 2011; Wang & Roman, 2011).

In addition to the syringe extrusion/drip technique, other techniques are developed to improve the reproducibility, stability, and uniformity of nanoparticles formed by IG and PC. This allows compounds with hydrophilic characteristics to be nanoencapsulated more efficiently (He et al., 2018). An example of this is the recent use of the flash nanocomplexation (FNC) technique (Figure 5) by He et al. (2017) to produce polyelectrolytic complexes based on chitosan with small diameters and uniform size distribution.

Santos et al. (2016) used FNC for the first time through adaptations of the flash nanoprecipitation technique (FNP). The adapted technique excludes the use of organic solvents and is induced only by the formation of polyelectrolytic complexes since in the PNF technique the complexes formed are precipitated by the addition of solvents (Santos et al., 2016). For the production of uniform nanoparticles, specific equipment must be used, such as a multi-inlet vortex mixer (MIVM) or a confined impinging jet mixer (CIJ) for a continuous flow process, which allows the production of nanoparticles with sizes between 30 and 150 nm and enables the use of this technology on a large scale. (He et al., 2018; He et al., 2017; Santos et al., 2016).

Although the FNC technique is very promising, specific equipment is necessary, which still compromises research in many laboratories. Therefore, developing biopolymer nanoparticles based on chitosan through ion gelatinization or polyelectrolytic complexation, and associating them with the titration/drip technique is still the most accessible, quick, and simple option to date.

Fig. 5. Methods of producing biopolymeric nanoparticles by polyelectrolyte complexation and ionic gelatinization.

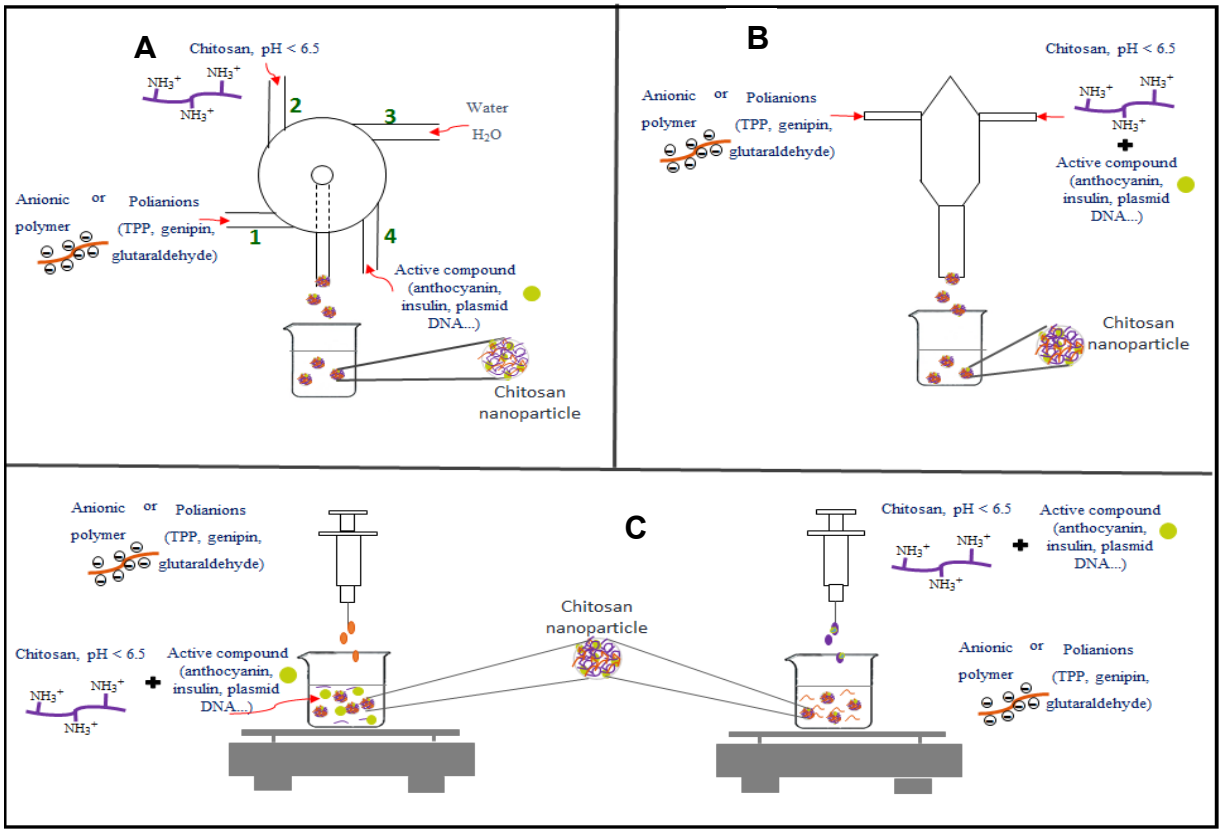

*(A) multi-inlet vortex mixer (MIVM); (B) confined impinging jet (CIJ) mixer; (C) extrusion/drip method. Font: Own authorship (2022)

5. Recent advances in anthocyanin nanoencapsulation by polyelectrolytic complexation and ionic gelatinization

When working with nanoparticulate systems incorporated with sensitive bioactive compounds, high efficiency of encapsulation, better performance of biological activities, and good stability in mediums with wide pH variations (mainly with pH> 6) and high temperatures are sought. In recent years, different polymers have been used in the research area, which includes proteins and polysaccharides. Cellulose nanocrystals (CNC), chondroitin sulfate (CHS), β-lactoglobulin (β-lg), and zein are some examples of biopolymers used for anthocyanins nanoencapsulation and other bioactive and nutraceutical compounds.

Cellulose nanocrystals are crystalline and compact structures, isolated from acid hydrolysis, mainly with sulfuric acid, from cellulose fibers (Abdul Khalil et al., 2016). CNCs are in the form of elongated rods or filaments and have dimensions ranging from 5 to 25 nm in diameter and from 100 to 500 nm in length (Wang & Roman, 2011).

Among the properties of CNCs, low density, low cost, abundance in nature, good mechanical properties, large surface area, flexibility, barrier properties, and low thermal expansion stand out (Abdul Khalil et al., 2016). Additionally, CNCs can increase the stiffness of nanocomposites, even at low concentrations, when incorporated into polymeric matrices. This resistance effect is due to the high length-to-width ratio and the ability of CNCs to form structures through hydrogen bonding (Yadav, Behera, Chang, Chiu, 2020; Abdul Khalil et al., 2016).

The association of CNCs with cationic polymers, such as chitosan, has attracted the attention of several researchers due to the excellent properties conferred to these materials. Furthermore, the fact that CNCs are food grade and biocompatible makes it possible to use them in food formulations, packaging development, and development of controlled release systems for the pharmaceutical and food industries. (Mu et al., 2019; Vashist et al., 2018).

Wang, Jung, and Zhao (2017) encapsulated blueberry extract in chitosan-CNC nanoparticles for the first time and achieved EE = 98% and yield of approximately 6.9 g, with an average particle size of 64.8 nm. The authors also produced chitosan-TPP particles and used the same parameters to the CNC. As a result, microparticles with an average size of 33.88 μm, a yield of 0.3 g and EE = 32.54% were formed. Furthermore, when studying controlled release in vitro, the authors found that nanoparticles with CNC were more stable at pH 7.4 than microparticles with TPP.

Chondroitin sulfate (CHS), originated from animal tissues and some bacteria, is a heteropolysaccharide from the group of glycosaminoglycans (GAG), unbranched, and negatively charged (Liang, Zhang & Jing, 2019). Its structure is composed of repeated units of alternating sulfated disaccharides (glucuronic acid and N-acetylgalactosamine residues), linked by glycosidic bonds β-(1 → 3). The sulfonate groups of chondroitin sulfate occur mainly in the hydroxyls in C4 and C6 of the N-acetylgalactosamine unit, and C2 of the glucuronic acid (Kumari, & Badwaik, 2019).

Besides composing a large part of the extracellular matrix of various connective tissues such as skin, bone, cartilage, ligaments, and tendons, CHS is involved in several biochemical activities such as antioxidants, anticoagulants, and anti-inflammatory. (Kumari, & Badwaik, 2019; Shariatinia, & Barzegari, 2019). This natural polysaccharide has also been the subject of much research in the field of nanotechnology, including the formation of nanostructured systems with chitosan.

Liang, Zhang & Jing (2019) encapsulated black rice extract anthocyanins in chitosan-CHS nanoparticles by IG method and found that there was an influence on pH, the mass

proportion of polymers, and the concentration of anthocyanins in the development of nanoparticles. The encapsulation efficiency of 88.32% and an average size of 350 nm were achieved. Moreover, nanoencapsulated anthocyanins significantly reduced the viability of colon cancer cells.

Tan et al. (2018) nanoencapsulated blueberry anthocyanins copigmented with epigallocatechin gallate (EGCG) in chitosan-CHS nanoparticles. It was found that the antioxidant capacity in ascorbic acid media of nanoencapsulated anthocyanins with EGCG was greater than free anthocyanins and encapsulated anthocyanins without EGCG. Nanoencapsulated anthocyanins in the presence of EGCG inhibited 82% and 70% of DPPH and FRAP radicals, respectively.

Another advance in research to overcome the problems in the production of chitosan nanoparticles is through the modification of the chitosan surface, as in the case of chitosan hydrochloride and carboxymethyl chitosan. Good results in particle size and encapsulation efficiency have been achieved for several compounds, including doxorubicin hydrochloride, with EE = 72% and 279.3 nm (Feng et al., 2013); quercetin, with EE = 70% and 386.3 nm (Yan et al., 2018) and green tea polyphenols, with EE = 83% and 407 nm (Liang et al., 2011). For anthocyanins, the encapsulation efficiency may be further improved, and in studies of He et al. (2017) and Ge et al. (2018), the maximum values obtained for $EE_{\text{blueberry extract}}$ were 64.2% and 44%, respectively.

Some authors report that biopolymeric nanoparticles produced by the drip / extrusion method are not very suitable for hydrophilic compounds nanoencapsulation, because the structures formed are porous and metastable. This accelerates the oxygen permeation through the matrix and facilitates the diffusion of the bioactive compound in a shorter time. In this way, the functionality of the formed nanoparticles becomes limited, with a consequent reduction in the encapsulation efficiency. (Sharif et al., 2020; Bulatao et al., 2018; Kurozawa & Hubinger, 2017; Joye, Davidov-Pardo, McClements, 2014).

Despite the still considerable anthocyanin losses in these systems, other strategies can also be used together to minimize these effects. An example is the use of copigmentation before the formation of nanoparticles (Tan et al., 2018), the combination of IG and PC techniques (Bulatao et al., 2016), and the formation of polyelectrolytic complexes associated with proteins, such as β -lactoglobulin (Ge et al., 2019) and zein (Prietto et al., 2018) to encapsulate anthocyanins.

As for the association with proteins, zein is a promising protein in the encapsulation area. In addition to having a hydrophobic characteristic, zein is considered to be GRAS, has excellent mucoadhesive properties, and is capable of resisting the gastric environment. Thus, zein can be used as a vehicle for the controlled release of active compounds sensitive to the action of enzymes and pH in the gastrointestinal tract (Luo et al., 2012; Paliwal e Palakurthi, 2014).

Considering the instability and low bioavailability of anthocyanins in the large intestine, besides the fact chitosan-TPP nanoparticles are a metastable systems (Furtado et al., 2018; Wang, Jung & Zhao, 2017; Tsai, Chen, Bai, Chen, 2011), zein could be used to coat chitosan nanoparticles loaded with anthocyanins stabilizing them. Moreover, zein can act as a polyanion in the formation of complexes with chitosan through hydrogen bonds between the hydroxyls present in its structure and the amino groups of chitosan (Ren et al., 2019). An example is the coating of chitosan-TPP nanoparticles incorporated with sodium selenite. After zein coating, EE increased from 60% to 95% and the release profile got better control compared to selenite in free form (Luo, Zhang, Cheng & Wang, 2010).

Given all the factors mentioned above and the low stability of anthocyanins, the incorporation of these molecules in chitosan nanoparticles is considered a challenge. Several factors, isolated or combined, contribute to the stability of nanoparticles formed by PC and IG. They can be classified into three groups: I) intrinsic factors of polyions, such as the nature of ionic groups, molecular weight, and charge density; II) extrinsic factors of polyions, such as polyelectrolyte concentration, pH, ionic strength of the medium, order of addition (addition of the polyanion dispersion in the polycation dispersion or vice versa); III) other factors, such as the use of ultrasound.

The structure of the nanoparticle is directly influenced by the factors described (Al-Rashed, Niknezhad, and Jana, 2019; Rampino et al., 2013), and they are not only affected by the preparation but also during storage (Rampino et al., 2013). Therefore, correct planning, with control of the variables that mainly affect EE, particle size, and the bioavailability of anthocyanins can result in highly stable systems.

5.1 pH Effect

It is known that the pH value that anthocyanin acquires in its most stable form varies between 1 and 3, which restricts the pH ranges that can be used in the preparation of polymeric dispersions. Chitosan is a promising polymer for anthocyanin nanoencapsulation because it is

a weak polyelectrolyte. Chitosan charge density varies according to the solution pH, so its degree of protonation may be changed by variations in the dispersion pH (Al-Rashed, Niknezhad, & Jana, 2019).

The highest protonation degrees of the primary chitosan amino groups occurs in pH values <6.5. Therefore, it is possible to work with dispersions in pH values between 3 and 4 (Abdel-Hafez, Hathout, & Sammour, 2014), which contributes to the greater stability of anthocyanin molecules. However, in media with pH values <4, the chitosan molecules exhibit extended conformation. This is due to the high protonation of amino groups, and even more when the degree of deacetylation of chitosan is high (> 85%). Thus, the electrostatic repulsion between the chitosan chains is intensified, which provides an increase in the exposure of the ionizable amino groups. As a result, interactions with the polyanion intensify and provide an increase in the size of the particles formed (Tsai, Chen, Bay & Chen, 2011).

Another point to be considered is the nature of the polyanion. Regarding ionic gelation, it is known that the most crosslinking agent used is TPP. The pH of a 0.01 M TPP aqueous solution is 9.7 (Wu, Tao, Zhang, & Su, 2011). Depending on the volume and concentration of the TPP solution and the initial pH of the chitosan dispersion, the pH of the reaction medium may increase to a value that is capable of destabilizing the anthocyanin molecules by hydrating the *flavilium* cation. In this case, there is a nucleophilic attack on carbon 2, which leads to the formation of carbinol (colorless) pseudo bases and even chalcones. These changes in the chemical structure of anthocyanin can hinder the nanoencapsulation of these molecules and even their biological activity (Arroyo-Maya & McClements, 2015).

In polyelectrolytic complexes, the structure, morphology, and functionality of the nanoparticles formed are even more affected by pH variations, since the polyanion is also a polymeric structure and, in addition to its main functional groups, pH can also interfere in the intramolecular interactions of the anionic polymer and highlight hydrophobic interactions and hydrogen bonds (Luo e Wang, 2014). These interactions can restrict access to anionic groups since the polymeric chain will be presented in a compact form at pH values close to the pKa of its functional groups. Therefore, the nanoparticles formation and the final yield will be reduced (Laleveé et al., 2017).

5.2 Effect of deacetylation degree, molecular weight and chitosan concentration

The main disadvantage of chitosan-based nanosystems application is the lack of understanding and consensus between the different production protocols reported in scientific

articles (Sreekumar et al., 2018). This hinders the ability to reproduce these nanoparticles, especially in relation to size, since the mass ratio of chitosan:polyanion is considered instead of molar ratios. Moreover, experimental factors such as deacetylation degree and molar mass of chitosan are often not prioritized. However, these factors are very important since the density of ionizable groups available for interaction is extremely significant in systems that have electrostatic interactions ~~such~~ as the main intermolecular force for interaction, besides hydrophobic interactions (Sreekumar et al., 2018; Abdel-Hafez, Hathout, & Sammour, 2014).

The molecular weight refers to the average size of the individual chitosan chains. In general, high molar mass chitosan form larger particles compared to low molar mass chitosan (Wu et al. 2020; Luo & Wang, 2014). In addition, polyelectrolytes with weak ionic groups, a large difference in molecular weight and polymerization degree should be chosen during polymers and/or polyanions selection to produce stable chitosan nanoparticles. The guest-host theory confirms this claim, which the excess polymer ("host") has a higher polymerization degree than the "guest" polymer (Siyawamwaya, Choonara, Bijukumar, Kumar, Du Toit & Pillay, 2015). Under these conditions, the polyelectrolytes are mixed at a non-stoichiometric molar ratio, that is, with a ratio of cationic functional groups: anionic > 1.

Wu et al. (2017) were able to produce stable sodium chitosan-heparin-hyaluronate nanoparticles in a medium with physiological pH and ionic strength by selecting chitosan with an appropriate degree of deacetylation (50%) and molecular mass (10^3 kg.mol^{-1}). The nanoparticles obtained were of the core-shell type, with the shell showing hydrophilic characteristics and a diffuse interface.

As for the deacetylation degree (DD), this is related to the charge density of chitosan, which is associated with the degree of substitution of acetyl groups with free amino groups, and is very important in the development of chitosan nanoparticles. According to Laleveé et al. (2017) high degree of deacetylation (DD = 86%) of chitosan increased its charge density. Therefore, chitosan was able to interact more with the sodium hyaluronate molecules, resulting in larger and stable particles. However, by reducing the DD, the charge density of chitosan was reduced, and fewer groups of sodium hyaluronate interacted with the amino groups of chitosan. The result was smaller particles with greater polydispersity.

Another factor that should be considered to obtain high polydispersity of nanoparticulated systems based on polysaccharides is the material batch. Chitosan and other commercial polysaccharides do not have a homogeneous molar mass, that is, the chains of this polysaccharide are polydispersed. This hinders the reproducibility of the experiments, due to the great

influence of the charge density and molar mass on the morphology and size of the particles formed.

Rampino et al. (2013) reported that they achieved unexpected results in terms of size or flocculation of particles upon studying the formation of nanoparticles of chitosan-TPP. The authors attributed these practical difficulties to the variation between batches of chitosan. Morris et al. (2011) also found differences in the size of polymer chains between batches and within the same batch of chitosan when producing nanoparticles cross-linked with TPP. The authors found a variation of up to 30 nm in the size of the nanoparticles, and the samples that had higher molecular mass were the same ones that originated larger nanoparticles.

Based on these reports, it is suggested to use samples from the same batch when carrying out experiments. Thus, large variations in molar mass and deacetylation degree of the collected samples can be avoided. Also, it is considered important to perform as many repetitions and replicates as possible.

5.3 Effect of ionic strength and surfactants

Particle aggregation is also an undesirable factor in colloidal systems and indicates system instability. The control of all variables mentioned so far allows stable colloidal systems to be obtained. However, some strategies can also be used to achieve these results more effectively.

The presence of monovalent ions such as NaCl in the formation of chitosan-TPP nanoparticles contributes to greater stability and smaller particle size in the system, depending on the concentration used. Jonassen, Kjøniksen, & Hiorth (2012) studied the effect of ionic strength on the formation and size of chitosan nanoparticles - TPP. It was verified that the nanoparticles prepared in medium with 50 mM and 150 mM saline concentration presented less polydispersity than those prepared without the addition of NaCl. However, nanoparticles produced in the presence of NaCl 150 mM became more aggregated and presented a larger size compared to those produced with less salt concentration.

The surfactants use in suitable proportions relative to the polymer mass also contributes to the formation of a more stable colloidal system. Yeon et al. (2019) produced chitosan-TPP nanoparticles for immobilization of the glucose oxidase enzyme and used Tween 20 (0.5% v / v) to prevent agglomeration of the particles during the ionic gelation process.

5.4 Ultrasound effect

Another device that can be used to prevent the aggregation of nanoparticles in the redispersion step is the use of an ultrasound probe. Ultrasound can help break down particles, as well as reduce size and polydispersity through cavitation effects (Floris, Meloni, Lai, Marongiu, Maccioni, & Sinico, 2013). However, care must be taken to particles be not disintegrated by the action of cavitation, avoiding re-agglomeration (Gokce, Cengiz, Yildiz, Calimli, & Aktas, 2014). Therefore, low powers should be used in this process, and the ideal is to carry out the preliminary study of factors that interfere in this stage.

6. Applications of nano and microstructured anthocyanins

Evidence from clinical and laboratory research has shown that free anthocyanins have beneficial health properties, such as cancer (Thibado et al. 2018) and cardiovascular disease prevention (Alvarez-Suarez, et al. 2014), diabetes control (Guo et al. 2018), antioxidant (Ahmad et al. 2018), neuroprotective properties (Jeong et al. 2012), and reduction on tumor activity (Jeong et al. 2016). In addition to the benefits found in the prevention and control of various diseases, anthocyanins also have the potential to replace synthetic dyes in the food (Khoo et al. 2017) and textiles (Haddar et al. 2017) industries.

The instability of the anthocyanin structures and the degradation in the organism before its absorption in the gastrointestinal environment are factors that reduce the aforementioned properties and due to this, become major obstacles for some applications. To solve these difficulties, during the last few years, researchers have directed efforts towards the improvement of nano/microstructure development techniques to protect and minimize anthocyanins degradation by the action of extrinsic factors such as pH, temperature, light, oxygen, and strength ionic (Sharif, Khoshnoudi-Nia, & Jarafi, 2020).

6.1 History and lack of effective applications

Contrary to the numerous applications of free anthocyanins found in the literature, the number of studies that apply micro / nanostructures containing anthocyanins in a product is scarce.

When keywords “Anthocyanins microencapsulation” or “Anthocyanins nanoencapsulation” are searched on ScienceDirect, for example, there is a reduction of more than 900 scientific articles to a few dozen articles that performed applications and found the size of these structures.

For the development of this work and description of the application areas of the nanoparticles produced by PC and IG techniques, other criteria were also adopted: particle size up to 500 nm, studies carried out with chitosan, the encapsulated compound should be a source of anthocyanins, and PC and IG techniques for the production of nanoparticles. However, the search resulted in few studies, which justifies examples of other nanostructures in the discussion of this topic.

Therefore, we present in Table 2 the researches that focused on the development of anthocyanin stabilization techniques by nano/microstructures formation in the last 10 years and carried out application studies. Additionally, the research lines, classifications of structure type, production method, the composition of wall material, and size of the nano/microstructures were highlighted for food and packaging.

6.2 Food applications

The development of nano/microstructures with optimal characteristics for applicability in food is ~~an~~ extensive, costly, and even impractical research in a short time~~,~~ due to the numerous factors and levels of study to be analyzed. One of the ways to develop processes and technologies with greater efficiency is through the use of response surface methodology (RSM). This tool allows determining optimal conditions, among the factors and responses evaluated, to obtain an optimized treatment, which saves time, reagents, and makes it possible to evaluate synergistic or antagonistic effects between independent variables. From this, research that uses RSM for development and application of nano/anthocyanin protective microstructures is frequently observed.

Table 2. Applications in the last 10 years of anthocyanins nano/microstructures.

Research line	Application	Structure classification	Production method	Composition of wall material	Size (µm)	Source
Food	Milk	Nanoliposomes	Ultrasonication	Lecithin/Cholesterol	0.053	Chi et al., (2019)
	Beverage	Nanoparticles	Ionic gelation	Carboxymethyl chitosan /Chitosan hydrochloride	0.219	He et al., (2017)
	Soft drink	Microcapsules	Spray-drying	Maltodextrin (MC), Maltodextrin/Gum arabic (MG), and Maltodextrin/ γ-Cyclodextrin (MC)	M > 500 MG < 200 MC < 50	Burin, Rossa, Ferreira-Lima, Hillmann, & Boirdignon-Luiz (2010)
Medicine	Tumor therapy	Nanocomplex	Mixing method in water	Chondroitin sulfate/ Doxorubicin hydrochloride	0.174 to 0.269	Jeong, Bae, Park, & Na (2016)
Packaging	Active biodegradable films	Microcapsules	Freeze-drying	Maltodextrin	below 150	Stoll et al., (2015)
	Active biodegradable films	Microcapsules	Freeze-drying	Gum arabic/Maltodextrin	below 200	Stoll, Costa, Jablonski, Flôres, & de Oliveira (2015)
Controlled release	Intestinal bioavailability and accessibility in humans	Microcapsules	Emulsification, thermal gelation, and spray-drying	Whey protein (WPC), and pectin (CPC)	WPC = 200 CPC = 250 to 500	Mueller et al., (2018)
Sensors	Detection of pH and borate additives	Nanoparticles	Advanced Stöber	Mesoporous sílica matrix	0.10 to 0.50	Ha, Lien, Anh, & Lam (2017)

Font: Own authorship (2022)

Chi et al. (2019) used the RSM tool to optimize anthocyanin-loaded nanoliposomes (AN), focusing on the particle size reduction and increase of anthocyanin retention rate. The AN optimization increased the anthocyanins' stability evaluated in vitro analysis over 30 days, at 4 ºC and 25 ºC, in the presence and absence of light, compared to free anthocyanins. When applying the optimized AN in milk, improvement in the protection of anthocyanins and with slow-release rate during intestinal digestion in vitro was observed. These results indicated the use of nanoliposomes as a potential functional ingredient for milk. However, new studies should be developed in milk to assess sensory quality, combined with anthocyanin retention rate and maintenance of bioactive effects until the expiration date.

He et al. (2017) also used the RSM tool to optimize chitosan nanoparticles with hydrochloride and carboxymethyl chitosan as constituents of wall material. When comparing EE% with work developed by Chi et al., (2019), it was noticed that nanoliposomes had 91.13 %, while chitosan nanoparticles showed 61.80 %. However, anthocyanin retention rate was persistent over time at 4 ºC and maintained at 84.5 % after 21 days of beverage storage (He et al. 2017). On the other hand, in Chi et al.'s (2019) study practically equal retention rate in milk was possible in just five days of storage at 4 ºC. Increased protection of anthocyanins by chitosan nanoparticles is dependent on the compositional of food matrices and copigmentation effect promoted by chitosan structures, which prevents hydration of flavilium cation and reduces instability of anthocyanins (Dangles & Brouillard, 1992).

The protection promoted by chitosan structures is proven by verifying that the release rate of anthocyanins in the gastric fluid after 120 minutes was 55 % for nanoliposomes and 47.73 % for chitosan nanoparticles. However, it is recommended that further research be carried out with anthocyanins from the same source to better understand the effect of each wall material on the stabilization of anthocyanins.

Burin et al. (2010) compared degradation kinetics of microencapsulated anthocyanins with different wall materials and applied them to soft drinks. It was observed that a combination of maltodextrin/Arabic-gum produced an increase in half-life time and lowest degradation constant in all evaluated conditions. This was justified by the action of Arabic-gum on the microcapsule wall as film-forming agent, which promoted better trapping of anthocyanins and made flavilium cation less vulnerable to hydrolysis (Dangles & Brouillard, 1992).

6.3 Food Packaging applications

Anthocyanins act as primary antioxidants due to the interruption of the lipid oxidation reaction chain when donating hydrogen to peroxy radicals, forming flavonoid radicals, which in turn reacts with another free radical and ends propagation chain (Reis et al. 2016; Griendling et al. 1994). They are also secondary antioxidants. They reduce the speed of oxidation initiation through chelation with metal ions and anti-peroxidative activity forming non-radical species (Reis et al. 2016). These characteristics allow its application in another area of science, such as the development of active packaging through the incorporation of anthocyanins in a polymeric matrix for food protection, since one of the main causes of reduced shelf life is oxidation processes.

Active packages are defined as those that intentionally interact with food to improve some of its characteristics (Soares, 1998). However, the low stability of flavonoids and, in some cases, lack of compatibility with the polymeric matrix makes it necessary to form micro/nanostructures for incorporation in packaging. In this sense, Stoll et al. (2015) produced active films based on cassava starch incorporated with anthocyanin microcapsules for application in extra virgin olive oil. Oxidation stability of oil in active packaging was maintained until the 8th day, while in polypropylene packaging degradation was observed on the 4th day. Insertion of anthocyanins in polymeric packaging for foods susceptible to oxidation is promising, however, further research is needed to evaluate the efficiency of the active effect throughout the storage period and comparisons with free anthocyanins in the polymeric matrix.

Soll et al. (2015) evaluated the antioxidant activity and compatibility of anthocyanin microcapsules formed by gum arabic (GA) and maltodextrin (MD) for application in active films. GA microcapsules showed antioxidant activity 2.44 times greater than structures formed by MD. This occurrence was justified by greater solubility of GA in water, which provided greater release and performance of anthocyanins in aqueous systems. However, when incorporating microcapsules of anthocyanins and MD into cassava starch films, a greater protective effect against the peroxides formation in sunflower oil was verified, as well as better compatibility with the polymeric matrix than GA-based microcapsules. Films containing MD-based microcapsules showed greater resistance to traction, greater percentage elongation, and less permeability to water vapor than active films with GA.

Implementation of active packaging in the food industry requires research to understand the mechanisms of anthocyanin diffusion to the food matrix. Besides, it is necessary to study the stability of microcapsules, the oxygen permeability through the films, and films' biodegradability capacity. Although antimicrobial or antioxidant properties of active packaging to be

evaluated throughout the storage period, the same does not occur with other physical-chemical characterizations. The mechanical, sensory, thermal and barrier properties to water vapor and oxygen are often analyzed shortly after manufacture. This is a problem for the implementation of active packaging in commerce, since these and other properties are practically not studied during storage conditions.

7. Conclusions and future trends

Anthocyanins are bioactive compounds extremely sensitive to changes in pH, temperature, light, enzymes, and other variables in the environment in which they are found. Therefore, it is necessary to employ artifices and technologies for their wide use in ~~both~~ the food and pharmaceutical sectors. This review addressed the main limitations of anthocyanins in terms of stability and, in particular, was directed towards a more in-depth approach on the encapsulation of this class of bioactive compounds in biopolymeric nanoparticles developed by the techniques of polyelectrolytic complexation and ionic gelatinization.

These two methodologies have been widespread in recent years due to their simplicity and because they do not require the use of toxic solvents during the preparation stage. The main limitations in the development of these nanoparticulate systems were also discussed. It can be seen that there is still a long way to go in this area of nanotechnology, especially with regard to the development of stable colloidal nanoparticles in mediums with physiological pH and high encapsulation efficiency.

Several strategies were also pointed out to improve anthocyanin nanoencapsulation, such as the use of new biopolymers for complexing with chitosan, including cellulose nanocrystal, zein, and chondroitin sulfate; modulation of ionic strength; use of non-stoichiometric proportions between polyions; adequate molar proportions; and use of surfactants in appropriate proportions.

There is a lack of studies on the behavior of nanoparticles in food or the body ~~and~~ that assesses the changes caused in these environments, leading to the development of research that aims to apply and evaluate the behavior of nanoparticles in different systems. Despite the excellent results obtained in vitro, it is inconceivable to expect the same effects in commercial products or in living organisms that present complex physicochemical conditions. It can be observed incompatibility, reduction and/or even inactivation of the effects of the active compounds in the polymeric matrix.

In addition, we suggest new research trends in order to minimize the aforementioned problems, such as: giving more attention to structure-property-function relations when planning

the nanostructures; analyzing the effectiveness and possible active function of anthocyanin degradation products; characterizing the physical-chemical properties over the storage time; and optimizing micro/nanostructures in the conditions of the commercialized matrix. These proposals can lead to a greater understanding of the effect of micro/nanostructures containing anthocyanins, in addition to providing discoveries and efficient implementation in living organisms and/or food and pharmaceutical products.

Acknowledgments

The authors thank the Coordenação de Aperfeiçoamento de Pessoal e Nível Superior (CAPES), Conselho de Desenvolvimento Ciêntífico e Tecnológico (CNPq) and the Fundação de Amparo à Pesquisa do Estado de Minas Gerais (FAPEMIG) for their financial support.

References

Abdel-Hafez, S. M., Hathout, R. M., & Sammour, O. A. (2014). Towards better modeling of chitosan nanoparticles production: screening different factors and comparing two experimental designs. *International journal of biological macromolecules*, 64, 334-340. doi: 10.1016/j.ijbiomac.2013.11.041

Abdul Khalil H.P.S., Saurabh, C. K., Adnan, A. S., Fazita, M. N., Syakir, M. I., Davoudpour, Y., ... & Dungani, R. (2016). A review on chitosan-cellulose blends and nanocellulose reinforced chitosan biocomposites: Properties and their applications. *Carbohydrate polymers*, *150*, 216-226. https://doi.org/10.1016/j.carbpol.2016.05.028

Ahmad, M., Ashraf, B., Gani, A., & Gani, A. (2018). Microencapsulation of saffron anthocyanins using β glucan and β cyclodextrin: Microcapsule characterization, release behaviour & antioxidant potential during in-vitro digestion. *International Journal of Biological Macromolecules*, 109, 435–442. doi:10.1016/j.ijbiomac.2017.11.122

Akhavan, S., & Jafari, S. M. (2017). Chapter 6-Nanoencapsulation of natural food colorants. *Nanoencapsulation of food bioactive ingredients*, 223-60. doi: 10.1016/B978-0-12-809740-3.00006-4

Ali, A., & Ahmed, S. (2018). A review on chitosan and its nanocomposites in drug delivery. *International journal of biological macromolecules*, *109*, 273-286. https://doi.org/10.1016/j.ijbiomac.2017.12.078

Al-Rashed, M. M., Niknezhad, S., & Jana, S. C. (2019). Mechanism and factors influencing formation and stability of chitosan/lignosulfonate nanoparticles. Macromolecular Chemistry and Physics, 220(1), 1800338. https://doi.org/10.1002/macp.201800338

Alvarez-Suarez, J. M., Giampieri, F., Tulipani, S., Casoli, T., Di Stefano, G., González-Paramás, A. M., Santos-Buelga, C., Busco, F., Quiles, J. L., Cordero, M. D., Bompadre, S., Mezzeti, B., & Battino, M. (2014). One-month strawberry-rich anthocyanin supplementation ameliorates cardiovascular risk, oxidative stress markers and platelet activation in humans. *The Journal of Nutritional Biochemistry*, 25(3), 289–294. doi:10.1016/j.jnutbio.2013.11.002

Amin, F. U., Shah, S. A., Badshah, H., Khan, M., & Kim, M. O. (2017). Anthocyanins encapsulated by PLGA@ PEG nanoparticles potentially improved its free radical scavenging capabilities via p38/JNK pathway against Aβ 1–42-induced oxidative stress. *Journal of nanobiotechnology*, *15*(1), 12. doi:10.1186/s12951-016-0227-4

Arpagaus, C., Collenberg, A., Rütti, D., Assadpour, E., & Jafari, S. M. (2018). Nano spray drying for encapsulation of pharmaceuticals. *International journal of pharmaceutics*, *546*(1-2), 194-214. doi: 10.1016/j.ijpharm.2018.05.037

Arroyo-Maya, I. J., & McClements, D. J. (2015). Biopolymer nanoparticles as potential delivery systems for anthocyanins: Fabrication and properties. *Food research international*, *69*, 1-8. https://doi.org/10.1016/j.foodres.2014.12.005

Asiri, S. M., Khan, F. A., & Bozkurt, A. (2018). Synthesis of chitosan nanoparticles, chitosan-bulk, chitosan nanoparticles conjugated with glutaraldehyde with strong anti-cancer proliferative capabilities. *Artificial Cells, Nanomedicine, and Biotechnology*, *46*(sup3), S1152-S1161. doi: 10.1080/21691401.2018.1533846

Askar, K. A., Alsawad, Z. H., & Khalaf, M. N. (2015). Evaluation of the pH and thermal stabilities of rosella anthocyanin extracts under solar light. *Beni-Suef University Journal of Basic and Applied Sciences*, 4(3), 262-268. https://doi.org/10.1016/j.bjbas.2015.06.001

Atnip, A. A., Sigurdson, G. T., Bomser, J., & Giusti, M. M. (2017). Time, concentration, and pH-dependent transport and uptake of anthocyanins in a human gastric epithelial (NCI-N87) cell line. *International Journal of Molecular Sciences*, 18(2), 446. doi: 10.3390/ijms18020446

Babaloo, F., & Jamei, R. (2018). Anthocyanin pigment stability of Cornus mas–Macrocarpa under treatment with pH and some organic acids. *Food science & nutrition*, *6*(1), 168-173. https://doi.org/10.1002/fsn3.542

Bazana, M. T., Codevilla, C. F., & de Menezes, C. R. (2019). Nanoencapsulation of bioactive compounds: challenges and perspectives. *Current opinion in food science*, *26*, 47-56. https://doi.org/10.1016/j.cofs.2019.03.005

Bimpilas, A., Panagopoulou, M., Tsimogiannis, D., & Oreopoulou, V. (2016). Anthocyanin copigmentation and color of wine: The effect of naturally obtained hydroxycinnamic acids as cofactors. *Food Chemistry*, *197*, 39-46. https://doi.org/10.1016/j.foodchem.2015.10.095

Bobbio, F. O., & Bobbio, P. A. (2003). *Introdução à química de alimentos*. São Paulo: Livraria Varela.

Brouillard, R., Chassaing, S., Isorez, G., Kueny-Stotz, M., & Figueiredo, P. (2010). The visible flavonoids or anthocyanins: From research to applications. https://doi.org/10.1002/9781444323375.ch1

Bueno, J. M., Sáez-Plaza, P., Ramos-Escudero, F., Jiménez, A. M., Fett, R., & Asuero, A. G. (2012). Analysis and antioxidant capacity of anthocyanin pigments. Part II: chemical structure, color, and intake of anthocyanins. *Critical Reviews in Analytical Chemistry*, *42*(2), 126-151. https://doi.org/10.1080/10408347.2011.632314

Bulatao, R. M., Samin, J. P. A., Salazar, J. R., & Monserate, J. J. (2017). Encapsulation of anthocyanins from black rice (Oryza Sativa L.) bran extract using chitosan-alginate nanoparticles. *J. Food Res.*, *6*(3), 40. doi: 10.5539/jfr.v6n3p40

Burin, V. M., Rossa, P. N., Ferreira-Lima, N. E., Hillmann, M. C. R., & Boirdignon-Luiz, M. T. (2010). Anthocyanins: optimisation of extraction from Cabernet Sauvignon grapes, microcapsulation and stability in soft drink. *International Journal of Food Science & Technology*, 46(1), 186–193. doi:10.1111/j.1365-2621.2010.02486.x

Cahyana, Y., & Gordon, M. H. (2013). Interaction of anthocyanins with human serum albumin: Influence of pH and chemical structure on binding. *Food chemistry*, *141*(3), 2278-2285. doi: 10.1016/j.foodchem.2013.05.026

Cai, Y., & Lapitsky, Y. (2014). Formation and dissolution of chitosan/pyrophosphate nanoparticles: is the ionic crosslinking of chitosan reversible?. *Colloids and Surfaces B: Biointerfaces*, *115*, 100-108. https://doi.org/10.1016/j.colsurfb.2013.11.032

Castañeda-Ovando, A., de Lourdes Pacheco-Hernández, M., Páez-Hernández, M. E., Rodríguez, J. A., & Galán-Vidal, C. A. (2009). Chemical studies of anthocyanins: A review. *Food chemistry*, *113*(4), 859-871. https://doi.org/10.1016/j.foodchem.2008.09.001

Chen, B. H., & Stephen Inbaraj, B. (2019). Nanoemulsion and nanoliposome based strategies for improving anthocyanin stability and bioavailability. *Nutrients*, *11*(5), 1052. doi: 10.3390/nu11051052

Chi, J., Ge, J., Yue, X., Liang, J., Sun, Y., Gao, X., & Yue, P. (2019). Preparation of nanoliposomal carriers to improve the stability of anthocyanins. *LWT*, 109, 101–107. doi:10.1016/j.lwt.2019.03.070

Comin, V. M., Lopes, L. Q., Quatrin, P. M., de Souza, M. E., Bonez, P. C., Pintos, F. G., ... & Santos, R. C. (2016). Influence of Melaleuca alternifolia oil nanoparticles on aspects of Pseudomonas aeruginosa biofilm. *Microbial pathogenesis*, 93, 120-125. doi: 10.1016/j.micpath.2016.01.019

Costalat, M., Alcouffe, P., David, L., & Delair, T. (2015). Macro-hydrogels versus nanoparticles by the controlled assembly of polysaccharides. *Carbohydrate polymers*, 134, 541-546. doi: 10.1016/j.carbpol.2015.07.071

Czank C, Cassidy A, Zhang Q, Morrison DJ, Preston T, Kroon PA, et al. Human metabolism and elimination of the anthocyanin, cyanidin-3-glucoside: a 13C-tracer study. *Am J Clin Nutr*. 2013;97:995–1003. doi: 10.3945/ajcn.112.049247

Dangles, O. & Brouillard, R. (1992). A spectrophotometric method based on the anthocyanin copigmentation interaction and applied to the quantitative study of molecular complexes. *Journal Chemical Society Perkin Trans*, 2, 247–257. https://doi.org/10.1039/P29920000247

De Robertis, S., Bonferoni, M. C., Elviri, L., Sandri, G., Caramella, C., & Bettini, R. (2015). Advances in oral controlled drug delivery: the role of drug–polymer and interpolymer non-covalent interactions. *Expert opinion on drug delivery*, *12*(3), 441-453. doi: 10.1517/17425247.2015.966685

Ertan, K., Türkyılmaz, M., & Özkan, M. (2018). Effect of sweeteners on anthocyanin stability and colour properties of sour cherry and strawberry nectars during storage. *Journal of food science and technology*, *55*(10), 4346-4355. doi: 10.1007/s13197-018-3387-4

Esfanjani, A. F., & Jafari, S. M. (2016). Biopolymer nano-particles and natural nano-carriers for nano-encapsulation of phenolic compounds. *Colloids and Surfaces B: Biointerfaces*, *146*, 532-543. https://doi.org/10.1016/j.colsurfb.2016.06.053

Espitia, P. J. P., Soares, N. D. F. F., Teófilo, R. F., dos Reis Coimbra, J. S., Vitor, D. M., Batista, R. A., ... & Medeiros, E. A. A. (2013). Physical–mechanical and antimicrobial properties of nanocomposite films with pediocin and ZnO nanoparticles. *Carbohydrate polymers*, *94*(1), 199-208.

Fan, W., Yan, W., Xu, Z., & Ni, H. (2012). Formation mechanism of monodisperse, low molecular weight chitosan nanoparticles by ionic gelation technique. *Colloids and surfaces B: Biointerfaces*, *90*, 21-27. https://doi.org/10.1016/j.colsurfb.2011.09.042

Fathi, M., Martin, A., & McClements, D. J. (2014). Nanoencapsulation of food ingredients using carbohydrate based delivery systems. *Trends in food science & technology*, *39*(1), 18-39. https://doi.org/10.1016/j.tifs.2014.06.007

Feng, C., Wang, Z., Jiang, C., Kong, M., Zhou, X., Li, Y., ... & Chen, X. (2013). Chitosan/o-carboxymethyl chitosan nanoparticles for efficient and safe oral anticancer drug delivery: in vitro and in vivo evaluation. *International journal of pharmaceutics*, *457*(1), 158-167. doi: 10.1016/j.ijpharm.2013.07.079

Fidan-Yardimci, M., Akay, S., Sharifi, F., Sevimli-Gur, C., Ongen, G., & Yesil-Celiktas, O. (2019). A novel niosome formulation for encapsulation of anthocyanins and modelling intestinal transport. *Food chemistry*, *293*, 57-65. https://doi.org/10.1016/j.foodchem.2019.04.086

Floris, A., Meloni, M. C., Lai, F., Marongiu, F., Maccioni, A. M., & Sinico, C. (2013). Cavitation effect on chitosan nanoparticle size: A possible approach to protect drugs from ultrasonic stress. *Carbohydrate polymers*, 94(1), 619-625. https://doi.org/10.1016/j.carbpol.2013.01.017

Furtado, G. T. F. D. S., Fideles, T. B., Cruz, R. D. C. A. L., Souza, J. W. D. L., Rodriguez Barbero, M. A., & Fook, M. V. L. (2018). Chitosan/NaF Particles Prepared Via Ionotropic Gelation: Evaluation of Particles Size and Morphology. *Materials Research*, 21(4). https://doi.org/10.1590/1980-5373-mr-2018-0101

Ge, J., Yue, P., Chi, J., Liang, J., & Gao, X. (2018). Formation and stability of anthocyanins-loaded nanocomplexes prepared with chitosan hydrochloride and carboxymethyl chitosan. *Food Hydrocolloids*, *74*, 23-31. https://doi.org/10.1016/j.foodhyd.2017.07.029

Ge, J., Yue, X., Wang, S., Chi, J., Liang, J., Sun, Y., ... & Yue, P. (2019). Nanocomplexes composed of chitosan derivatives and β-Lactoglobulin as a carrier for anthocyanins: Preparation, stability and bioavailability in vitro. *Food Research International*, 116, 336-345. doi: 10.1016/j.foodres.2018.08.045

Gokce, Y., Cengiz, B., Yildiz, N., Calimli, A., & Aktas, Z. (2014). Ultrasonication of chitosan nanoparticle suspension: Influence on particle size. *Colloids and Surfaces A: Physicochemical and Engineering Aspects*, *462*, 75-81. https://doi.org/10.1016/j.colsurfa.2014.08.028

Griendling, K. K., Minieri, C. A., Ollerenshaw, J. D., & Alexander, R. W. (1994). Angiotensin II stimulates NADH and NADPH oxidase activity in cultured vascular smooth muscle cells. *Circulation Research*, 74(6), 1141–1148. doi:10.1161/01.res.74.6.1141

Gu, B., Linehan, B., & Tseng, Y. C. (2015). Optimization of the Büchi B-90 spray drying process using central composite design for preparation of solid dispersions. *International journal of pharmaceutics*, *491*(1-2), 208-217. doi: 10.1016/j.ijpharm.2015.06.006

Guldiken, B., Gibis, M., Boyacioglu, D., Capanoglu, E., & Weiss, J. (2018). Physical and chemical stability of anthocyanin-rich black carrot extract-loaded liposomes during storage. *Food research international*, *108*, 491-497. doi:10.1016/j.foodres.2018.03.071

Guo, H., & Xia, M. (2018). Anthocyanins and diabetes regulation. In *Polyphenols: Mechanisms of Action in Human Health and Disease* (pp. 135-145). Academic Press. doi:10.1016/b978-0-12-813006-3.00012-x

Ha, C. T., Lien, N. T. H., Anh, N. D., & Lam, N. L. (2017). Development of Natural Anthocyanin Dye-Doped Silica Nanoparticles for pH and Borate-Sensing Applications. *Journal of Electronic Materials*, 46(12), 6843–6847. doi:10.1007/s11664-017-5743-y

Haddar, W., Ben Ticha, M., Meksi, N., & Guesmi, A. (2017). Application of anthocyanins as natural dye extracted from Brassica oleracea L. var. capitata f. rubra: dyeing studies of wool and silk fibres. *Natural Product Research*, 32(2), 141–148. doi:10.1080/14786419.2017.1342080

Hamman, J. H. (2010). Chitosan based polyelectrolyte complexes as potential carrier materials in drug delivery systems. *Marine drugs*, *8*(4), 1305-1322. doi: 10.3390/md8041305

He, B., Ge, J., Yue, P., Yue, X., Fu, R., Liang, J., & Gao, X. (2017). Loading of anthocyanins on chitosan nanoparticles influences anthocyanin degradation in gastrointestinal fluids and stability in a beverage. *Food chemistry*, 221, 1671-1677. https://doi.org/10.1016/j.foodchem.2016.10.120

He, Z., Liu, Z., Tian, H., Hu, Y., Liu, L., Leong, K. W., ... & Chen, Y. (2018). Scalable production of core–shell nanoparticles by flash nanocomplexation to enhance mucosal transport for oral delivery of insulin. *Nanoscale*, 10(7), 3307-3319. https://doi.org/10.1039/C7NR08047F

He, Z., Santos, J. L., Tian, H., Huang, H., Hu, Y., Liu, L., ... & Mao, H. Q. (2017) Scalable fabrication of size-controlled chitosan nanoparticles for oral delivery of insulin. *Biomaterials*, 130, 28-41. https://doi.org/10.1016/j.biomaterials.2017.03.028

Isik, B. S., Altay, F., & Capanoglu, E. (2018). The uniaxial and coaxial encapsulations of sour cherry (Prunus cerasus L.) concentrate by electrospinning and their in vitro bioaccessibility. *Food chemistry*, *265*, 260-273. https://doi.org/10.1016/j.foodchem.2018.05.064

Iosub, I., Kajzar, F., Makowska-Janusik, M., Meghea, A., Tane, A., & Rau, I. (2012). Electronic structure and optical properties of some anthocyanins extracted from grapes. *Optical Materials*, *34*(10), 1644-1650. https://doi.org/10.1016/j.optmat.2012.03.020

Jafari, S. M. (2017). An overview of nanoencapsulation techniques and their classification. In *Nanoencapsulation technologies for the food and nutraceutical industries* (pp. 1-34). Academic Press. doi: 10.1016/B978-0-12-809436-5.00001-X

Jeong, D., Bae, B., Park, S., & Na, K. (2016). Reactive oxygen species responsive drug releasing nanoparticle based on chondroitin sulfate–anthocyanin nanocomplex for efficient tumor therapy. *Journal of Controlled Release*, 222, 78–85. doi:10.1016/j.jconrel.2015.12.009

Jeong, D., & Na, K. (2012). Chondroitin sulfate based nanocomplex for enhancing the stability and activity of anthocyanin. *Carbohydrate Polymers,* 90(1), 507–515. doi:10.1016/j.carbpol.2012.05.072

Jiang, T., Mao, Y., Sui, L., Yang, N., Li, S., Zhu, Z., ... & He, Y. (2019). Degradation of anthocyanins and polymeric color formation during heat treatment of purple sweet potato extract at different pH. *Food chemistry*, 274, 460-470. https://doi.org/10.1016/j.foodchem.2018.07.141

Jonassen, H., Kjøniksen, A. L., & Hiorth, M. (2012). Effects of ionic strength on the size and compactness of chitosan nanoparticles. *Colloid and Polymer Science*, *290*(10), 919-929. DOI: 10.1007/s00396-012-2604-3

Joye, I. J., Davidov-Pardo, G., & McClements, D. J. (2014). Nanotechnology for increased micronutrient bioavailability. *Trends in food science & technology*, *40*(2), 168-182. https://doi.org/10.1016/j.tifs.2014.08.006

Joye, I. J., & McClements, D. J. (2014). Biopolymer-based nanoparticles and microparticles: Fabrication, characterization, and application. *Current Opinion in Colloid & Interface Science*, *19*(5), 417-427. https://doi.org/10.1016/j.cocis.2014.07.002

Ju, M., Zhu, G., Huang, G., Shen, X., Zhang, Y., Jiang, L., & Sui, X. (2020). A novel pickering emulsion produced using soy protein-anthocyanin complex nanoparticles. *Food Hydrocolloids*, *99*, 105329. https://doi.org/10.1016/j.foodhyd.2019.105329

Jung, Y. K., Joo, K. S., Rho, S. J., & Kim, Y. R. (2020). pH-dependent antioxidant stability of black rice anthocyanin complexed with cycloamylose. *LWT*, 109474. https://doi.org/10.1016/j.lwt.2020.109474

Karaoglan, H. A., Keklik, N. M., & Isıklı, N. D. (2019). Degradation kinetics of anthocyanin and physicochemical changes in fermented turnip juice exposed to pulsed UV light. *Journal of food science and technology*, 56(1), 30-39. https://doi.org/10.1007/s13197-018-3434-1

Kay, C. D., Pereira-Caro, G., Ludwig, I. A., Clifford, M. N., & Crozier, A. (2017). Anthocyanins and flavanones are more bioavailable than previously perceived: A review of recent evidence. *Annual Review of Food Science and Technology*, 8, 155-180. doi: 10.1146/annurev-food-030216-025636

Khoo, H. E., Azlan, A., Tang, S. T., & Lim, S. M. (2017). Anthocyanidins and anthocyanins: colored pigments as food, pharmaceutical ingredients, and the potential health benefits. *Food & Nutrition Research*, 61(1), 1361779. doi: 10.1080/16546628.2017.1361779

Ko, A., Lee, J. S., Sop Nam, H., & Gyu Lee, H. (2017). Stabilization of black soybean anthocyanin by chitosan nanoencapsulation and copigmentation. *Journal of Food Biochemistry*, *41*(2), e12316. https://doi.org/10.1111/jfbc.12316

Koley, T. K., Singh, S., Khemariya, P., Sarkar, A., Kaur, C., Chaurasia, S. N. S., & Naik, P. S. (2014). Evaluation of bioactive properties of Indian carrot (Daucus carota L.): A chemometric approach. *Food research international*, 60, 76-85.

Kumari, L., & Badwaik, H. R. (2019). Polysaccharide-based nanogels for drug and gene delivery. In Polysaccharide Carriers for Drug Delivery (pp. 497-557). Woodhead Publishing. https://doi.org/10.1016/B978-0-08-102553-6.00018-0

Kurozawa, L. E., & Hubinger, M. D. Hydrophilic food compounds encapsulation by ionic gelation. *Current Opinion in Food Science*, v. 15, p. 50-55, 2017. https://doi.org/10.1016/j.cofs.2017.06.004

Lalevée, G., Sudre, G., Montembault, A., Meadows, J., Malaise, S., Crépet, A., ... & Delair, T. (2016). Polyelectrolyte complexes via desalting mixtures of hyaluronic acid and chitosan—Physicochemical study and structural analysis. *Carbohydrate polymers*, *154*, 86-95. https://doi.org/10.1016/j.carbpol.2016.08.007

Lee, J. H., & Choung, M. G. (2011). Identification and characterisation of anthocyanins in the antioxidant activity-containing fraction of Liriope platyphylla fruits. *Food Chemistry*, *127*(4), 1686-1693. https://doi.org/10.1016/j.foodchem.2011.02.037

Liang, T., Zhang, Z., & Jing, P. (2019). Black rice anthocyanins embedded in self-assembled chitosan/chondroitin sulfate nanoparticles enhance apoptosis in HCT-116 cells. *Food chemistry*, *301*, 125280. https://doi.org/10.1016/j.foodchem.2019.125280

Luo, Y., & Wang, Q. (2014). Recent development of chitosan-based polyelectrolyte complexes with natural polysaccharides for drug delivery. *International journal of biological macromolecules*, *64*, 353-367. https://doi.org/10.1016/j.ijbiomac.2013.12.017

Luo, Y., Zhang, B., Cheng, W. H., & Wang, Q. (2010). Preparation, characterization and evaluation of selenite-loaded chitosan/TPP nanoparticles with or without zein coating. *Carbohydrate Polymers*, 82(3), 942-951. doi : 10.1016/j.carbpol.2010.06.029

Mazza, G., & Brouillard, R. (1987). Recent developments in the stabilization of anthocyanins in food products. *Food chemistry*, *25*(3), 207-225. https://doi.org/10.1016/0308-8146(87)90147-6

Meka, V. S., Sing, M. K., Pichika, M. R., Nali, S. R., Kolapalli, V. R., & Kesharwani, P. (2017). A comprehensive review on polyelectrolyte complexes. *Drug discovery today*, *22*(11), 1697-1706. https://doi.org/10.1016/j.drudis.2017.06.008

Mohammed, M. A., Syeda, J., Wasan, K. M., & Wasan, E. K. (2017). An overview of chitosan nanoparticles and its application in non-parenteral drug delivery. *Pharmaceutics*, *9*(4), 53. DOI: 10.3390/pharmaceutics9040053

Morais, C. A., de Rosso, V. V., Estadella, D., & Pisani, L. P. (2016). Anthocyanins as inflammatory modulators and the role of the gut microbiota. *Journal of Nutritional Biochemistry*, *33*, 1–7. https://doi.org/10.1016/j.jnutbio.2015.11.008

Morris, G. A., Castile, J., Smith, A., Adams, G. G., & Harding, S. E. (2011). The effect of prolonged storage at different temperatures on the particle size distribution of tripolyphosphate (TPP)–chitosan nanoparticles. Carbohydrate polymers, 84(4), 1430-1434. https://doi.org/10.1016/j.carbpol.2011.01.044

Mu, R., Hong, X., Ni, Y., Li, Y., Pang, J., Wang, Q., ... & Zheng, Y. (2019). Recent trends and applications of cellulose nanocrystals in food industry. *Trends in Food Science & Technology*, *93*, 136-144. https://doi.org/10.1016/j.tifs.2019.09.013

Mueller, D., Jung, K., Winter, M., Rogoll, D., Melcher, R., Kulozik, U., Schwarz, K., & Richling, E. (2018). Encapsulation of anthocyanins from bilberries – Effects on bioavailability and intestinal accessibility in humans. *Food Chemistry*, 248, 217–224. doi:10.1016/j.foodchem.2017.12.058

Norkaew, O., Thitisut, P., Mahatheeranont, S., Pawin, B., Sookwong, P., Yodpitak, S., & Lungkaphin, A. (2019). Effect of wall materials on some physicochemical properties and release characteristics of encapsulated black rice anthocyanin microcapsules. *Food chemistry*, *294*, 493-502. https://doi.org/10.1016/j.foodchem.2019.05.086

Oehlke, K., Adamiuk, M., Behsnilian, D., Gräf, V., Mayer-Miebach, E., Walz, E., & Greiner, R. (2014). Potential bioavailability enhancement of bioactive compounds using food-grade engineered nanomaterials: a review of the existing evidence. *Food & function*, *5*(7), 1341-1359. doi: 10.1039/c3fo60067j

Paliwal, R., & Palakurthi, S. (2014). Zein in controlled drug delivery and tissue engineering. *Journal of Controlled Release*, 189, 108-122. https://doi.org/10.1016/j.jconrel.2014.06.036

Patil, J. S., Kamalapur, M. V., Marapur, S. C., & Kadam, D. V. (2010). Ionotropic gelation and polyelectrolyte complexation: the novel techniques to design hydrogel particulate sustained, modulated drug delivery system: a review. *Digest Journal of Nanomaterials and Biostructures*, *5*(1), 241-248.

Peixoto, F. M., Fernandes, I., Gouvêa, A. C. M., Santiago, M. C., Borguini, R. G., Mateus, N., ... & Ferreira, I. M. (2016). Simulation of in vitro digestion coupled to gastric and intestinal transport models to estimate absorption of anthocyanins from peel powder of jabuticaba, jamelão and jambo fruits. *Journal of functional foods*, 24, 373-381. https://doi.org/10.1016/j.jff.2016.04.021

Pina, F., Melo, M. J., Laia, C. A., Parola, A. J., & Lima, J. C. (2012). Chemistry and applications of flavylium compounds: a handful of colours. *Chemical Society Reviews*, *41*(2), 869-908. doi: 10.1039/c1cs15126f

Pisoschi, A. M., Pop, A., Cimpeanu, C., Turcuş, V., Predoi, G., & Iordache, F. (2018). Nanoencapsulation techniques for compounds and products with antioxidant and antimicrobial activity-A critical view. *European journal of medicinal chemistry*, *157*, 1326-1345. https://doi.org/10.1016/j.ejmech.2018.08.076

Pola, C. C., Moraes, A. R., Medeiros, E. A., Teófilo, R. F., Soares, N. F., & Gomes, C. L. (2019). Development and optimization of pH-responsive PLGA-chitosan nanoparticles for triggered release of antimicrobials. *Food chemistry*, 295, 671-679. https://doi.org/10.1016/j.foodchem.2019.05.165

Prietto, L., Pinto, V. Z., El Halal, S. L. M., de Morais, M. G., Costa, J. A. V., Lim, L. T., ... & Zavareze, E. D. R. (2018). Ultrafine fibers of zein and anthocyanins as natural pH indicator. *Journal of the Science of Food and Agriculture*, *98*(7), 2735-2741. doi: 10.1002/jsfa.8769

Pujana, M. A., Pérez-Álvarez, L., Iturbe, L. C. C., & Katime, I. (2013). Biodegradable chitosan nanogels crosslinked with genipin. *Carbohydrate Polymers*, *94*(2), 836-842. doi: 10.1016/j.carbpol.2013.01.082

Qian, B. J., Liu, J. H., Zhao, S. J., Cai, J. X., & Jing, P. (2017). The effects of gallic/ferulic/caffeic acids on colour intensification and anthocyanin stability. *Food chemistry*, *228*, 526-532. doi: 10.1016/j.foodchem.2017.01.120

Ramasamy, T., Tran, T. H., Cho, H. J., Kim, J. H., Kim, Y. I., Jeon, J. Y., ... & Kim, J. O. (2014). Chitosan-based polyelectrolyte complexes as potential nanoparticulate carriers: physicochemical and biological characterization. *Pharmaceutical research*, *31*(5), 1302-1314. https://doi.org/10.1007/s11095-013-1251-9

Rampino, A., Borgogna, M., Blasi, P., Bellich, B., & Cesàro, A. (2013). Chitosan nanoparticles: preparation, size evolution and stability. *International journal of pharmaceutics*, 455(1-2), 219-228. doi: 10.1016/j.ijpharm.2013.07.034

Ravanfar, R., Tamaddon, A. M., Niakousari, M., & Moein, M. R. (2016). Preservation of anthocyanins in solid lipid nanoparticles: Optimization of a microemulsion dilution method using the Placket–Burman and Box–Behnken designs. *Food chemistry*, *199*, 573-580. doi: 10.1016/j.foodchem.2015.12.061

Reis, J. F., Monteiro, V. V. S., de Souza Gomes, R., do Carmo, M. M., da Costa, G. V., Ribera, P. C., & Monteiro, M. C. (2016). Action mechanism and cardiovascular effect of anthocyanins: a systematic review of animal and human studies. *Journal of Translational Medicine*, *14*(1), 315. https://doi.org/10.1186/s12967-016-1076-5

Ren, X., Hou, T., , Q., Zhang, X., Hu, D., Xu, B., ... & Ma, H. (2019). Effects of frequency ultrasound on the properties of zein-chitosan complex coacervation for resveratrol encapsulation. *Food chemistry*, *279*, 223-230. https://doi.org/10.1016/j.foodchem.2018.11.025

Robert, P., & Fredes, C. (2015). The encapsulation of anthocyanins from berry-type fruits. Trends in foods. *Molecules*, *20*(4), 5875-5888. doi: 10.3390/molecules20045875

Roobha, J. J., Saravanakumar, M., Aravindhan, K. M., & devi, P. S. (2011). The effect of light, temperature, ph on stability of anthocyanin pigments in Musa acuminata bract. Research in Plant Biology, 1(5). Retrieved from https://updatepublishing.com/journal/index.php/ripb/article/view/2597

Santos-Buelga, C., & González-Paramás, A. M. (2018). Anthocyanins. *Reference Module in Food Science*, 1–12. https://doi.org/10.1016/B978-0-08-100596-5.21609-0

Santos, J. L., Ren, Y., Vandermark, J., Archang, M. M., Williford, J. M., Liu, H. W., ... & Mao, H. Q. (2016). Continuous production of discrete plasmid DNA-polycation nanoparticles using flash nanocomplexation. *Small*, *12*(45), 6214-6222. doi: 10.1002/smll.201601425

Shariatinia, Z., & Barzegari, A. (2019). Polysaccharide hydrogel films/membranes for transdermal delivery of therapeutics. In *Polysaccharide Carriers for Drug Delivery* (pp. 639-684). Woodhead Publishing. https://doi.org/10.1016/B978-0-08-102553-6.00022-2

Sharif, N., Khoshnoudi-Nia, S., & Jafari, S. M. (2020). Nano/microencapsulation of anthocyanins; a systematic review and meta-analysis. *Food Research International*, *132*, 109077. https://doi.org/10.1016/j.foodres.2020.109077

Shim, H. R., Lee, J. S., Nam, H. S., & Lee, H. G. (2016). Nanoencapsulation of synergistic combinations of acai berry concentrate to improve antioxidant stability. *Food science and biotechnology*, *25*(6), 1597-1603. https://doi.org/10.1007/s10068-016-0246-9

Shovsky, A., Varga, I., Makuška, R., & Claesson, P. M. (2009). Formation and stability of water-soluble, molecular polyelectrolyte complexes: effects of charge density, mixing ratio, and polyelectrolyte concentration. *Langmuir*, 25(11), 6113-6121. https://doi.org/10.1021/la804189w

Singh, S., Kalia, P., Meena, R. K., Mangal, M., Islam, S., Saha, S., & Tomar, B. S. (2020). Genetics and Expression Analysis of Anthocyanin Accumulation in Curd Portion of Sicilian Purple to Facilitate Biofortification of Indian Cauliflower. *Frontiers in plant science*, *10*, 1766. https://doi.org/10.3389/fpls.2019.01766

Sipahli, S., Mohanlall, V., & Mellem, J. J. (2017). Stability and degradation kinetics of crude anthocyanin extracts from H. sabdariffa. *Food Science and Technology*, 37(2), 209-215. http://dx.doi.org/10.1590/1678-457x.14216

Siyawamwaya, M., Choonara, Y. E., Bijukumar, D., Kumar, P., Du Toit, L. C., & Pillay, V. (2015). A review: overview of novel polyelectrolyte complexes as prospective drug bioavailability enhancers. *International Journal of Polymeric Materials and Polymeric Biomaterials*, *64*(18), 955-968. doi: 10.1080/00914037.2015.1038816

Soares, N. F. F. (1998). Bitterness reduction in citrus juice through naringinase immobilized into polymer film. Ph.D. *Dissertation*. Cornell University, New York, 130.

Sreekumar, S., Goycoolea, F. M., Moerschbacher, B. M., & Rivera-Rodriguez, G. R. (2018). Parameters influencing the size of chitosan-TPP nano-and microparticles. Scientific reports, 8(1), 1-11. https://doi.org/10.1038/s41598-018-23064-4

Srivastava, J., & Vankar, P. S. (2010). Canna indica flower: New source of anthocyanins. *Plant physiology and biochemistry*, *48*(12), 1015-1019. https://doi.org/10.1016/j.plaphy.2010.08.011

Stoll, L., Costa, T. M. H., Jablonski, A., Flôres, S. H., & de Oliveira Rios, A. (2015). Microencapsulation of Anthocyanins with Different Wall Materials and Its Application in Active Biodegradable Films. *Food and Bioprocess Technology*, 9(1), 172–181. doi:10.1007/s11947-015-1610-0

Stoll, L., Silva, A. M., Iahnke, A. O. e S., Costa, T. M. H., Flôres, S. H., & Rios, A. de O. (2017). Active biodegradable film with encapsulated anthocyanins: Effect on the quality attributes of extra-virgin olive oil during storage. *Journal of Food Processing and Preservation*, 41(6), e13218. doi:10.1111/jfpp.13218

Suket, N., Srisook, E., & Hrimpeng, K. (2014). Antimicrobial activity of the anthocyanins isolated from purple field corn (Zea mays L.) Cob against Candida spp. *IOSR J Pharm Biol Sci*, *9*, 40-4. DOI: 10.9790/3008-09424044

Tarone, A. G., Cazarin, C. B. B., & Junior, M. R. M. (2020). Anthocyanins: New techniques and challenges in microencapsulation. *Food Research International*, 133, 109092. https://doi.org/10.1016/j.foodres.2020.109092

Tan, C., Celli, G. B., & Abbaspourrad, A. (2018). Copigment-polyelectrolyte complexes (PECs) composite systems for anthocyanin stabilization. *Food Hydrocolloids*, *81*, 371-379. https://doi.org/10.1016/j.foodhyd.2018.03.011

Tan, C., Celli, G. B., Selig, M. J., & Abbaspourrad, A. (2018). Catechin modulates the copigmentation and encapsulation of anthocyanins in polyelectrolyte complexes (PECs) for natural colorant stabilization. *Food chemistry*, *264*, 342-349. https://doi.org/10.1016/j.foodchem.2018.05.018

Tan, C., Selig, M. J., & Abbaspourrad, A. (2018). Anthocyanin stabilization by chitosan-chondroitin sulfate polyelectrolyte complexation integrating catechin co-pigmentation. Carbohydrate polymers, 181, 124-131. https://doi.org/10.1016/j.carbpol.2017.10.034

Terefe, N. S., Netzel, G. A., & Netzel, M. E. (2019). Copigmentation with Sinapic Acid Improves the Stability of Anthocyanins in High-Pressure-Processed Strawberry Purees. *Journal of Chemistry*, *2019*. https://doi.org/10.1155/2019/3138608

Thibado, S., Thornthwaite, J., Ballard, T., & Goodman, B. (2017). Anticancer effects of Bilberry anthocyanins compared with NutraNanoSphere encapsulated Bilberry anthocyanins. *Molecular and Clinical Oncology*, 8(2), 330-335. doi:10.3892/mco.2017.1520

Tong, Y., Deng, H., Kong, Y., Tan, C., Chen, J., Wan, M., ... & Li, L. (2020). Stability and structural characteristics of amylopectin nanoparticle-binding anthocyanins in Aronia melanocarpa. *Food chemistry*, *311*, 125687. https://doi.org/10.1016/j.foodchem.2019.125687

Tsai, M. L., Chen, R. H., Bai, S. W., & Chen, W. Y. (2011). The storage stability of chitosan/tripolyphosphate nanoparticles in a phosphate buffer. *Carbohydrate Polymers*, *84*(2), 756-761. https://doi.org/10.1016/j.carbpol.2010.04.040

Vashist, A., Kaushik, A., Vashist, A., Bala, J., Nikkhah-Moshaie, R., Sagar, V., et al. (2018). Nanogels as potential drug nanocarriers for CNS drug delivery. *Drug Discovery Today*, 23(7), 1359–6446. https://doi.org/10.1016/j.drudis.2018.05.018

Wallace, T. C., & Giusti, M. M. (2015). Anthocyanins. *Advances in Nutrition*, 6(5), 620-622. https://doi.org/10.3945/an.115.009233

Wang, F., Yang, Y., Ju, X., Udenigwe, C. C., & He, R. (2018). Polyelectrolyte complex nanoparticles from chitosan and acylated rapeseed cruciferin protein for curcumin delivery. *Journal of agricultural and food chemistry*, *66*(11), 2685-2693. doi: 10.1021/acs.jafc.7b05083

Wang, W., Jung, J., & Zhao, Y. (2017). Chitosan-cellulose nanocrystal microencapsulation to improve encapsulation efficiency and stability of entrapped fruit anthocyanins. *Carbohydrate polymers*, *157*, 1246-1253. https://doi.org/10.1016/j.carbpol.2016.11.005

Wang, H., Qian, C., & Roman, M. (2011). Effects of pH and salt concentration on the formation and properties of chitosan–cellulose nanocrystal polyelectrolyte–macroion complexes. *Biomacromolecules*, *12*(10), 3708-3714. https://doi.org/10.1021/bm2009685

Wang, H., & Roman, M. (2011). Formation and properties of chitosan− cellulose nanocrystal polyelectrolyte− macroion complexes for drug delivery applications. *Biomacromolecules*, 12(5), 1585-1593. https://doi.org/10.1021/bm101584c

Wen, J., Gailani, M. A., & Yin, N. (2018). Filled hydrogel particles. *Emulsion-based systems for delivery of food active compounds: formation, application, health and safety*. John Wiley & Sons, Hoboken, 161-180. https://doi.org/10.1002/9781119247159.ch7

Wu, D., Ensinas, A., Verrier, B., Cuvillier, A., Champier, G., Paul, S., & Delair, T. (2017). Ternary polysaccharide complexes: Colloidal drug delivery systems stabilized in physiological media. *Carbohydrate Polymers*, *172*, 265-274. https://doi.org/10.1016/j.carbpol.2017.05.051

Wu, D., Zhu, L., Li, Y., Zhang, X., Xu, S., Yang, G., & Delair, T. (2020). Chitosan-based Colloidal Polyelectrolyte Complexes for Drug Delivery: A Review. *Carbohydrate Polymers*, 116126. https://doi.org/10.1016/j.carbpol.2020.116126

Wu, S., Tao, Y., Zhang, H., & Su, Z. (2011). Preparation and characterization of water-soluble chitosan microparticles loaded with insulin using the polyelectrolyte complexation method. *Journal of Nanomaterials*, *2011*. https://doi.org/10.1155/2011/404523

Yadav, M., Behera, K., Chang, Y. H., & Chiu, F. C. (2020). Cellulose Nanocrystal Reinforced Chitosan Based UV Barrier Composite Films for Sustainable Packaging. *Polymers*, 12(1), 202. https://doi.org/10.3390/polym12010202

Yan, L., Gao, S., Shui, S., Liu, S., Qu, H., Liu, C., & Zheng, L. (2018). Small interfering RNA-loaded chitosan hydrochloride/carboxymethyl chitosan nanoparticles for ultrasound-triggered release to hamper colorectal cancer growth in vitro. *International Journal of Biological Macromolecules*, *162*, 1303-1310. https://doi.org/10.1016/j.ijbiomac.2020.06.246

Yeon, K. M., You, J., Adhikari, M. D., Hong, S. G., Lee, I., Kim, H. S., ... & Sajomsang, W. (2019). Enzyme-immobilized chitosan nanoparticles as environmentally friendly and highly effective antimicrobial agents. *Biomacromolecules*, *20*(7), 2477-2485. https://doi.org/10.1021/acs.biomac.9b00152

Yousuf, B., Gul, K., Wani, A. A., & Singh, P. (2016). Health benefits of anthocyanins and their encapsulation for potential use in food systems: a review. *Critical reviews in food science and nutrition*, *56*(13), 2223-2230. https://doi.org/10.1080/10408398.2013.805316

Yuan, Y., & Huang, Y. (2019). Ionically crosslinked polyelectrolyte nanoparticle formation mechanisms: the significance of mixing. *Soft Matter*, *15*(48), 9871-9880. https://doi.org/10.1039/C9SM01441A

Zapata, I. C., Álzate, A. F., Zapata, K., Arias, J. P., Puertas, M. A., & Rojano, B. (2019). Effect of pH, temperature and time of extraction on the antioxidant properties of Vaccinium meridionale Swartz. *Journal of Berry Research*, *9*(1), 39-49. DOI: 10.3233/JBR-18299

Zhao, L. M., Shi, L. E., Zhang, Z. L., Chen, J. M., Shi, D. D., Yang, J., & Tang, Z. X. (2011). Preparation and application of chitosan nanoparticles and nanofibers. *Brazilian Journal of Chemical Engineering*, *28*(3), 353-362. https://doi.org/10.1590/S0104-66322011000300001

Zhao, L., Temelli, F., & Chen, L. (2017). Encapsulation of anthocyanin in liposomes using supercritical carbon dioxide: Effects of anthocyanin and sterol concentrations. *Journal of Functional Foods*, *34*, 159-167. https://doi.org/10.1016/j.jff.2017.04.021

Artigo 2 *

* Formatado de acordo com as diretrizes da revista *Carbohydrates Polymers*

Design, optimization and evaluation of intermolecular interaction, morphological characteristics and thermal stability nanocomplexes formed between chitosan and cellulose nanocrystal

Rafaela Venancio Flores [a,*], Lucas de Souza Soares[b], Mariane Oliveira de Araujo [a], Laura Pereira [a], Sukarno Olavo Ferreira [c], Eduardo Basílio de Oliveira [a], Paulo César Stringheta [a], Taíla Veloso de Oliveira [a], Nilda de Fátima Ferreira Soares [a]

[a] Food Technology Department, Viçosa Federal University, Universitary Campus, s/n, 36570-900, Viçosa, MG, Brazil.

[b] Engineering College, Grande Dourados Federal University, Dourados road - Itahum km 12, 79804-970, Dourados, MS, Brazil.

[c] Physical Department, Viçosa Federal University, Universitary Campus, s/n, 36570-900, Viçosa, MG, Brazil.

∗Corresponding author: R. V. Flores.
E-mail address: rafavenacio2@gmail.com

Abstract: The polyelectrolyte complexation has been used to produce nanostructures obtained from different biopolymers in order to improve their technological performance. Thus, a Box-Behnken design involving pH_{NCC}, NaCl concentration and molar ratio of chitosan (CH):cellulose nanocrystal (NCC) variables was employed to optimize the formation of nanocomplexes, presenting a Z-average of < 200 nm and Zeta potential next to +40 mV. Moreover, higher complexation yields (~8%) were obtained at higher pH and lower [NaCl] ($p < 0.05$). Then, nanocomplexes obtained at $pH_{NCC} = 5.0$, absence of NaCl and CHI:NCC = 3:1, 6.5:1 or 10:1 were evaluated. Atomic force microscopy exhibited height ~30 nm and oval shape for CH:NCC nanocomplexes. XRD and TGA/DTG exhibited a higher thermal resistance of nanocomplexes and crystallinity modifications, compared to chitosan. The absence of microscopic changes indicated the thermal stability for CH:NCC = 3:1 nanocomplex stored during 30 days, at 7ºC e 25ºC.

Keywords: Polyelectrolyte complexation, Box-Behnken design, nanostructures, biopolymers.

Graphical abstract:

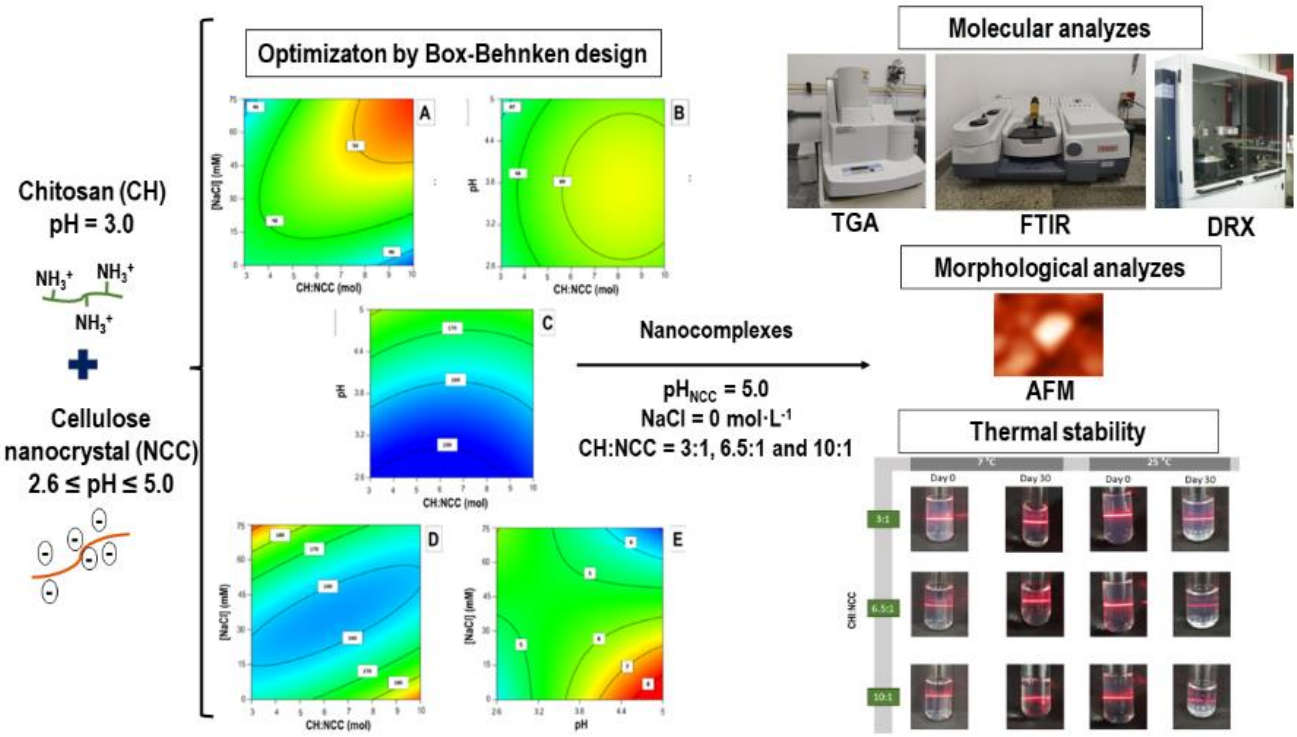

1. Introduction

The demand for improved materials in terms of functionalities and performance stimulates the adoption of new technologies in the food and pharmaceutical industries. Development of systems for controlled release of compounds, production of nanocomplexes/nanostructures and preparations of hydrogels are examples of strategies implemented in the development of formulations for innovative materials production. Moreover, ecofriendly materials from natural and renewable sources have greatly gained much of the scientists' attention, in the last two decades, to support the demand for sustainable processes and/or products.

In this context, polyelectrolytes have attracted the attention of the scientific community and industrial sectors, being one of the most attractive topics in the field of research and technological innovation (Meka et al., 2017). Polyelectrolytes (PEs) are polymers with ionizable groups that are capable of forming polyelectrolytic complexes (PECs) when mixed in a conductive medium free of organic solvents, surfactants and chemical ligands with opposite charges. Consequently, it can occur the release of counterions to the surrounding medium, resulting in an interpolymeric ionic condensation (Wu et al., 2020; Wang & Roman, 2011).

Among the PEs, chitosan, a natural polymer obtained by partial N-acetylation of chitin, the second most abundant polymer in the world, has aroused great interest because it is considered non-toxic, biocompatible, biodegradable and has good mucoadhesive properties (Xu et al., 2019). Chitosan is composed of glucosamine residues linked by β-1,4 bonds and randomly distributed N-acetyl-D-glucosamine units (Wu et al., 2020). The cationic nature of chitosan allows it to form complexes with a range of polymers and other anionic chemical compounds, such as sodium alginate (Bulatao, Samin, Salazar, & Monserate, 2017), carboxymethylcellulose (Ferreira et al., 2022), nanocrystal of cellulose (Wang, Jung & Zhao, 2017), glutaraldehyde and sodium tripolyphosphate (Paulraj et al., 2017).

Cellulose derivatives are also highlighted in the natural origin PEs' scope, including cellulose nanocrystals (NCC), which are materials obtained through the partial hydrolysis of cellulose fibers, where the amorphous part is removed. The result is a crystalline material with a high aspect ratio (length/diameter), large specific surface area, high mechanical and hydrophilic strength (Akhlaghi, Tiong, Berry, & Tam, 2014). Sulfuric acid is commonly used for the hydrolysis of cellulose fibers, which allows part of the polymer chain to be functionalized with sulfonate groups. This effect gives the NCC an anionic characteristic

dependent on the pH of the medium in which it is inserted (Xie, Du, Yang, & Si, 2018). In this way, NCC is able to interact with cationic polymers such as chitosan and form new structures and materials, acting both as a filler of interpolymer spaces and film reinforcement, as well as a controlled release agent for drugs and other active ingredients through the nanocomplexes formation (Abdull Khalil et al., 2016).

The chitosan-NCC nanocomplexes formation gained prominence with the study carried out by Wang & Roman (2011), showing that the density charge of ionizable groups of each of the polymer directs the complexes' formation. These nanostructures can be used as a controlled release due to acquired characteristics (positive net surface charge and size < 10 μm) when the proportion of chitosan amino groups is 1.33 times greater than the sulfonate groups of NCC. Wang, Jung & Zhao (2017) demonstrated the possibility of encapsulating anthocyanins with 94% encapsulation efficiency in nanocomplexes formed by chitosan and NCC. In addition, the nanocomplexes with NCC were more rigid and stable when compared to the chitosan nanoparticles with sodium tripolyphosphate. Abo-Elseoud et al. (2018) also achieved high encapsulation efficiency of repaglinide in chitosan nanoparticles with both NCC and oxidized NCC (carboxyl groups present on the polymer surface).

Among the studies with chitosan-based nanocomplexes and other natural polymers studies, many authors report low mechanical strength (Jonassen, Kjøniksen, & Hiorth, 2012), formation of porous hydrogels (Joye, Davidov-Pardo, & McClements, 2014) and metastable systems (Furtado et al., 2018; Wang, Jung & Zhao, 2017), which interferes on the stability on the system, encapsulation efficiency of active ingredients and the effectiveness of the materials developed. Although NCCs are an excellent alternative to overcome these problems, much remains to be studied so that the goals of encapsulation of drugs and active ingredients can be predicted and achieve better performance depending on the environment in which they will be inserted.

Several parameters influence the formation of chitosan-based nanocomplexes, many of which have been extensively studied, such as pH, ionic strength, chitosan molecular weight, the proportion between polymers, stirring speed, among others (Jonassen, Kjøniksen, & Hiorth, 2012). However, when referring to the chitosan and NCC complexes, little information is found, since most studies focus on the encapsulation of the active compound and do not prioritize the structure of the complex itself, difficulting to reproduce the methodologies available in the literature. (Sreekumar, Goycoolea, Moerschbacher, & Rivera-Rodriguez, 2018).

An excellent way to assess the simultaneous influence of variables on the process is through optimization experiments with response surface methodologies (Kalam et al., 2016). In this context, the present study aims, for the first time, to optimize the production process of chitosan and NCC nanocomplexes through the Box-Behnken design in order to evaluate the effects of one of the main parameters that influence the formation of the nanocomplexes. Physicochemical and morphological characteristics of the nanocomplexes were evaluated as a function of the monovalent salt, the molar proportion of ionizable groups and the pH to be optimized in terms of yield, particle size and zeta potential. The materials were also analyzed for their calorimetric, structural and crystalline properties.

2. Material and methods

2.1 Material

Chitosan (low molecular weight, Sigma-Aldrich Corporation, USA; Product ID = 448869) from fresh shrimp shells *Pandalus boralis* was bought from Sigma- Aldrich Corporation (USA). Cellulose Nanocrystal (Product ID = NCV100) was bought from CelluForce Corporation (Canada). Other chemicals were of analytical grade and used without any purification process: hydrochloric acid (Neon, Brazil, 37 wt. % in H_2O), NaCl (FMaia, Brazil, 99% purity), sodium hydroxide (Dinâmica, Brazil). Deionized water was obtained from a Milli-Q system (18.2 $M\Omega.cm^{-1}$, 25 ^oC, Millipore, Italy).

2.2 Experimental design

Box-Behnken experimental design was used to study the effects of the molar ratio of chitosan and cellulose nanocrystal ionizable groups (CH:NCC), pH of NCC dispersion (pH), NaCl molar concentration ([NaCl]) and the interaction among these independent variables on Z-average (nm), Zeta-potential (mV), and Yield (%). A design matrix comprising 13 experimental runs was built, and systems resulting from the combination of independent variables were summarized in Table 1. The central point (CP) was represented by the 13 system, and five repetitions were performed to the CP.

Table 1. Coded and uncoded variables of Box-Behnken experimental design used to optimize the formation of CH-NCC nanocomplexes.

Systems	Coded Variables			Uncoded Variables		
	CH:NCC (mol) (X_1)	pH (X_2)	[NaCl] (mM) (X_3)	CH:NCC (mol) (X_1)	pH (X_2)	[NaCl] (mM) (X_3)
1	-1	-1	0	3	2.6	37.5
2	1	-1	0	10	2.6	37.5
3	-1	1	0	3	5	37.5
4	1	1	0	10	5	37.5
5	-1	0	-1	3	3.8	0
6	1	0	-1	10	3.8	0
7	-1	0	1	3	3.8	75
8	1	0	1	10	3.8	75
9	0	-1	-1	6.5	2.6	0
10	0	1	-1	6.5	5	0
11	0	-1	1	6.5	2.6	75
12	0	1	1	6.5	5	75
13*	0	0	0	6.5	3.8	37.5

*Central point (CP) of Box-Behnken experimental design.

2.3 Preliminary procedures

2.3.1 Removal of chitosan impurities

Chitosan was washed in order to eliminate salts residues and water-soluble chitooligosaccharides and impurities. Firstly, chitosan was sequentially washed three times with deionized water and vacuum-filtered (MA039, Marconi, Brazil) using qualitative paper

(Cat No 1004 125, Whatman) to recover the insoluble fraction (Ferreira et al., 2022; Soares et al., 2019). Then, washed chitosan was frozen at −80.0 °C, lyophilized (FreeZone, 2,5 L, LABCONCO), vacuum-packed, and stored inside a desiccator, at 20 °C ± 2 °C.

2.3.2 Viscometric average molar mass of chitosan

Viscometric average molar mass of chitosan (M_v) was estimated by viscometric-average methodology (Soares et al., 2019; Amorim et al., 2016). Firstly, 0.25 g·(100 g)$^{-1}$ chitosan was dispersed in acetic acid-sodium acetate buffer (0.2 mol L^{-1} acetic acid + 0.1 mol L^{-1} sodium acetate; pH = 4.41 and ionic strength = 0.1 mol L^{-1}), and kept under magnetic stirring during 24 h, at 25 °C ± 1 °C (Kasaai 2007). Chitosan dispersion was vacuum-filtered using qualitative paper in order to remove any non-dispersed material. Then, the filtrate was diluted, and other four dispersions were obtained. Flow times of chitosan dispersions were measured in a Cannon-Fenske viscometer (model 513 20, Schott, Germany), 25.0 °C ± 0,1 °C. Then, the average intrinsic viscosity ($[\underline{\eta}]$) was calculated, and the Mv was estimated as 463 ± 25 kDa (for details, see Supplementary Material; Figure SM1).

2.3.3 Degree of deacetylation and density of the amino groups (NH_2) of chitosan

Fourier transform infrared spectroscopy (FTIR) approach was applied to study the deacetylation degree (DD) of chitosan using a spectrophotometer (Nicolet 6700, Thermo Scientific, USA). First, the degree of acetylation (DA) was estimated from the empirical relationship between normalized absorbances of the peaks at wavenumbers 1320 cm^{-1} and 1420 cm^{-1} after deconvolution in Lorentz components using the PeakFit software (v.4.12, SeaSolve Software Inc., 1999-2003) (Brugnerotto et al., 2001; Kasaai, 2008). DD was obtained by simple difference [DD(%) = 100% – DA(%)]. The DD value of the chitosan used in the present study was estimated as 69.10% (for details, see Supplementary Material; Figure SM2). Then, the density of the amino groups of chitosan (CH) was estimated as 3.9681 ± 0.54 mol·kg^{-1}, according to Eq. 1.

$$\frac{nNH_3}{m_{CHI}} = \frac{DD}{DD \times MM_D + (1 - DD) \times MM_A} \quad (1)$$

In Eq. 1, nNH_3 is the number of moles of amino groups in chitosan chains; m_{CHI} is the weight of chitosan; DD is the degree of deacetylation of chitosan, MM_D = 161.1558 g·mol^{-1} is the

molar mass of the deacetylated chitosan unit; and MM_A = 203.1925 g·mol^{-1} is the molar mass of the unit of the acetylated chitosan unit.

2.3.4 Density of the sulfonate groups (-O-SO_3^-) of cellulose nanocrystal

Cellulose nanocrystal (NCC) dispersion (0.55 % wt) was prepared and dialyzed using milli-Q water, during three days with successive water until constant values for pH and conductivity are reached (Beck, Méthot & Bouchard, 2015). Ion-exchange resin (DOWEX™ Monosphere™ 88 H Cation Exchange, DOW Chemical Company, USA) was utilized after the dialysis process in order to promote the total protonation of the sulfonate groups on the NCC surfaces (Beck, Méthot & Bouchard, 2015). Then, the recovered dispersion was diluted (0.15% or 0.15 g NCC.100 mL^{-1}) using 2 mL of NaCl 0.1 M solution and milli-Q water. Then, the density of the sulfonate groups was determined by conductimetric titration using a digital conductivimeter (145A+, Thermo, Orion, USA). Finally, the density of the sulfonate groups of NCC was obtained as 216.87 ± 9.01 mmol (OSO_3^-)·kg^{-1} (for details, see Supplementary Material; Figure SM3).

2.4 Preparation of biopolymer dispersions and nanocomplexes formation

Previously, 0.5 mg·mL^{-1} CH was mixed to with a 0.6343 mol·L^{-1} HCl solution (pH = 3.0), and this material was kept under magnetic stirring at 25 °C, for 24 h. Then, CH dispersion was filtered using a black ribbon quantitative filter followed by a 2nd filtration, using blue ribbon quantitative filter. Amounts of NaCl (Table 1) were added to CH dispersions, and the resulting aqueous media were stirred during for an additional 2 h. Finally, CH dispersions containing NaCl were filtered according to the procedure above-mentioned. Analogously, 1.0 mg·mL^{-1} NCC was added to Milli-Q water, placed into an ice bath, and dispersed using an ultrasound (Unique, desruptor model – 19 KHz) device (420 W), for 10 min. Then, NCC dispersion was filtered using a 0.45 μm syringe filter (Millipore), and adequate NaCl amounts (Table 1) were added to aqueous media. The pH of CH was set at 3.0 and the NCC pH dispersions were adjusted to values from 2.6 to 5.0 (Table 1), using NaOH 1 mol·L^{-1} or HCl 1 mol·L^{-1}.

During the nanocomplexes preparation, adequate amounts of NCC dispersions was added to 5 mL CH dispersions at 0.5 mL·min^{-1} (according to results of the density of chitosan and NCC's amino and sulfonate groups) (Table 1), using a 0.13 mm x 45 mm syringe coupled with a peristaltic pump (TECNOPON, LAP-101-3 model). CH dispersion was kept under magnetic stirring during NCC addition, and the agitation was maintained for 10 min, after the

end of the NCC addition. Systems containing CH and NCC were placed in 50 mL Falcon tubes, and centrifuged at 13,000 x g, at 4 ± 0.5 ºC, for 30 min. Then, the supernatants were removed, and the pellets were added to deionized water, placed into an ice bath, and redispersed using an ultrasound device (420 W), for 6 min. Resulting systems were stored at 7 ± 0.5 ºC ºC until use.

2.5 Yield (%) of nanocomplexes

Firstly, the weight of 50 mL Falcon tubes (empty) were recorded. Then, aliquots of systems were transferred to these tubes, and their weights were recorded again. After centrifugation at 13,000 x g, at 4 ± 0.5 ºC, for 30 min, the supernatants were removed, whereas the nanocomplexes left at the bottom of the tube were weighed with the tube. Thus, the yield (Y, %) obtained from was calculated using Eq. 2 (Wang, Jung, & Zhao, 2017).

$$Y\ (\%) = \frac{W\ -\ W_0}{W_D\ -\ W_0} \times 100 \tag{2}$$

In Eq. 2, W_o is the weight of 50 mL Falcon tubes empty, W_D is the weight of 50 mL Falcon tubes containing the systems, and W is the weight of 50 mL Falcon tubes containing the nanocomplex.

2.6 Z-average, polydispersity index (PDI) and ζ potential

Z-average, PDI, and ζ potential of CH, NCC and nanocomplexes dispersions were evaluated by dynamic light scattering (DLS) (Zetasizer Nano ZS90, Malvern Instruments, UK), at 25.0 ± 0.1 °C. Thus, aliquots of aqueous media were placed in a cuvette in order to obtain the distribution of diameters by means of the amplitude of the decay rate, which is obtained by fitting the normalized temporal intensity correlation functions. This analysis was conducted in three replications. Then, the polydispersity index (PDI) could be calculated. PDI was estimated from the hydrodynamic average diameter (dh) and standard deviation (SD) relationship (PDI = $(SD/d_h)^2$) for each particle distribution.

ζ potential of dispersed particles was estimated from the electrophoretic mobility phenomena. Thus, aliquots of the above-mentioned aqueous media were placed into a folded capillary cell (DTS1070; Malvern Instruments, UK), and analyzed using the Zetasizer Nano ZS90. Then, the cuvette was subjected to a controlled electric field, and ζ potential values could be calculated considering the Smoluchowski model for the double electrical layer.

2.7 Atomic force microscopy (AFM)

Atomic force microscopy was used to study the diameters of CH:NCC nanoparticles and their morphological characteristics. Thus, aliquots of CH:NCC nanoparticles in aqueous media were diluted and spread over a mica surface. Then, after solvent evaporation, CH:NCC nanoparticles were analyzed using an atomic force microscope (NTEGRA Prima, NT-MDT, Russia). Measurements were performed in intermittent contact mode (probe with radius of curvature = 10 nm; 10 N/m force constant; and resonance frequency ~ 280 kHz).

2.8 X-ray diffractometry (XRD)

The XRD patterns of CHS, NCC, and nanocomplexes (CH:NCC = 3:1; 6.5:1; or 10:1) were studied using a X-ray diffractometer (D8 Advance, Bruker, Germany) equipped with Cu-Kα radiation (λ = 0.1542 nm), at 40 kV and 40 mA. The scan data were recorded from angles between 10° and 50°, at a scanning rate of 0.5 degree·s^{-1}. Diffractograms obtained were analyzed and their differences indicated the nanocomplex formation. Moreover, XRD was used to analyze the effects of the CH:NCC ratio in the crystallinity degree and presence of amorphous regions of nanocomplexes. Then, the crystallinity index (CI, %) was calculated as proposed by Segal et al. (1962) (Eq. 3):

$$CI\ (\%) = \frac{I_{002} - I_{am}}{I_{002}} \times 100 \qquad (3)$$

In Eq. 3, CI (%) expresses the relative crystallinity degree, I_{002} is the maximum intensity (arb. u.) of the 002 lattice diffraction, and l_{am} is the intensity of diffraction in the same units at 2θ = 18°.

2.9 Attenuated total reflectance with Fourier-transform infrared spectroscopy (ATR-FTIR)

FT-IR analyses were performed using a spectrophotometer (Nicolet 6700, Thermo Scientific, USA) in order to study molecular interactions between CH and NCC in nanocomplexes. A range of 4000 cm^{-1} to 400 cm^{-1} scans was accumulated for each spectrum at a spectral resolution of 4 cm^{-1} and 32 scans. Thus, pellets obtained after centrifugation were previously freeze-dried, and the analyses were carried out directly on the nanocomplexes.

2.10 Thermal gravimetric analysis (TGA)

Thermal behavior analysis of CH, NCC, and nanocomplexes (CH:NCC = 3:1; 6.5:1; or 10:1) was performed using a thermal gravimetric analyzer (Shimadzu, 60H, Japan). 3-5 mg freeze-dried samples were weighed in the TGA microbalance, and heated at 20 °C/min from 25 to 700 °C. Nitrogen gas was used as a heating medium with a 20 $mL \cdot min^{-1}$ flow rate.

2.11 Macroscopic and microscopic thermal stability

The stability of systems (CH:NCC = 3:1; 6.5:1; or 10:1) stored at 7 ± 0.5 ºC or 25 ± 0.5 ºC was monitored during 30 days (Morris et al., 2011). Thus, preliminarily, changes in the visual aspect of systems and Tyndall scattering effects were observed. Then, Zeta-potential, Z-average and PDI of nanocomplexes were also studied.

2.12 Data analysis

Minitab software version 17.0 (Minitab Software Systems, State College, PA) was used to proceed with the statistical analysis. The Response surface methodology (RMS) was applied to experimental data in order to optimize the formation of the nanocomplexes, and to observe the effect and/or correlation for independent variables (CH:NCC, pH, and/or [NaCl]) on dependent responses (Z-average, Zeta-potential, and/or Yield). Thus, the nonlinear quadratic model was fitted according to Eq. 4.

$$Y = b_0 + b_1X_1 + b_2X_2 + b_3X_3 + b_{12}X_1X_2 + b_{13}X_1X_3 + b_{23}X_2X_3 + b_{11}{X_1}^2 + b_{22}{X_2}^2 + b_{33}{X_3}^2 \qquad (4)$$

In Eq. 4, Y is the measured response associated with each factor level combination; b_0 is an intercept, and b_1 to b_{33} are regression coefficients computed from the observed experimental values of Y; X_1 (molar ratio between ionizable groups of chitosan and NCC or CH:NCC), X_2 (pH of NCC dispersion or pH_{NCC}) and X_3 (NaCl molar concentration or [NaCl]) are the coded levels of independent variables. X_1X_2, X_1X_3 and X_2X_3 represent the interaction terms, while X_1^2, X_2^2 and X_3^2 represent the quadratic terms.

Regression models were used to study the interactions between temperature and storage-time obtained from a factorial experiment on Zeta-potential, Z-average and PDI dependent variables.

Macroscopic visual aspect and Tyndall Effects were analyzed and textually described. Data from AFM, XRD, ATR-FTIR and TGA of nanocomplexes were compared with CH and NCC, and results presented in qualitative terms.

3. Results and discussion

3.1. Optimization

In order to find conditions that optimize the nanocomplexes formation, minimizing the Z-average value and maximizing the Zeta-potential or Yield values, a Box-Behnken design involving CH:NCC, pH_{NCC} and [NaCl] independent variables was performed. Results for Z-average, PDI, Zeta-potential and Yield evaluated from the experimental design are shown in Table 2.

Table 2. Z-average, Zeta-potential and Yield values for systems of the Box-Behnken experimental design.

System	CH:NCC	pH_{NCC}	[NaCl] (mM)	Z-average (nm)	PDI	Zeta-potential (mV)	Yield (%)
1	3	2.6	37.5	151.23	0.27	47.60	5.07
2	10	2.6	37.5	156.23	0.26	49.47	5.83
3	3	5	37.5	178.40	0.28	45.87	5.71
4	10	5	37.5	175.20	0.28	47.97	6.30
5	3	3.8	0	164.70	0.26	46.83	7.01
6	10	3.8	0	189.97	0.3	44.57	6.66
7	3	3.8	75	193.87	0.27	45.73	4.69
8	10	3,8	75	165.47	0.27	51.30	2.59
9	6.5	2.6	0	157.80	0.3	45.13	2.80
10	6.5	5	0	195.33	0.29	47.90	8.05
11	6.5	2.6	75	163.03	0.26	48.17	6.14
12	6.5	5	75	191.00	0.26	47.93	3.33
13*	6.5	3.8	37.5	158.04	0.27	49.29	5.87

*Mean value of the Central point (CP), corresponding to five repetitions.

In Table 2, it can be observed that in all systems, the Z-average, zeta potential and PDI exhibited adequate values, since it becomes more suitable to obtain nanocomplexes with smaller diameters (< 200 nm), values in zeta potential modulus > 30 mV and PDI ≤ 0.3. The ranges noted in the optimization study (151.23 – 195.33 nm for diameter, 44.57 – 51.30 for zeta potential and 0.25 – 0.3 for PDI) are ideal for applications in both the food and pharmaceutical (Delan et al., 2020; De Pinho Neves et al., 2014), since reduced particle diameters contribute to the improvement of adhesion and penetration of nanostructures in cell membranes. As for the zeta potential, the nanocomplexes formed in all systems (Table 2) exhibited a positive value, indicating the prevalence of chitosan structures on the surface of the formed nanocomplexes. For zeta potential analysis, it is assumed that nanoparticles and nanocomplexes with a net surface charge > 30 mV (in module) are less unstable, and this value is sufficient to prevent particle aggregation (De Pinho Neves et al., 2014). Finally, when considering the PDI, values below 0.3 indicate a high homogeneity of dispersed particle diameters.

In order to study the effects of independent variables (CH:NCC, pH_{NCC} and [NaCl]) on dependent responses (Z-average, Zeta-potential and Yield), coefficients of regression models were estimated, and the results are displayed in Table 3. In addition, contours plots are illustrated in Figure 1. The responses were individually fitted to the models using linear regression (simple and multiple), and the coefficient of determination (R2) was estimated. ANOVA was conducted to identify the significant terms of the chosen model in the responses. Model terms with a p-value <0.05 were considered statistically significant. Considering that the R2 values of the models presented are high, and to keep the results more realistic, the non-significant terms were kept in the models.

The Quadratic model was adjusted for Z-average and Zeta-potential data, while the 2FI model to Yield. The mentioned models were significant ($p < 0.05$), presenting R^2 values > 0.7 and were not significant for the lack of fit. The Quadratic model fitted to Z-average and Zeta-potential data showed a positive effect for CH:NCC, pH_{Ncc} and [NaCl]. For Z-average, the Quadratic model presented a negative effect for the interactions between CH:NCC*pH_{Ncc}, CH:NCC*[NaCl] and pH_{Ncc}*[NaCl], and only the interaction CH:NCC*[NaCl] was significant ($p<0.05$).

Table 3. Descriptive statistics, regression models for Z-average, Zeta-potential or Yield (%), and fitting indicators of models.

Variable	Mean	Std. Dev.	Model	F-value	p-value	Regression model	R^2	Lack of Fit
Z-average	168.97	4.53	Quad-ratic	19.4	0.0004	Z-average = 127.98258 + 0.898367 X_1 + 0.031948 X_2 + 2.23743 X_3 - 0.102222 X_1*X_2 - 0.488095 X_1*X_3 - 0.053130 X_2*X_3 + 0.364796 X_1^2 + 0.011373 X_2^2 + 1.91522 X_3^2	0.9615	0.5768*
Zeta potential	47.94	0.98	Quad-ratic	5.52	0.0174	Zeta-potential = 37.13685 + 0.568719 X_1 + 0.065216 X_2 + 4.12106 X_3 + 0.014921 X_1*X_2 + 0.013889 X_1*X_3 – 0.016667 X_2*X_3 – 0.070884 X_1^2 – 0.000932 X_2^2 – 0.481481 X_3^2	0.8765	0.1047*
Yield (%)	5.45	1.00	2FI	4.35	0.0300	Yield = - 2.16588 + 0.123033 X_1 + 0.166021 X_2 + 2.11485 X_3 - 0.003328 X_1*X_2 -0.009953 X_1*X_3 - 0.044809 X_2*X_3	0.7655	0.4117*

*not significant;

**X_1 = CH:NCC, X_2 = pH_{NCC}, and X_3 = [NaCl].

On another hand, for Zeta-potential, a positive effect was observed in the interactions between CH:NCC*pH_{Ncc} and CH:NCC*[NaCl], while a negative effect on the pH_{Ncc}*[NaCl] interaction occurred. This negative effect was expected, since in polyelectrolytes, such as CH and NCC, changes in pH values shift the ionization degree of their respective functional groups, causing coulombic interactions to intensify. However, a concomitant increase in the ionic strength of the medium is capable of reversing this behavior, since depending on the concentration of ions, they can promote the attenuation of the charges of the polyelectrolytes (Wang, Qian, & Roman, 2011). Moreover, all quadratic terms presented a positive effect in the model adjusted for Z-average data, and a negative effect for Zeta-average data. The 2FI model fitted to Yield data showed a positive effect for CH:NCC, pH_{Nc} and [NaCl], while a negative

effect was observed for the interactions between CH:NCC*pH_{Nc}, CH:NCC*[NaCl] and pH_{Nc}*[NaCl].

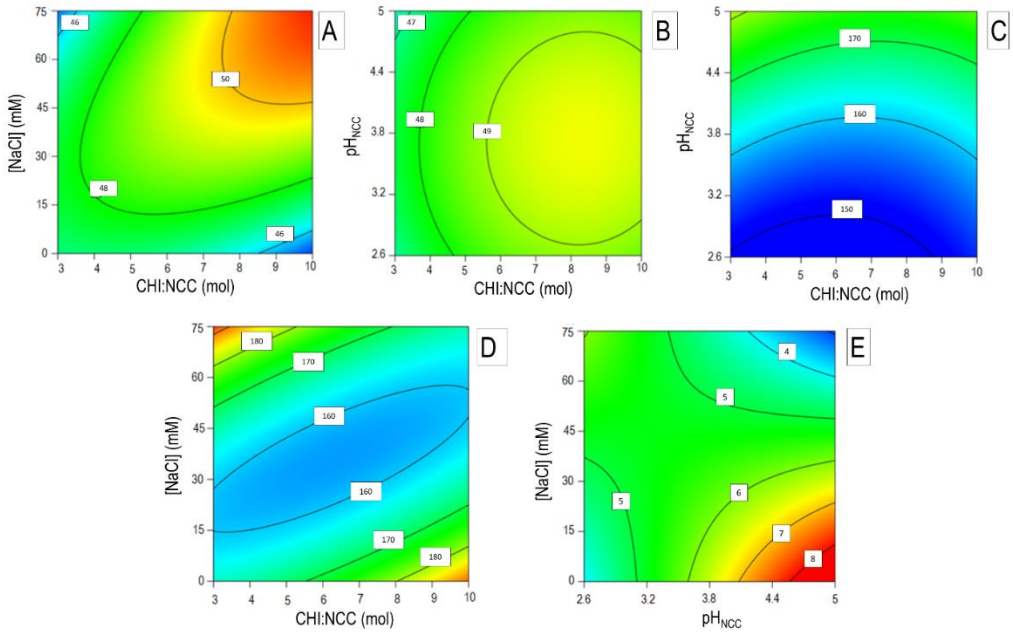

Figure 1. Contour graphics for Zeta-potential (A and B), Z-average (C and D), and Yield (E)

A significant interaction ($p < 0.05$) between CH:NCC and [NaCl] was observed for Zeta-potential. Figure 1-A displayed an increase in Zeta-potential values at conditions with higher CH:NCC and higher [NaCl], which shows the small effect of NaCl addition on the nanocomplexes superficial charge density. The study corroborated with Prathapan, Thapa, Garnier, & Tabor (2016) who observed when they found that Na^+ and Cl^- ions do not significantly affect the cellulose nanocrystals' zeta potential under acidic or basic condictions. Moreover, the authors affirmed that ions with hydrophobic characteristics, belonging to the Hofmeister series, reduced even more the zeta potential of these colloidal particles. On the other hand, the interaction between pH_{NCC} and CH:NCC was not significant ($p > 0.05$) within the studied ranges. Figure 1-B displayed Zeta-potential values, wich were not changed by the increase in these variables. Despite the highlighted observations, regardless of the values adopted for the variables under study, the zeta potential remained positive and above +40 mV, indicating the high stability of nanocomplexes in dispersion. Therefore, to optimize this response variable under the conditions studied, lower proportions of CHI:NCC could also be adopted for the production of nanocomplexes in the absence of NaCl.

Analyzing the interaction between CH:NCC and pHNcc (Figure 1-C), it was observed that regardless of the proportion adopted within the studied range, the Z-average values were

not significantly altered in pHNcc values from 2.6 to 5.0. As well as the observed values for zeta potential, the Z-average values are suitable for the production of nanostructures, with values below 200 nm. The interaction between CH:NCC and [NaCl] was significant ($p < 0.05$), and lower Z-average values were observed under two conditions in Figure 1-D: i) higher [NaCl] concentrations and higher CH:NCC ratio; or ii) lower [NaCl] concentrations and lower CH:NCC ratios. Such observation demonstrated that to reach diameters of up to 160 nm there is a relation between the NaCl maximum concentration and the pHNcc values to be used when CHI:NCC 7:1 proportions are adopted. From this limit, the minimum and maximum NaCl concentrations increase. One explanation can be the fact that the ionization degree of NCC and CH are different at the same pH value. For example at pH 3.8, chitosan has a higher ionization degree and a more extended conformation than NCC. Thus, the presence of an electrolyte will partially reduce the excess charge and allow the chitosan molecules to assume a less "extended" conformation, resulting in a partial folding in the particles formed (Wang, Qian, & Roman 2011).

Regarding the Yield (%), it was observed in Figure 1-E that the maximum yield was obtained at higher pH values and lower [NaCl], and the interaction between these factors was significant ($p < 0.05$). The nanocomplexes yield ranged from 8 to 9% when NaCl concentrations were up to 10 mM and the pHNcc between 4.5 and 5.0 allow. Considering that nanocomplexes are studied and formulated to be applied in the food, pharmaceutical and cosmetic industries, among the answers of this study, the high yield would be essential for the scaling of a process. Thus, we chose the best formulations based on this response variable. Furthermore, as mentioned, Z-average, zeta potential and PDI values found in this study were satisfactory, regardless of the levels of the factors studied. Following this line of reasoning, it was decided to conduct the characterization and stability analyzes of the nanocomplexes at pHNcc = 5.0, without NaCl addition. As for the proportions, it was decided to evaluate the molar ratio of 3:1, 6.5:1 and 10:1, in relation to the Z-average, for values of pH = 5.0, they presented a practically constant value, regardless of the proportion used. In this way, it is possible to evaluate and compare nanostructures in terms of other properties, such as crystallinity, intermolecular interactions, thermal properties and stability, and then define and direct their application.

3.2. Atomic Force Microscopy (AFM)

The morphology of the nanocomplexes was analyzed by atomic force microscopy. The preparation of suspensions for this analysis requires drying on glass slides. Due to water surface tension, the particles present in the suspension were directed to the edges of the glass slides, agglomerating and forming distorted images, which difficult the material identification. Through the Figure (5-A), it can be observed the cellulose nanocrystal structure, with a needle-like shape and an average height of 2 nm. Figures 4-B, 4-C and 4-D refer to nanocomplexes with molar ratio QUI:NCC 10:1, being those in which it was possible to analyze the structure formed. Note that the nanocomplexes have an oval structure, with sizes between 20 and 30 nanometers.

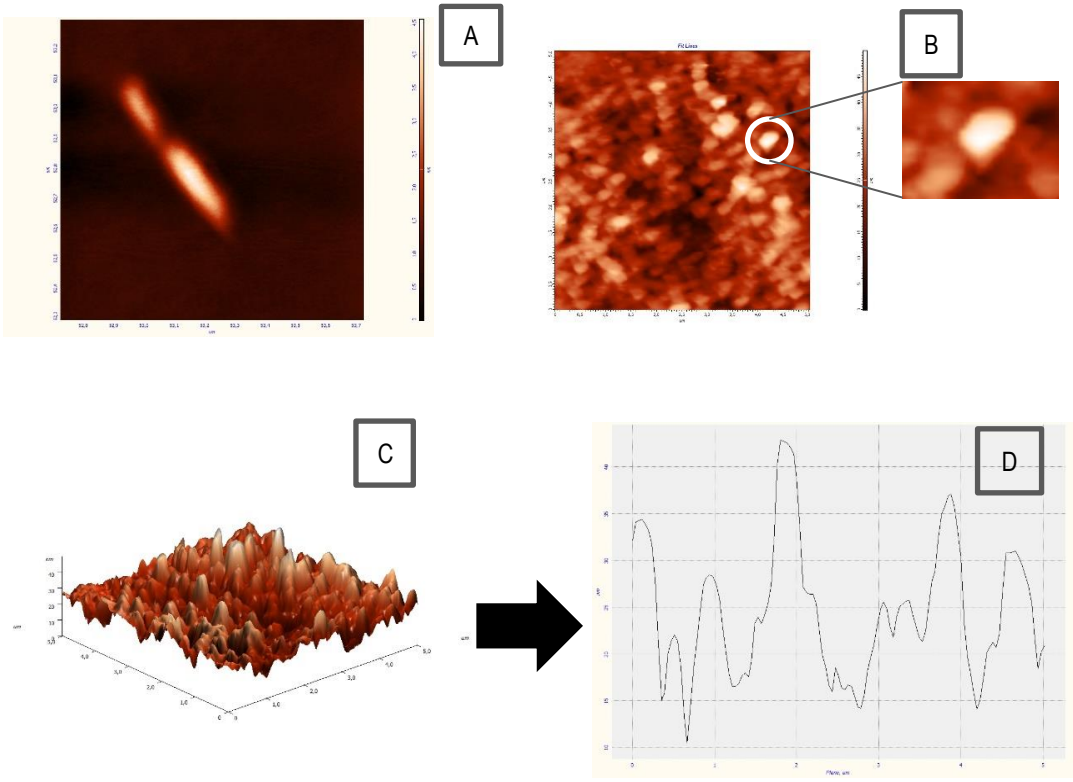

Figure 5. Atomic force microscopy (AFM) images of cellulose nanocrystal (A) and CH:NCC 10:1 nanocomplex (B, C and D).

Comparing the mean diameters of NCC and nanocomplexes obtained by AFM and DLS techniques, a huge difference can be noted. The greater mean diameter estimated by DLS may be caused by the measurement principle, that is based on the movement and dragging of particles in dispersion, taking into account the electrical double layer, which contributes to the increase in the calculated particle diameter. The same divergence was observed by

Mukhopadhyay et al., (2013) when studying the incorporation of insulin in chitosan nanoparticles cross-linked with tripolyphosphate. The authors found particle sizes between 80 and 120 nm by AFM and between 200 and 550 nm by DLS.

3.3. X-ray diffractometry (XRD)

Figure 6 illustrates the diffractograms of the nanocomplexes and their individual components. The respective crystallinity indices were calculated from the diffractograms presented.

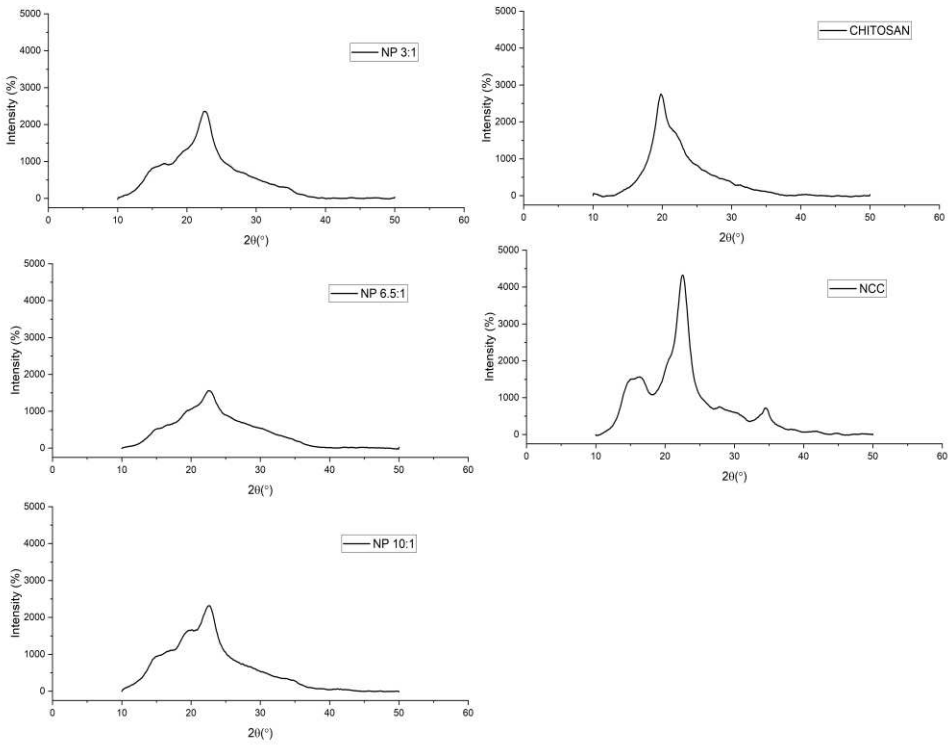

Figure 6. X-ray diffractograms of nanocomplexes at different molar ratio of ionizable groups (CHI:NCC), CH and NCC.

CH exhibited two characteristic peaks, one at 2θ = 19.85º and the other at 2θ = 21.75º, which corresponds to (020) and (120) planes, respectively, in agreement with results found by other researchers (Ferreira et al., 2022; Wildan & Lubis, 2021; Anand, Sathyapriya, Maruthupandy, & Beevi, 2018). The crystallinity degree of chitosan was 47.89%, which represents a semi-crystalline material, resulting from partial organization structure provided by strong inter and intramolecular interactions, mainly of the hydrogen bond type, established

between the amine, alcohol and amide groups of chitosan (Zhang et al., 2019). In addition, it is known that chitosan properties, such as molecular weight, degree of deacetylation and amino groups density, also have a strong influence on the physicochemical and structural properties of the molecule (Jampafuang, Tongta, & Waiprib, 2019).

As for the nanocrystal, it was characterized mainly due to its well-known cellulose I crystal structure with 2θ peaks centered at 15.05º, 16.35º and 22.5°, attributed to the -110, 110 and 200 planes (Celebi, & Kurt, 2015). Another lower intensity peak at 2θ = 34.5° was also identified. This peak can be attributed to in-plane diffraction (0 0 4) (Abo-Elseoud et al., 2018). The crystallinity index of the NCC was 79.33%, being close to the value specified by the manufacturer (Ic= 88%).

In relation to the nanocomplexes, they presented more diffuse and wider peaks, with less evidence of 2θ = 15º and 2θ = 16º peaks and disappearance of 2θ = 34.5º and 2θ = 21.75º peaks, referring to NCC and chitosan, respectively. It shows the polymeric chains rearrangement in the nanocomplexes formation and consequent change in the crystal structure. The results found in the XRD analyzes corroborate those of AFM, which show the new structures formed. Another evidence of nanocomplexes formation was the reduction in peak intensity 2θ = 19.8º as the moles' number of chitosans' NH_3^+ groups decreased in relation to those of NCC. It is also important to note that at the CHI:NCC = 3:1 ratio this reduction is even more pronounced. This can be explained by the number of chitosan and NCC interaction sites being closer. Therefore, much of the chitosan present in the medium is directed to interactions with the NCC, which changes the arrangement of crystals present in the nanocomplexes. This fact can still be supported by the crystallinity values found in the nanocomplexes, being 68.6%, 51.84% and 37.3% for QUI:NCC = 10:1, 6.5:1 and 3:1, respectively, where the increase in the crystallinity of the nanocomplexes also implies in the greater organization of the formed supramolecular structure.

3.4. Fourier Transform Infrared Spectroscopy (FT-IR)

The chemical structure of the nanocomplexes was analyzed by infrared spectroscopy, and their spectra can be seen in Figure 5. The spectra of chitosan and cellulose nanocrystals were similar due to the similarity of chemical groups present in the molecular structures of chitosan and cellulose.

The chitosan spectrum presented a broad band between 3050 - 3600 cm^{-1} due to N-H and O-H stretching vibrations and alcohols associated by hydrogen bonds, a band at 2867 cm^{-1}

due to the axial deformation of C-H, a peak at 1648 cm^{-1} referring to the angular deformation and C=O stretching of amide II, related to the acetylated groups peak from quitin, at 1589 cm^{-1} related to N-H bending vibration, peak at 1060 cm^{-1} referring to C-N stretching vibrations, and peak between 890 cm^{-1} and 1149 cm^{-1} due to N-H angular movement of primary, secondary amines and amides and ether bond, respectively (Barbosa, 2007).

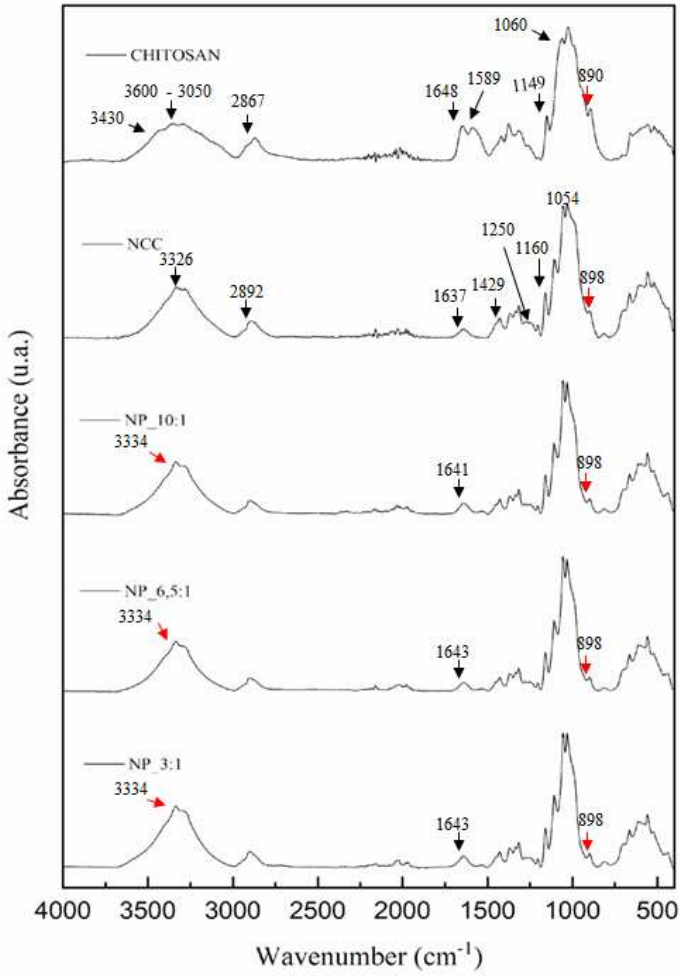

Figura 7. FT-IR spectrums of CH, NCC, and CH:NCC nanocomplexes at different molar ratio.

As for the NCC, it presented a band between 3580 and 3100 cm^{-1}, also related to the vibration of the bonds of the –OH groups envolved at hydrogen bonds. The bands at 2892 cm^{-1} and between 1500 and 1250 cm^{-1} are related to stretching and bending vibrations of CH and CH2, respectively. These bands are characteristic of cellulosic materials and the values are in agreement with those found by Abo-Elseoud et al. (2018) and Wang & Roman (2011). The peaks at 1429 cm^{-1}, 1160 cm^{-1} and 1054 cm^{-1} refer to CH_2 angular deformation, glycosidic bonds, and primary hydroxyl and C-O secondaries groups, respectively (Abo-Elseoud et al., 2018).

The nanocomplexes presented spectra very similar to NCC, without any characteristic peak of chitosan, which indicates the predominant presence of NCC in the formed structures. However, subtle changes in intensity with respect to chitosan and NCC such as the peak at 896 cm^{-1} related to N-H angular movement of primary, secondary amines and amides, and the shift from the 1648 cm^{-1} peak referring to amide II angular deformation of chitosan, which varied between 4 and 6 cm^{-1} between the nanocomplexes, were noticed when NCC was added. This indicates that even the NCC being in greater quantity, interactions between it and the chitosan were established and prioritized, mainly those of the hydrogen bond type, a fact that can be supported by the disappearance of the band at 3430 cm^{-1} referring to the N-H stretching vibration associated with chitosan, and displacement and increase in peak intensity 3334 cm^{-1} of the nanocomplexes when compared to the NCC at 3326 cm^{-1} (De Pinho Neves et al., 2014; Abo-Elseoud et al., 2018). Abo-Elseoud et al. (2020) also obtained spectra with the same characteristics when encapsulating ketoprofen in chitosan/cellulose nanocrystal nanoparticles cross-linked with sodium tripolyphosphate. No interfering peaks were in the nanocomplexes' spectrum, however, subtle shifts were observed in the peak 1648 cm^{-1}, referring to the angular deformation of chitosan amide II. The authors attributed this mainly to the hydrogen bonds formed between the active compound and the other components that form the nanoparticles.

3.5. Thermal gravimetric analysis (TGA)

Thermogravimetric analysis was carried out on the chitosan samples, NCC and on the nanocomplexes formed (CHI:NCC 3:1, CHI:NCC 6.5:1 and CHI:NCC 10:1). The TGA and DTG curves can be seen in figure (8).

In table 4 it is possible to observe the temperatures referring to each thermal event of the studied systems and the percentage of mass loss associated with them (for details, see Supplementary Material; Figures SM4 and SM5). Chitosan was degraded in three stages In the first event, the percentage of mass loss in this region was 9.33%, attributed to the evaporation of water adsorbed inside the polymer (López, Mercê, Alguacil, & López-Delgado, 2008). The second event, observed between 254 and 345 ºC, is considered the most important by López, Mercê, Alguacil, & López-Delgado (2008), as it is associated with the depolymerization of chitosan, including deacetylation and cleavage of glycosidic bonds by dehydration and deamination, with an onset pointed to the breakage of the C-O-C bond (López, Mercê, Alguacil, & López-Delgado, 2008; Xu et al., 2018). The third event, between 360 and 420 ºC, corresponds to the degradation of the cross-linked chitosan residues and corresponds to 23.7%

of mass loss. It is also possible to identify through the DTG curves the maximum thermal decomposition rate of 0.0058 mg/ºC. At the end of the process, it is noticed the existence of mass, indicating the presence of non-volatile components in chitosan (Ferreira et al., 2022). Similar behavior can be observed for the NCC and the formed nanocomplexes.

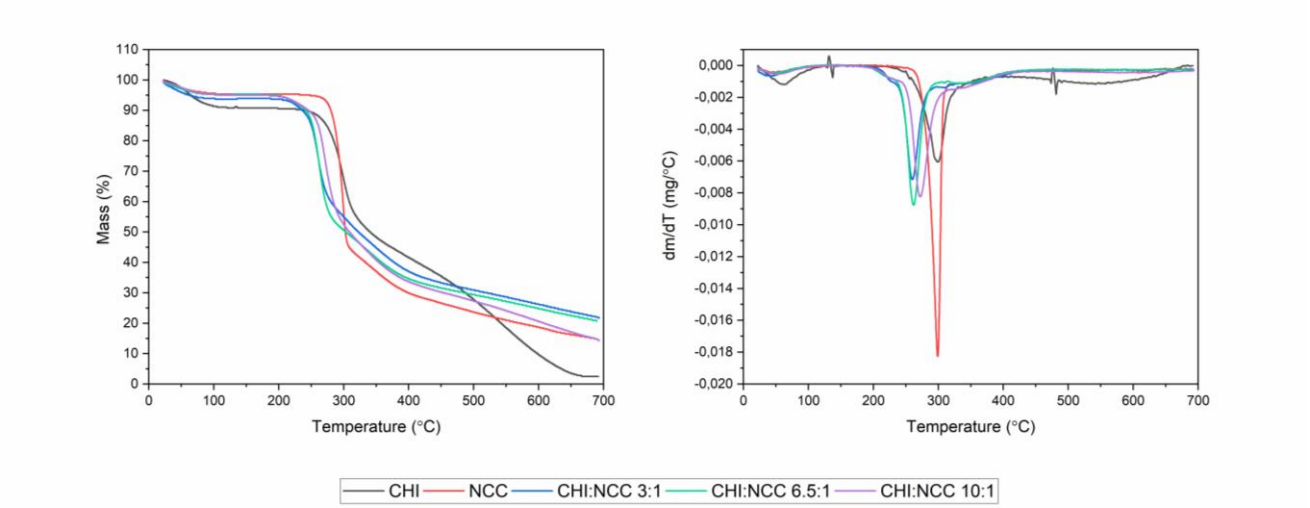

Figure 8. TGA and DTG thermograms of CH, NCC, and nanocomplexes at different molar ratio of ionizable groups (CHI:NCC).

For the NCC, the first event occurred between 32 and 108 ºC, corresponding to a mass loss of 3.65% due to evaporation of the adsorbed and bound water in the cellulosic structure and/or adsorbed low molecular weight compounds (Henrique et al., 2015). The peak between 273 and 318 ºC is attributed to several NCC degradation processes, such as depolymerization, dehydration and decomposition of the glycosidic units (Roman & Winter, 2004), presenting a high rate of degradation (0.0177 mg/ºC) and mass loss of 48.7%. The third degradation event, which occurred between 318 and 423.8 ºC, is mainly attributed to the oxidation and breakdown of charged fragments with the formation of low molecular weight gaseous products (Roman & Winter, 2004).

The thermograms of the nanocomplexes exhibited degradation peaks in similar regions, totaling three thermal events. The first one, with a minimum temperature between 41 ºC and 51 ºC and a percentage of mass loss between 4 and 6% is attributed to the loss of physically adsorbed water and that strongly bound through hydrogen bonds in pure polymers and nanocomplexes (Delan et al., 2020; Celebi & Kurti, 2015). The second event, with a minimum temperature of 262.6 ºC, 269 ºC and 272 ºC for CHI:NCC 3:1, CHI:NCC 6.5:1 and CHI:NCC 10:1, respectively, corresponds to mass loss due to polymeric chains degradation of CHI, NCC

and nanocomplexes, and decomposition of the pyranose structure due to dehydration, with the consequent opening of the rings (Bonardd et al., 2018).

Table 4. Thermal decomposition temperatures and mass loss (%) of chitosan, NCC and nanocomplexes.

SYSTEM		T_I*	$T_{inflection\ point}$	T_F**	Weight loss (%)	Total weight loss (%)
CHITOSAN	1	25	63	116	9.33	74.75
	2	254	304.6	345	41.68	
	3	441.4	561	686.8	23.74	
NCC	1	32	45.7	108.2	3.65	69.48
	2	273.9	305.09	318.3	48.68	
	3	318.3	364.7	423.78	17.15	
CHI:NCC 3:1	1	25	41.7	104.9	5.63	64.97
	2	230.3	262.6	290.8	33.34	
	3	332.8	367	433.5	26	
CHI:NCC 6.5:1	1	30	51.9	105	3.94	65.5
	2	235	269	299	40.45	
	3	322.7	355.5	436	21.11	
CHI:NCC 10:1	1	25	50.6	106.6	4.32	65.39
	2	248.5	272.2	298.3	39.63	
	3	320	352.7	415	21.44	

*Initial Temperature; **Final Temperature

A reduction in the thermal stability of the nanocomplexes was also observed with an increase in the content of sulfonate groups ($-OSO_3^-$) when compared to pure polymers. This fact can be explained by the greater sensitivity of these groups to heating, which facilitates the thermal degradation of the nanocomplexes (Patel, Dutta, Ganguly, & Lim, 2021). In addition, with the reduction in the amount of NCC moles in the system, fewer electrostatic interactions and hydrogen bonds are established with chitosan, which requires lower temperature and,

consequently, less energy to degrade the structures formed (Ferreira et al., 2022; Bonardd et al., 2018). The third event, with minimum temperatures at 367 ºC, 355.5 ºC and 352.7 ºC for CHI:NCC 3:1, CHI:NCC 6.5:1 and CHI:NCC 10:1, respectively, equivalent to a percentage of mass loss equivalent to 26%, 21.11% and 21.44%, which is related to the carbonization of residues of polymeric materials and the oxidation and volatilization reactions of low molecular weight compounds (Patel, Dutta, Ganguly, & Lim, 2021; Bonardd et al., 2018).

Despite the nanocomplexes degradation temperature being lower in relation to CHI and NCC, based on the total mass losses of CHI, NCC and nanocomplexes, the thermal stability is enough to support the processes in the food area. Furthermore, the thermal stability of these nanocomplexes is targeted, since they can be used to protect thermosensitive compounds, which in pure form they are not capable of.

3.6. Macroscopic and microscopic thermal stability

Visual aspect and Tyndall scattering effects of systems (CH:NCC = 3:1; 6.5:1; and 10:1) stored at 25 ºC and 7 ºC were recorded in order to observe changes in their macroscopic stability during 30 days, and results are presented in Figure 2.

All developed nanocomplexes were presented as colloidal dispersions, that is, systems without formation of aggregates or sedimented particles, a fact that is supported by the polymers concentrations (0.5 $mg.mL^{-1}$ for CHI and 1 $mg.mL^{-1}$ for NCC) and proportions used. Opalescent colloidal systems with fine particles in suspension are mostly formed by diluted polyelectrolyte dispersions in non-stoichiometric proportions, characterizing the polyelectrolytic complexes (Rathee, Sidky, Sikora, & Whitmer, 2018). The opalescence of the dispersions increased as the CHI:NCC decreased. This can be explained by the ratio in mol of functional groups (NH_3^+ for CHI and $0S0_3^-$ for NCC) of the polyelectrolytes approaching 1, intensifying inter and intramolecular interactions, resulting in greater formation of nanocomplexes (Wang & Roman, 2011).

The Tyndall effect is the phenomenon in which particles in a colloid scatter the light beams that are directed at them. Regarding the formation of complexes, when the polyelectrolytes involved present ionic groups of opposite charge in a non-stoichiometric mixing ratio and under dilute conditions, the complexes formed are able to scatter visible light, characterizing the Tyndall effect (Ferreira et al., 2022). In this case, the intensity of the scattered light depends on the density of the colloidal particles as well as the frequency of the incident light.

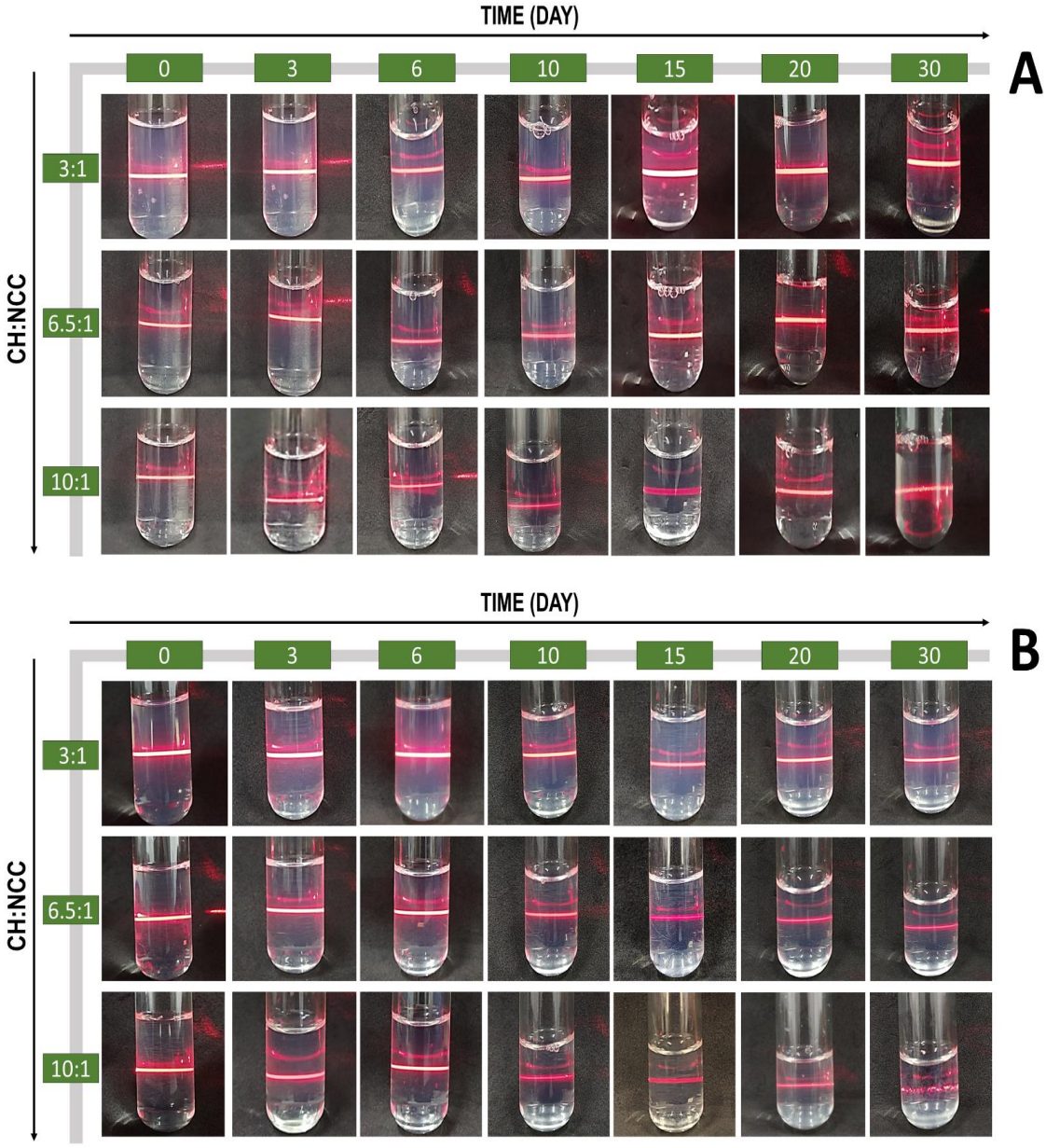

Figure 2. Visual aspect and Tyndall effect of systems containing CH:NCC nanocomplexes at different molar ratio stored during 30 days at 7 °C (A) and 25 °C (B).

In figures 2 and 3 we can verify this effect in the produced nanocomplexes. For the temperature of 25ºC, greater instability was observed in the proportions 10:1 and 6.5:1, and on the 30th day, the formation of evident flakes was observed in the CHI:NCC 10:1 nanocomplex, preventing the laser from passing in a similar way to be continued. The same can be noticed in the 6.5:1 and 10:1 dispersions when stored at 7ºC, and the higher proportion, as well as at 25ºC, promoted greater laser refraction.

In order to verify the behavior of the studied variables, interaction plots were obtained for each one. The analysis of the factorial experiment showed that the interaction effects of time and temperature, and CHI:NCC and temperature were significant ($p<0.05$) for all variables studied. Figure 4 shows the interaction graphs of the adjusted mean values of size, zeta potential and PDI as a function of CHI:NCC (Figures A, C and E) and time (Figures B, D and F) at 7ºC and 25ºC, making it possible to evaluate the apparent interaction effects and the behavior of z-average, zeta potential and PDI as a function of the aforementioned variables.

When evaluating the size of the nanocomplexes, it is noted that among the proportions studied, CHI:NCC = 10:1 proved to be more unstable. The nanocomplexes produced in this proportion presented larger initial sizes when compared to those referring to CHI:NCC = 3:1 and CHI:NCC = 6.5:1, in addition to increasing over the storage time, as shown in figures 2 and 3. One of the main factors governing the formation and stability of PECs formed by weak polyelectrolytes is pH. The formulated systems were produced at pH_{Ncc} = 5 and redispersed in Milli-Q water. In the absence of salts, the formation of PECs is rapid and may contribute to a thermodynamically more unstable system due to the low osmotic pressure of the diluent (Wang, Qian & Roman, 2011). Then, water molecules can penetrate the nanocomplexes by osmosis and be able to cause swelling, a fact that may have led to an increase in size during the storage period (Tsai, Chen, Bai & Chen, 2011). In addition, the inherent motion of the dispersed particles, known as Brownian motion, may have intensified at moments of the storage period caused by small temperature variations. Thus, an increase in the collision between the nanocomplexes may have occurred and facilitated the adhesion of the particles, forming small flakes and/or aggregates at the end of storage (Tsai, Chen, Bai & Chen, 2011).

The PDI and zeta potential results complement the z-average, showing that after 15 days of storage at 25ºC, the CHI:NCC = 10:1 system becomes more heterogeneous, with PDI values > 0.3 and lower zeta potential values, mainly from the 20th day, reaching 26 mV. Reductions in zeta potential values and increased heterogeneity of the system during the storage period can be attributed to changes in pH values due to changes in the chemical balance of dispersions in the absence of salts (Jonassem, Kjøniksen, & Hiorth, 2012). Taking into account the data presented, in order of stability, we can list the formulations as follows: 3:1 > 6.5:1 > 10:1, with the QUI:NCC = 3:1 showing no sedimentation at the end of the 30 days of storage.

Figure 4. Interaction effects plots from the interaction between different independent variables for dependent variables: molar ratio and temperature for Z-average (A); molar ratio and time for Z-average (B); molar ratio and temperature for Zeta-potential (C); molar ratio and time for Zeta-potential (D), molar ratio and temperature for PDI (E); and molar ratio and time for PDI (F).

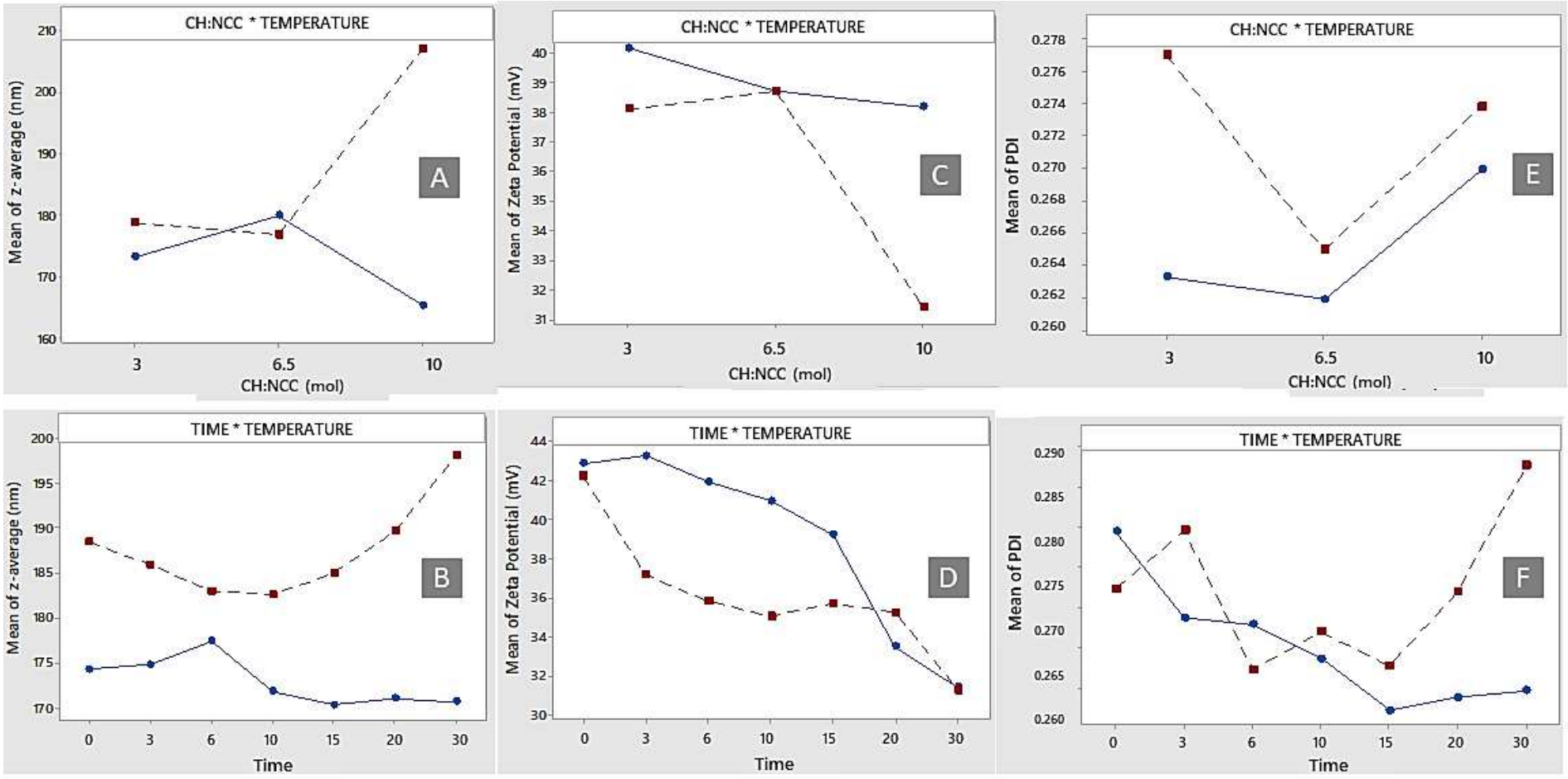

4. Conclusion

The optimization of the preparation of CH:NCC nanocomplexes was achieved, obtaining small particles with diameter ranging Z-average from 151.23 to 195.33 nm, low polydispersity (PDI values between 0.25 and 0.3), high values of Zeta potential (+44.57 to +51.30 mV) and high values for yield, reaching values next to 8%. Such results are quite innovative and demonstrate the successful use of electrolytic complexation in the synthesis of CH:NCC nanocomplexes, being this method considered simple, economically viable, ecofriendly and reproducible. Significant variables, as well as significant interactions between these variables, were observed from models adjusted to Z-average, Zeta potential and Yield, and nanocomplexes prepared at pH = 5.0, absence of NaCl and molar ratio CHI:NCC = 3:1, 6.5:1 and 10:1 were evaluated in terms of intermolecular interactions, morphological characteristics and thermal stability.

CH:NCC nanocomplexes prepared at pH 5.0, absence of NaCl and molar ratio = 3:1, 6.5:1 or 10:1 presented heights between 20 and 30 nm, and oval shape. In addition, nanocomplexes prepared in the above-mentioned conditions showed a different crystallinity from that common to chitosan or NCC polymer chains, their biopolymer precursors, indicating an interaction at the molecular level between their chains. The thermogravimetric analysis indicated that the existence of such intermolecular interactions between chitosan and NCC caused a lower stability of the nanocomplexes compared to the individual polymers; however, CH:NCC particles showed a lower total mass loss, presenting greater thermal resistance. Finally, the absence of macroscopic and microscopic changes indicated the thermal stability for CH:NCC = 3:1 nanocomplex stored during 30 days, at 7ºC e 25ºC, while a macroscopic destabilization was observed for the aqueous media containing nanocomplexes at molar ratio = 6.5:1 and 10:1 after 30 days storage-time.

Thus, the development of CH:NCC nanocomplexes is considered suitable for use in the food, pharmaceutical and biochemical fields, and the structures prepared at pH = 5.0, absence of NaCl and molar ratio CH:NCC = 3:1 showed similarities in terms of structure with others synthesized under different conditions, but showing greater thermal stability, which gives it a superior quality for future technological applications.

ACKNOWLEDGMENTS

Authors thank Universidade Federal de Viçosa (UFV), Coordenação de Aperfeiçoamento de Pessoal de Nível Superior (CAPES; Finance code 001), Fundação de

Amparo à Pesquisa do Estado de Minas Gerais (FAPEMIG), and Conselho Nacional de Desenvolvimento Científico e Tecnológico (CNPq) for the financial support.

5. Reference

Abdull Khalil, H.P.S., Saurabh, C. K., Adnan, A. S., Fazita, M. N., Syakir, M. I., Davoudpour, Y., ... & Dungani, R. (2016). A review on chitosan-cellulose blends and nanocellulose reinforced chitosan biocomposites: Properties and their applications. *Carbohydrate polymers*, *150*, 216-226.

Abo-Elseoud, W. S., Hassan, M. L., Sabaa, M. W., Basha, M., Hassan, E. A., & Fadel, S. M. (2018). Chitosan nanoparticles/cellulose nanocrystals nanocomposites as a carrier system for the controlled release of repaglinide. *International journal of biological macromolecules*, *111*, 604-613.

Abo-Elseoud, W. S., Hassan, M. L., Sabaa, M. W., Basha, M., Hassan, E. A., & Fadel, S. M. (2020). Use of cellulose nanocrystals in chitosan nanoparticles carrier system for the controlled release of ketoprofen. *OSP Journal of Nanomedicine and Nanotechnology*, *1*(1), 1-11.

Akhlaghi, S. P., Tiong, D., Berry, R. M., & Tam, K. C. (2014). Comparative release studies of two cationic model drugs from different cellulose nanocrystal derivatives. *European Journal of Pharmaceutics and Biopharmaceutics*, *88*(1), 207-215.

Anand, M., Sathyapriya, P., Maruthupandy, M., & Beevi, A. H. (2018). Synthesis of chitosan nanoparticles by TPP and their potential mosquito larvicidal application. *Frontiers in Laboratory Medicine*, *2*(2), 72-78.

Amorim, M. L., Ferreira, G. M. D., Soares, L. D. S., Soares, W. A. D. S., Ramos, A. M., Coimbra, J. S. D. R., ... & de Oliveira, E. B. (2016). Physicochemical aspects of chitosan dispersibility in acidic aqueous media: effects of the food acid counter-anion. *Food Biophysics*, *11*(4), 388-399.

Beck, S., Méthot, M., & Bouchard, J. (2015). General procedure for determining cellulose nanocrystal sulfate half-ester content by conductometric titration. *Cellulose*, *22*(1), 101-116.

Bonardd, S., Robles, E., Barandiaran, I., Saldías, C., Leiva, Á., & Kortaberria, G. (2018). Biocomposites with increased dielectric constant based on chitosan and nitrile-modified cellulose nanocrystals. *Carbohydrate polymers*, *199*, 20-30.

Brugnerotto, J., Lizardi, J., Goycoolea, F. M., Argüelles-Monal, W., Desbrieres, J., & Rinaudo, M. (2001). An infrared investigation in relation with chitin and chitosan characterization. *Polymer*, *42*(8), 3569-3580.

Bulatao, R. M., Samin, J. P. A., Salazar, J. R., & Monserate, J. J. (2017). Encapsulation of anthocyanins from black rice (Oryza Sativa L.) bran extract using chitosan-alginate nanoparticles. *J. Food Res.*, *6*(3), 40.

Celebi, H., & Kurt, A. (2015). Effects of processing on the properties of chitosan/cellulose nanocrystal films. *Carbohydrate polymers*, *133*, 284-293.

Delan, W. K., Zakaria, M., Elsaadany, B., ElMeshad, A. N., Mamdouh, W., & Fares, A. R. (2020). Formulation of simvastatin chitosan nanoparticles for controlled delivery in bone regeneration: Optimization using Box-Behnken design, stability and in vivo study. *International journal of pharmaceutics*, *577*, 119038.

De Pinho Neves, A. L., Milioli, C. C., Müller, L., Riella, H. G., Kuhnen, N. C., & Stulzer, H. K. (2014). Factorial design as tool in chitosan nanoparticles development by ionic gelation technique. *Colloids and Surfaces A: Physicochemical and Engineering Aspects*, *445*, 34-39.

Ferreira, D. C. M., Ferreira, S. O., de Alvarenga, E. S., Soares, N. D. F. F., dos Reis Coimbra, J. S., & de Oliveira, E. B. (2022). Polyelectrolyte complexes (PECs) obtained from chitosan and carboxymethylcellulose: A physicochemical and microstructural study. *Carbohydrate Polymer Technologies and Applications*, *3*, 100197.

Furtado, G. T. F. D. S., Fideles, T. B., Cruz, R. D. C. A. L., Souza, J. W. D. L., Rodriguez Barbero, M. A., & Fook, M. V. L. (2018). Chitosan/NaF Particles Prepared Via Ionotropic Gelation: Evaluation of Particles Size and Morphology. *Materials Research*, 21(4).

Henrique, M. A., Neto, W. P. F., Silvério, H. A., Martins, D. F., Gurgel, L. V. A., da Silva Barud, H., De Morais, L. C., & Pasquini, D. (2015). Kinetic study of the thermal decomposition of cellulose nanocrystals with different polymorphs, cellulose I and II, extracted from different sources and using different types of acids. *Industrial Crops and Products*, *76*, 128-140.

Jampafuang, Y., Tongta, A., & Waiprib, Y. (2019). Impact of crystalline structural differences between α-and β-chitosan on their nanoparticle formation via ionic gelation and superoxide radical scavenging activities. *Polymers*, *11*(12), 2010.

Jonassen, H., Kjøniksen, A. L., & Hiorth, M. (2012). Effects of ionic strength on the size and compactness of chitosan nanoparticles. *Colloid and Polymer Science*, *290*(10), 919-929.

Joye, I. J., Davidov-Pardo, G., & McClements, D. J. (2014). Nanotechnology for increased micronutrient bioavailability. *Trends in food science & technology*, *40*(2), 168-182.

Kalam, M. A., Khan, A. A., Khan, S., Almalik, A., & Alshamsan, A. (2016). Optimizing indomethacin-loaded chitosan nanoparticle size, encapsulation, and release using Box–Behnken experimental design. *International journal of biological macromolecules*, *87*, 329-340.

Kasaai, M. R. (2007). Calculation of Mark–Houwink–Sakurada (MHS) equation viscometric constants for chitosan in any solvent–temperature system using experimental reported viscometric constants data. *Carbohydrate polymers*, *68*(3), 477-488.

López, F. A., Mercê, A. L. R., Alguacil, F. J., & López-Delgado, A. (2008). A kinetic study on the thermal behaviour of chitosan. *Journal of Thermal Analysis and Calorimetry*, *91*(2), 633-639.

Meka, V. S., Sing, M. K., Pichika, M. R., Nali, S. R., Kolapalli, V. R., & Kesharwani, P. (2017). A comprehensive review on polyelectrolyte complexes. *Drug discovery today*, *22*(11), 1697-1706.

Morris, G. A., Castile, J., Smith, A., Adams, G. G., & Harding, S. E. (2011). The effect of prolonged storage at different temperatures on the particle size distribution of tripolyphosphate (TPP)–chitosan nanoparticles. *Carbohydrate polymers*, *84*(4), 1430-1434.

Mukhopadhyay, P., Sarkar, K., Chakraborty, M., Bhattacharya, S., Mishra, R., & Kundu, P. P. (2013). Oral insulin delivery by self-assembled chitosan nanoparticles: in vitro and in vivo studies in diabetic animal model. *Materials Science and Engineering: C*, *33*(1), 376-382.

Patel, D. K., Dutta, S. D., Ganguly, K., & Lim, K. T. (2021). Multifunctional bioactive chitosan/cellulose nanocrystal scaffolds eradicate bacterial growth and sustain drug delivery. *International Journal of Biological Macromolecules*, *170*, 178-188.

Paulraj, M. G., Ignacimuthu, S., Gandhi, M. R., Shajahan, A., Ganesan, P., Packiam, S. M., & Al-Dhabi, N. A. (2017). Comparative studies of tripolyphosphate and glutaraldehyde cross-linked chitosan-botanical pesticide nanoparticles and their agricultural applications. *International journal of biological macromolecules*, *104*, 1813-1819.

Prathapan, R., Thapa, R., Garnier, G., & Tabor, R. F. (2016). Modulating the zeta potential of cellulose nanocrystals using salts and surfactants. *Colloids and Surfaces A: Physicochemical and Engineering Aspects*, *509*, 11-18.

Rathee, V. S., Sidky, H., Sikora, B. J., & Whitmer, J. K. (2018). Role of associative charging in the entropy–energy balance of polyelectrolyte complexes. *Journal of the American Chemical Society*, *140*(45), 15319-15328.

Roman, M., & Winter, W. T. (2004). Effect of sulfate groups from sulfuric acid hydrolysis on the thermal degradation behavior of bacterial cellulose. *Biomacromolecules*, *5*(5), 1671-1677.

Segal, L.; Creely, J.; Martin, A.; Conrad, C. An empirical method for estimating the degree of crystallinity of native cellulose using the x-ray diffractometer.Tex Res J,, v. 29, p. 786, 1962.

Soares, L.S., Perim, R. B., de Alvarenga, E. S., de Moura Guimarães, L., de Carvalho Teixeira, A. V. N., dos Reis Coimbra, J. S., & de Oliveira, E. B. (2019). Insights on physicochemical aspects of chitosan dispersion in aqueous solutions of acetic, glycolic, propionic or lactic acid. *International journal of biological macromolecules*, *128*, 140-148.

Sreekumar, S., Goycoolea, F. M., Moerschbacher, B. M., & Rivera-Rodriguez, G. R. (2018). Parameters influencing the size of chitosan-TPP nano-and microparticles. *Scientific reports*, *8*(1), 1-11.

Tsai, M. L., Chen, R. H., Bai, S. W., & Chen, W. Y. (2011). The storage stability of chitosan/tripolyphosphate nanoparticles in a phosphate buffer. *Carbohydrate Polymers*, *84*(2), 756-761.

Xie, H., Du, H., Yang, X., & Si, C. (2018). Recent strategies in preparation of cellulose nanocrystals and cellulose nanofibrils derived from raw cellulose materials. *International Journal of Polymer Science*, *2018*.

Xu, K., Liu, C., Kang, K., Zheng, Z., Wang, S., Tang, Z., & Yang, W. (2018). Isolation of nanocrystalline cellulose from rice straw and preparation of its biocomposites with chitosan: Physicochemical characterization and evaluation of interfacial compatibility. *Composites Science and Technology*, *154*, 8-17.

Xu, Q., Ji, Y., Sun, Q., Fu, Y., Xu, Y., & Jin, L. (2019). Fabrication of cellulose nanocrystal/chitosan hydrogel for controlled drug release. *Nanomaterials*, *9*(2), 253.

Wang, H., & Roman, M. (2011). Formation and properties of chitosan− cellulose nanocrystal polyelectrolyte− macroion complexes for drug delivery applications. *Biomacromolecules*, *12*(5), 1585-1593.

Wang, H., Qian, C., & Roman, M. (2011). Effects of pH and salt concentration on the formation and properties of chitosan–cellulose nanocrystal polyelectrolyte–macroion complexes. *Biomacromolecules*, *12*(10), 3708-3714.

Wang, W., Jung, J., & Zhao, Y. (2017). Chitosan-cellulose nanocrystal microencapsulation to improve encapsulation efficiency and stability of entrapped fruit anthocyanins. *Carbohydrate polymers*, *157*, 1246-1253.

Wildan, M. W., & Lubis, F. I. (2021). Fabrication and Characterization of Chitosan/Cellulose Nanocrystal/Glycerol Bio-Composite Films. *Polymers*, *13*(7), 1096.

Wu, D., Zhu, L., Li, Y., Zhang, X., Xu, S., Yang, G., & Delair, T. (2020). Chitosan-based colloidal polyelectrolyte complexes for drug delivery: a review. *Carbohydrate polymers*, *238*, 116126.

Zhang, E., Xing, R., Liu, S., Qin, Y., Li, K., & Li, P. (2019). Advances in chitosan-based nanoparticles for oncotherapy. *Carbohydrate polymers*, *222*, 115004.

Supplementary Material for "Design, optimization and evaluation of intermolecular interaction, morphological characteristics and thermal stability nanocomplexes formed between chitosan and cellulose nanocrystal"

Rafaela Venancio Flores [a,*], Lucas de Souza Soares[b], Mariane Oliveira de Araujo [a], Laura Pereira [a], Sukarno Olavo Ferreira [c], Eduardo Basílio de Oliveira [a], Paulo César Stringheta [a], Taíla Veloso de Oliveira [a], Nilda de Fátima Ferreira Soares [a]

[a] Food Technology Department, Viçosa Federal University, Universitary Campus, s/n, 36570-900, Viçosa, MG, Brazil.

[b] Engineering College, Grande Dourados Federal University, Dourados road - Itahum km 12, 79804-970, Dourados, MS, Brazil.

[c] Physical Department, Viçosa Federal University, Universitary Campus, s/n, 36570-900, Viçosa, MG, Brazil.

∗Corresponding author: R. V. Flores.
E-mail address: rafavenacio2@gmail.com

I. Chitosan viscometric-avarage molar mass

From the flow times of chitosan dispersions [0.05; 0.1; 0.15 e 0.20·(100 mL)$^{-1}$ in acetate buffer (ácido acético 0,2 M + acetato de sódio 0,1 M; pH = 4,41 e força iônica = 0,1 M), measured in a Cannon-Fenske viscometer (model 513 10, Schott®, Germany), specific (ηsp) (Equation SM1) and relative viscosities (ηr) (Equation SM2) were calculated.

$$\eta_{sp} = \frac{t - t_0}{t_0} \qquad \textit{Equation SM1}$$

$$\eta_r = \eta_{sp} + 1 \qquad \textit{Equation SM2}$$

Where t (s) is the flow time of the chitosan dispersion; t_0 is the flow time of the acetate buffer solution.

The intrinsic viscosity, η (mL.g^{-1}) was calculated from the simple average of the intrinsic viscosities of Huggins (Eq.3) and Kraemer (Eq.4). These viscosities were obtained by extrapolating Equations SM3 and SM4.

$$\frac{\eta_{sp}}{c} = [\eta]_H + k_1[\eta]^2 c \qquad \textit{Equation SM3}$$

$$\frac{\ln(\eta_r)}{c} = [\eta]_K + k'_1[\eta]^2 c \qquad \textit{Equation SM4}$$

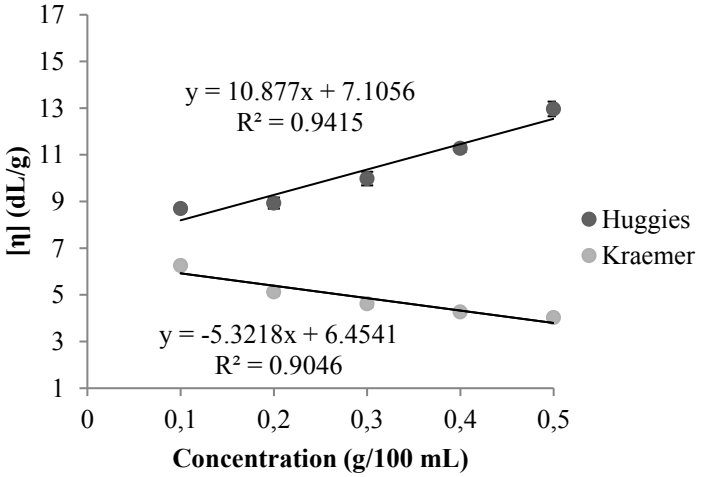

Figure SM2 – Adjustment of Huggins and Kraemer empirical models adjusted to viscometric-average experimental data from chitosan aqueous dispersions. (●) $\frac{\eta_{sp}}{c} = k_1[10.877]^2 \cdot c + [7.1056]$; R² = 0.941, (○) $\frac{\ln \eta_r}{c} = k'_1[-5.3218]^2 \cdot c + [6.4541]$; R² = 0.904.

Applying Kasaai (2007) (equations SM5 and SM6), the values of the constants *a* (1.31) and *k* (2.7×10^{-7} dL·g^{-1}), from the MHS equation were calculated and obtained as viscosimetric average molar mass for the chitosan used in this work, the value of 463 ± 25 kDa.

$$a = \left(0.6202 + \frac{0.699 \times x}{0.4806+x}\right) + [0.003(T - 20)] \qquad \textit{Equation SM5}$$

$$\log K \times 10^{-5} = -5.7676a + 5.9232 \qquad \textit{Equation SM6}$$

In equation (SM5), $x = DA/(pH \cdot \mu)$ and T tempetature in °C.

II. Degree of deacetylation (DD) of chitosan

The degree of deacetylation of chitosan was obtained by analyzing the FTIR spectrum (Figure SM1) of chitosan together with the deconvolution into Lorentz components of the individual intensities of the bands of interest (1320 and 1420 cm^{-1}), wich show the conversion of N-acetylglycosamine units into amino groups, and using the equation SM7.

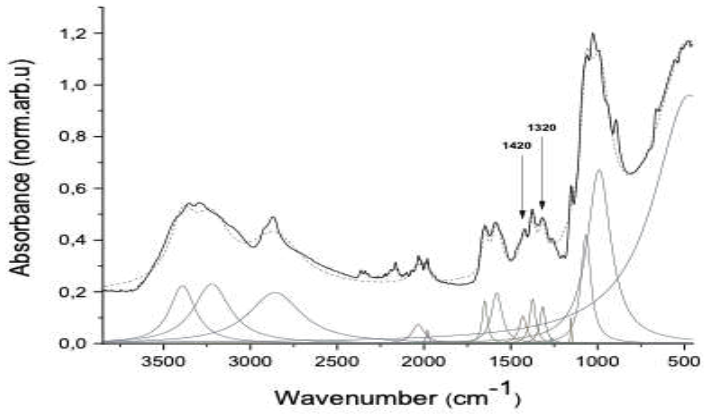

Figure SM1 - Chitosan spectrum of 450 – 3850 cm^{-1} followed by the deconvolution of highlighted bands in its Lorentzian components.

$$DD = 100 - \frac{(A_{1320}/A_{1420}) - 0.3822}{0.03133} \qquad \textit{Eq. SM7}$$

In equation $(SM7)$, A_{1320} and A_{1420} correspond to the absorbance of glucosamine.

III. Density of sulfonate groups by conductimetric titration

Figure 3 shows the NCC conductometric titration curve. The density of sulfonate groups in the NCC was 216.87 ± 9.01 mmol OSO_3^-/ kg NCC, close to the value specified by the manufacturer (246 – 261 mmol OSO_3^-/kg NCC).

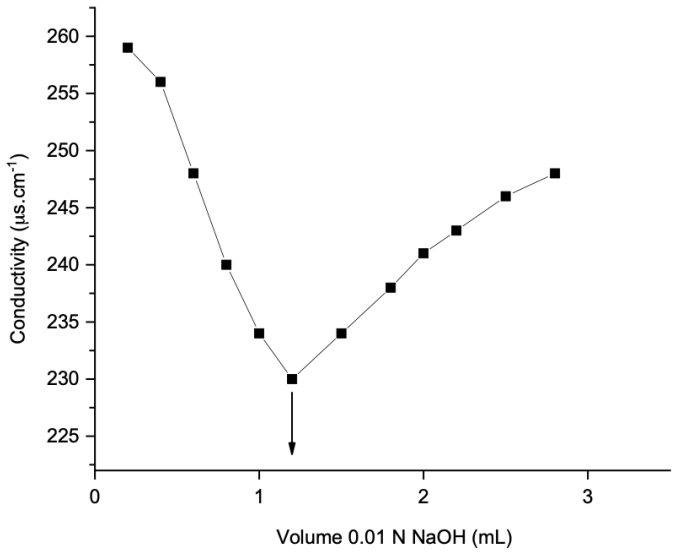

Figure SM2 – Representative curve of conductivity titration of the cellulose nanocrystal to determine the density of sulfonate groups (OSO_3^-).

IV. Determinations of weight loss (%) from TGA thermograms

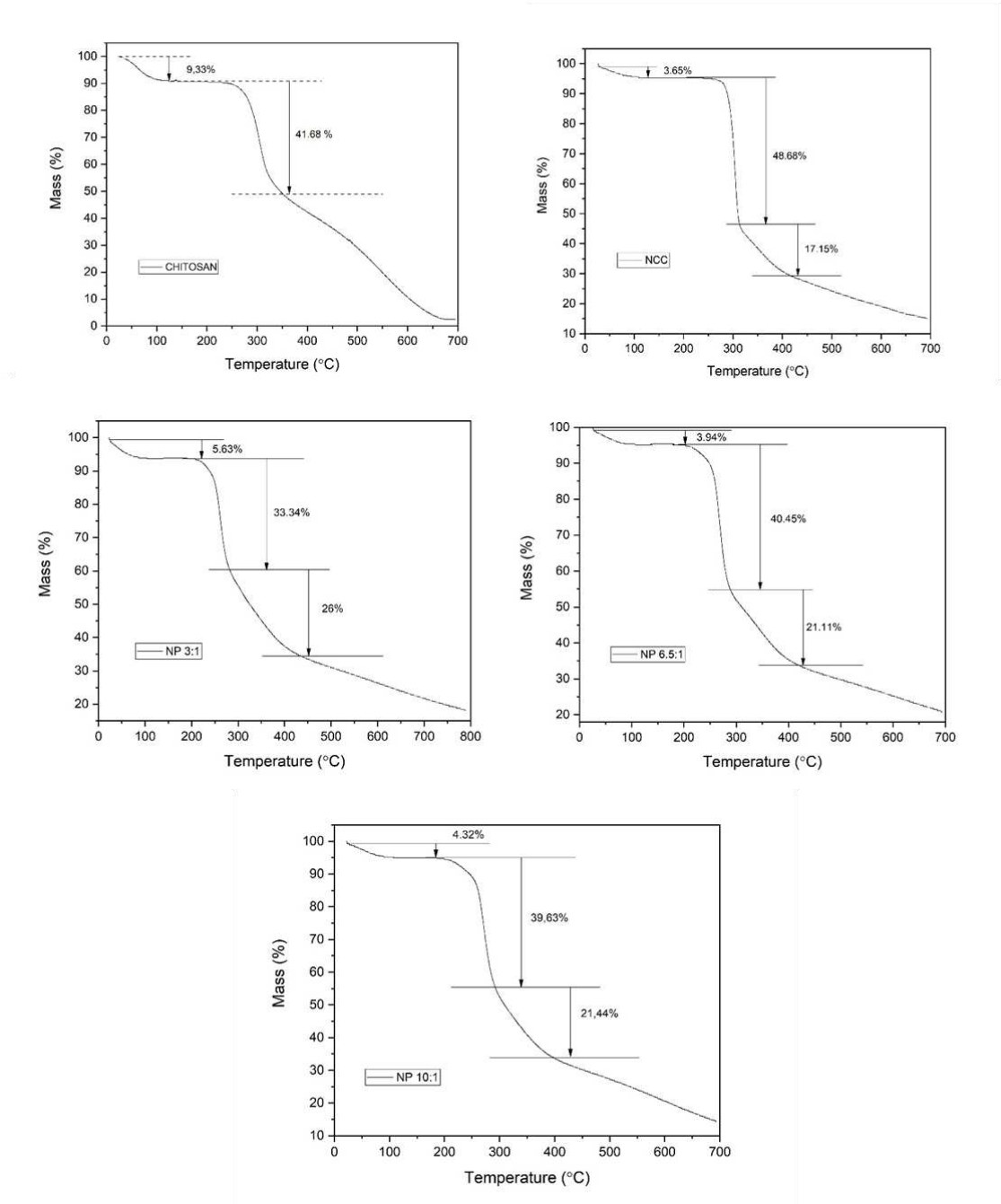

Figure SM3 - TG thermograms of chitosan, NCC, NP 3:1, NP 6.5:1 and NP 10:1.

V. Thermal degradations temperatures from DTG thermograms

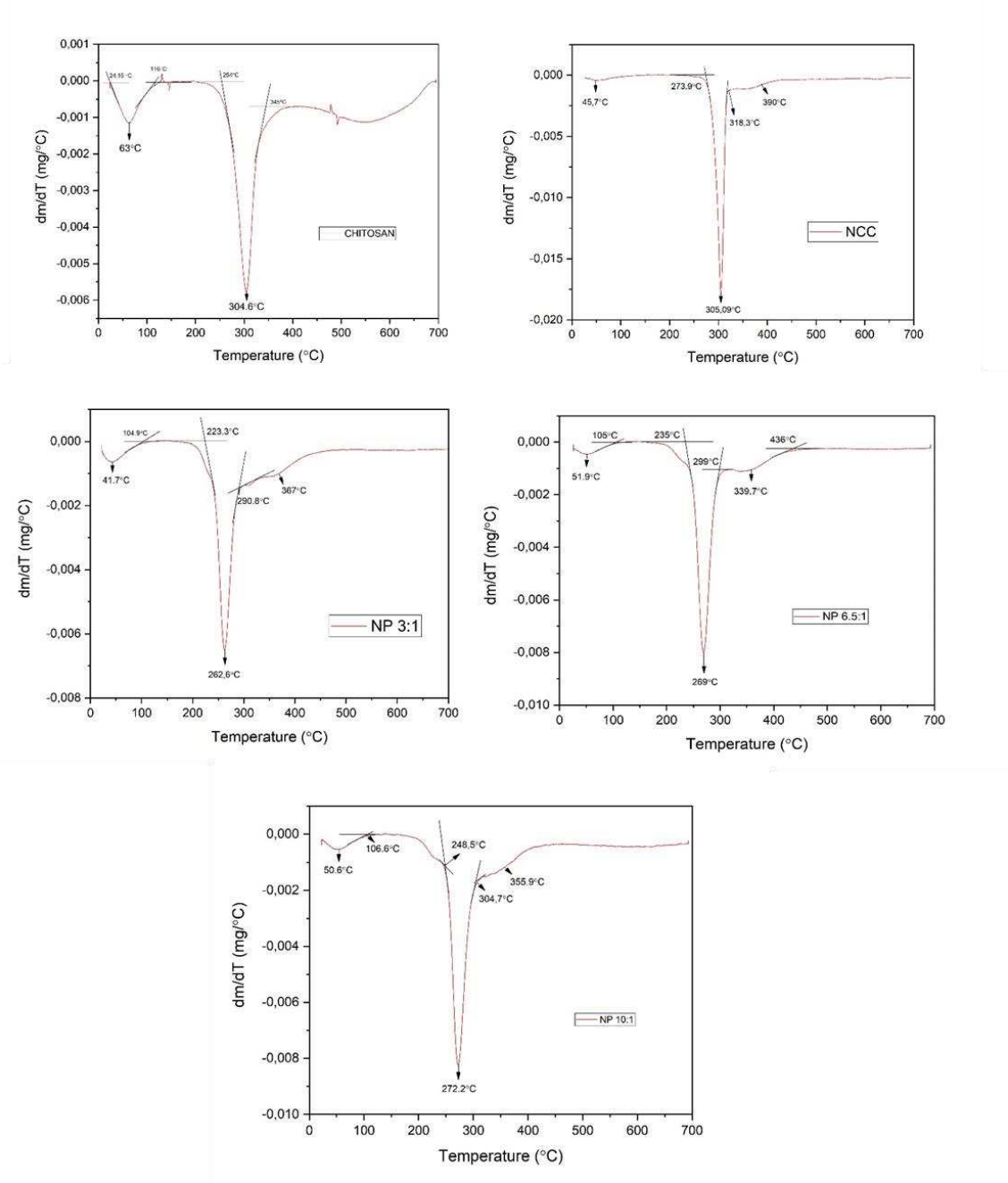

Figure SM4 - DTG thermograms of chitosan, NCC, NP 3:1, NP 6.5:1 and NP 10:1.

Artigo 3*

* Formatado de acordo com as diretrizes da revista *Carbohydrates Polymers*

The influence of the acid types and cellulose nanocrystal on the chitosan/PVA-based blend films added of Jussara (Euterpe edulis M.) extract: Effect on mechanical, molecular, and Physico-chemical properties

Rafaela Venancio Flores[a], Katia Silva Maciel[a], Kely de Paula Correa[b], Sukarno Olavo Ferreira [c], Paulo César Stringheta [a], Eduardo Basílio de Oliveira [a], Taíla Veloso de Oliveira [a], Nilda de Fátima Ferreira Soares [a]

[a] Food Technology Department, Viçosa University Federal, Universitary campus, s/n, 36570-900, Viçosa, MG, Brazil.

[b] Candido Tostes Dairy Institute – Agricultural Research Company of Minas Gerais, R. Tem. Luís de Freitas, 116 – Santa Terezinha, 36045-560, Juiz de Fora, MG, Brazil.

[c] Physics Department, Viçosa University Federal, Universitary campus, s/n, 36570-900, Viçosa, MG, Brazil.

∗Corresponding author: R. V. Flores.
E-mail address: rafavenacio2@gmail.com

Abstract: Chitosan previously dispersed in lactic and propionic solutions were used for the preparation of nanocomposite polyvinyl alcohol/chitosan (PVA/CS) films with antioxidant and mechanical and water vapor - barrier properties improved by the addiction of cellulose nanocrystal (CNC) and Jussara extract (*Euterpe edulis* M.). The molecular structure of the films was strongly affected by the type of acid used in chitosan dispersion. Films manufactured with lactic acid exhibited twice the moisture content compared to those with propionic acid. The color and antioxidant activity of the films were also significantly influenced by the type of acid. Films with propionic acid exhibited a purple color while those with lactic acid presented a red color and higher antioxidant activity (95%). The addition of CNC to the films increased the Young's modulus and reduced the tensile strength and elongation at break. The films formulated with lactic acid exhibited higher elongation at break (236%) and lower elastic modulus (30 MPa), while those with propionic acid (171.4% and 46.6 MPa). From the results, it can be noticed the importance of choosing the acid not only for chitosan dispersion, but also for achieving the best film properties according to its application.

Keywords: anthocyanin, active food packaging, antioxidant, lactic acid, propionic acid.

1. Introduction

Plastic packaging plays an essential role in the plastic materials market, especially in the food sector, where they are associated with proper packaging and preservation of food quality (Andrade, González-Martínez, & Chiralt, 2022; Kanatt & Makwana, 2020). However, these same materials have been one of the main guidelines in the management of environmental problems generated by solid waste.

The fact that most plastic packaging is not biodegradable and still contains additives in its composition (paints, resins, plasticizers, crosslinkers, and others), contributes to an increase in the environmental impact (Kanatt & Makwana, 2020). In this sense, researches have been directed toward developing packaging with biodegradable materials, aiming the sustainability of the production chain, and reducing environmental impacts (Kanatt, Muppalla, & Chawla, 2017). Therefore, several biopolymers, especially polysaccharides, can be explored. Cellulose and chitin stand out in this way since they are the most abundant natural polymers in the world.

Chitin is a linear polysaccharide composed of 1,4-N-acetylglucosamine units, located mainly in crustaceans exoskeleton. Despite the chitin accessibility in nature, its application is limited due to the large structural volume; hydrogen bonds between carbonyl, hydroxyl, and acetamido groups, and highly crystalline structure, making chitin not soluble in water and other commonly used solvents such as alcohol, chloroform, among others (Sivashankari & Prabaharan, 2017).

The largest chitin derivative is chitosan, which is obtained by N-deacetylation and composed of glucosamine and N-acetylglucosamine units. Chitosan (CHI) has attracted great attention in the biomedical, food, and materials fields due to its excellent properties and functions such as biodegradability, weak acid solubility, biocompatibility, and adhesiveness (Ali & Ahmed, 2018). Furthermore, chitosan has good film-forming properties, which makes it extremely attractive in the packaging field. However, some challenges are also encountered in formulating chitosan films, such as poor mechanical and thermal properties, dissolution in acidic solution, and small surface area (Perumal, Sellamuthu, Nambiar & Sadiku, 2018). To circumvent these problems, some strategies can be used, such as: I) optimization of polymer's properties through the modulation of the physicochemical characteristics and intermolecular interaction to packaging development; II) polymeric blend development through the mixture of chitosan with another polymer with a better mechanical, barrier and thermal properties; III) addition of nanomaterials with high aspect ratio and surface area as reinforcers of the developed

material. Many factors can interfere simultaneously in the development of chitosan-based packaging, so the combination of modulation of the strategies allows the manufacture of excellent films, expanding their applications.

When considering the first point, several factors can be highlighted, such as degree of deacetylation, molecular mass, ion concentration, type of acid, and pH, most of which are related to chitosan solubility (Pavoni, Luchese, & Tessaro). To form aqueous dispersions, this polymer requires an acidic environment. The amino groups in chitin's structure, in pH below 6.5 (pKa = 6.5), are high degree of protonation, allowing the dispersion of chitosan. Among the acids used for this purpose, the use of weak organic acids, especially acetic acid, is the most common when dealing with dispersions for film production (Melro et al., 2020; El Miri et al., 2015; Chen, & Zhao, 2012). However, acids allowed in foods, in general, can be used, including propionic, lactic, malic, citric, and others. The acids are known in the literature to influence the physicochemical properties of aqueous chitosan dispersions and their films. However, this effect has still not been elucidated.

Another way to modulate the properties of chitosan-based films is the association with other polymers. In this sense, polyvinyl alcohol (PVA) becomes a remarkably interesting alternative, presenting itself as a water-soluble, non-toxic, biodegradable synthetic polymer, in addition to having good resistance to solvents, oils, and greases and low permeability to oxygen gas (Perumal, Sellamuthu, Nambiar & Sadiku, 2018; Aranha & Lucas, 2001). Studies show that PVA and chitosan blends have good compatibility and superior thermal properties to films produced with individual polymers (El Miri et al., 2015; Bonilla et al., 2014). As for the water vapor barrier and high performance of mechanical properties, strategies using film reinforcers, such as cellulose nanocrystal (CNC), have been employed (Perumal et al., 2018; Luzi et al., 2017).

Cellulose nanocrystals are obtained by acid hydrolysis of cellulose fibers. During this process, the glycosidic bonds are broken, releasing the amorphous part of the cellulose structure and allowing only the crystalline domains to remain intact (Abdul Khalil et al., 2016). CNC features a high surface-to-volume ratio, high tensile strength (10 GPa), high rigidity (110–130 GPa), and high flexibility (Mali & Sherje, 2022; Perumal et al., 2018). Therefore, the CNC incorporation into chitosan films can provide better properties to these materials.

In addition, packaging with biodegradable polymers can also be used as carriers of additives, including antioxidant agents, in particular natural antioxidants such as plant extracts and essential oils, with the aim of to extend the shelf life of food. Packages with this direction

are classified as active packages, being defined as material that package the product, wich dynamically and intentionally interact with food intrinsic and/or extrinsic factors to modify desirable properties, while maintaining the food quality through the potentiation of the function packaging protection (Lim, 2015).

Among the natural antioxidants, we highlight anthocyanins, phenolic compounds belonging to the flavonoid class, responsible for the typical color of red fruits, especially the *Jussara* fruit, known as the *açaí* of the Brazilian Atlantic Forest. Anthocyanins, especially cyanidin-3-rutinoside and cyanidin-3-glycoside, are an important group of phenolic compounds found in *Jussara* fruit, being responsible for conferring a high antioxidant power to the fruit and intense purple color (Bicudo et al., 2015). This fruit, with a globular shape and a diameter of 10 to 15 mm, contains only one seed, occupying about 80% of its total volume, and has a chemical and mineral composition similar to or even superior to *açaí* (Euterpe oleracea) (Silva, Barreto, & Serodio, 2004). In recent years, several studies have been carried out aiming at the use of extracts sources of anthocyanins, showing the beneficial relationship of these phenolic compounds with cardiovascular, immunological, and inflammatory diseases, is considered a "super fruit" due to its high antioxidant capacity (Cardoso et al., 2018; De Barros Freitas et al., 2017). In addition, anthocyanins from fruits have been applied in research with active packaging, which further expands their use in the food sector (Wang et al., 2019; Yong et al., 2019).

Therefore, the objective of this study was to develop nanocomposite films with high performance in antioxidant and water vapor barrier properties. The films were manufactured through the association of techniques, including the PVA and chitosan blending, chitosan dispersion in two acid types, CNC incorporation as a nano-reinforcement agent, and EXTJ addition as a natural bioactive compound. To date, there are no studies approaching the concomitant effect of the addition of CNC and EXTJ in chitosan and PVA blends prepared with the different acid mediums. Moreover, this works aims to characterize the films in terms of their antioxidant, structural, mechanical, and barrier properties.

2. Material and methods

2.1 Material

Chitosan (low molecular weight; Product ID = 448869), Poly(vinyl alcohol) (PVA) (Mw 85,000-124,000, 99+% hydrolyzed), DPPH (2,2-diphenyl-1-picrylhydrazyl), TPTZ

(2,4,6-Tris(2-piridil)-s-triazina) (PM= 312,34 g/mol), and propionic acid were purchased from Sigma-Aldrich. Cellulose Nanocrystal (Product ID = NCV100) was bought from CelluForce Corporation (Canada). Lactic acid, acetic acid, glycerol, ferric chloride and ethyl alcohol were obtained from Dinâmica Company (Brazil). Hydrochloric acid (HCl) was purchased from SPLabor (Brazil) and Sodium acetate from Synth Company (Brazil).

2.2 Plant material preparation

Jussara (Euterpe edulis M.) was obtained from Canaã, Minas Gerais (Brazil). The plant material was immersed in a sodium hypochlorite solution (200 $mg.mL^{-1}$) for 15 min. After that, the Jussara fruits were were portioned, stored in polyethylene-nylon plastic bags, identified and frozen at conventional freezer until the extration.

2.3 Jussara extration

To prepare the Jussara extract (EXTJ), the sanitized fruit was left to stand for 20 minutes with water at 40°C ± 5°C. Then, the water was drained and the fruit was macerated to remove the seed. Then, 7 g of the fruit was added to 100 mL of 75% (v/v) ethanol and the pH was adjusted to 3.0 with hydrochloric acid. The flasks were covered with parafilm®, wrapped with aluminum paper and submitted to sonication in an ultrasound bath (Ultracleaner 1400A, Unique, Brazil) at 40 kHz/ 50 minutes/ 40°C. Then, the extract was centrifuged at 5000 x g/ 10°C/ 20 minutes, vacuum filtered in a Buchner funnel with Whatman 1 paper and evaporated in a rotary evaporator at 50 °C until a final volume corresponding to 5% of the original volume being obtained (Rocha et al., 2017). The extract was evaluated for total phenolic compounds content (Singleton and Rossi, 1965), total anthocyanins (Fuleki and Francis, 1968), and antioxidant capacity by FRAP (Larrauri,Rupérez,& Saura-Calixto, 1997) and DPPH (Brand-Williams, Cuvelier, &Berset, 1995) methods, presenting values of 6. 38 mg gallic acid/mL^{-1} extract, 1.42 mg total anthocyanins/mL concentrated extract, 833.74 µmol ferrous suffate/g^{-1} fresh fruit, and 1377.71 µmol Trolox/g^{-1} fresh fruit, respectively. The extract was frozen at - 80 °C and stored until the films were prepared.

2.4 Active nanocomposite films preparation

The formulation of nanocomposite films was according to Bonilla et al. (2014) with modifications. PVA was diluted in 100 mL of distilled water at 3.2% (wt) under magnetic stirring at 90 °C for 3h. Chitosan (0.8% wt) was dissolved in 100 mL of water with lactic acid

or propionic acid at the same mols quantity (15.82 mmol of acid) under magnetic stirring for 24 h. Then, the chitosan dispersion was added to PVA dispersión gradually and kept under stirring for 30 min. Then, glycerol 30% (wt) was added and subjected to stirring for another 15 minutes. Subsequently, determined volumes (Table 1) of the nanocrystal dispersion (20 mg/mL^{-1} in water, sonicated at 420 W, for 12 min, in an ice bath) were added to film-forming dispersion, and water was added to equalize the final volumes. The dispersions were kept under stirring for 15 min. After this period, 8.78 mL Jussara extract was added (1.5% of total phenolic compounds in relation to the total mass of polymer). The dispersions were stirred for another 20 minutes and then sonicated in an ultrasonic bath to remove bubbles. Then, they were poured onto glass plates (34 cm x 18.5 cm) and subjected to bench drying in the absence of light at 23°C and relative humidity 55%.

Table 1- Composition of nanocomposite CHI/PVA/EXTJ - based films.

TREATMENTS		**CNC (%)**	**V_{CNC} (mL)**	**V_{EXTJ} (mL)**
Lactic acid	**Propionic acid**			
ALCONT	APCONT	0	-	-
AL0%	AP0%	0	-	8.78
AL2%	AP2%	2	4	8.78
AL4%	AP4%	4	8	8.78
AL6%	AP6%	6	12	8.78
AL8%	AP8%	8	16	8.78

CNC: celullose nanocrystal; V_{CNC}: CNC dispersion' volumen added to the films; V_{EXTJ}: Jussara extract volumen added to the films; ALCONT: lactic acid polymeric blends without CNC and Jussara extract; APCONT: propionic acid polymeric blends without CNC and Jussara extract.

2.5 Nanocomposite CHI/PVA/EXTJ - based films characterization

2.5.1 Fourier transform infrared spectroscopy (FTIR)

FTIR spectra of the JEXT and the PVA/chitosan/JEXT-based films added or not with CNC were obtained using an FTIR spectrometer (Nicolet 6700, Thermo Sicientific) equipped with an attenuated total reflectance accessory of a germanium crystal. Spectra were performed

at 4 cm^{-1} of resolution, in the wavelength range of 4000 − 650 cm^{-1}, and 32 scans for each spectrum. The measurements were performed four times for each treatment.

2.5.2 Color characteristics and visual appearence

A Colorimeter (Colorquest® XE, HunterLab, USA), operating with D65 illuminant (average daylight) and field of view of 10◦ angle, was used to determine the film color coordinates L* (lightness), a* (red/ green) and b* (yellow/blue). The analysis were performed three times.

2.5.3 Moisture content and swelling degree (%)

The moisture content was determined by drying film sample at 105 °C to a constant weight (Yong et al., 2019).

$$Moisture\ (\%) = \frac{m_i - m_f}{m_i} \times 100$$

Where in which M_i and M_t were the initial and final masses of film sample, respectively.

For the swelling degree, dried film pieces (2 cm^2) were weighed individually and immersed in deionized water for 2 h. The film swelling behavior was quantified using Eq. (2) (De Oliveira et al., 2020):

$$SD = \frac{m_s - m_i}{m_i} \times 100$$

where m_s is the swelled film mass and m_i is the dried film mass

2.5.4 Thickness and mechanical properties

Thicknesses of the PVA/chitosan films were measured in fifteen random sample positions using a digital micrometer (Model 547-401, Mitutoyo, Japan).

A Universal Testing Machine (model 3367, Instron Corporation, USA) was used to obtain the mechanical properties of the films, namely tensile strength (TS), elongation at break (EB), and Young's modulus (YM). According to the ASTM D882 method (ASTM, 2012), the CHI/PVA/EXTJ-based film samples of 10 cm x 2.5 cm were stretched at a crosshead speed of 50 $mm.min^{-1}$. The measurements were carried out five times for each repetition.

2.5.5 Water Vapor Permeability (WVP)

The WVP of the nanocomposite CHI/PVA/JEXT-based films was determined gravimetrically according to ASTM method E96-95 with modifications. Before the analysis, the samples were conditioned at 25 °C ± 2 °C and 53% RH for 12 h. The films were sized 80 mm in diameter, placed under circular paraffin capsules, and sealed with liquid paraffin. Capsules were filled with $MgCl_2$ saturated solution (32.5% RH) and stored at 25 °C ± 2 °C in a desiccator containing a saturated solution of NaCl to maintain a RH of 75%. Samples were weighed every 3 h for 96 h, and WVP was calculated using three replicates and expressed in ($g \cdot m^{-2} \cdot s^{-1} \cdot kPa^{-1}$).

2.5.6 Determination of antioxidant capacity (DPPH)

The antioxidant capacity of the film was determined by DPPH radical scavenging test (Yun et al., 2019). Briefly, different amounts (4, 8, 12, 16, and 20 mg) of the film sample were weighed and individually placed in the test tubes. Then, 4 mL of 100 μM DPPH methanol solution was added to each tube and reacted with the film sample at 25 °C for 1 h in the dark. The absorbance of the reaction solution was measured at 517 nm. The DPPH radical scavenging activity of the film was calculated as follows:

$$DPPH\ radical\ scavenging\ activity\ (\%) = \frac{Abs_B - Abs_A}{Abs_B} \times 100$$

where Abs_B was absorbance of blank (without film) and Abs_A was absorbance of reaction solution containing film.

2.6 Statistical analysis

The experimental data were analyzed through analysis of variance (ANOVA) ($\alpha = 0.05$) and Tukey's studentized range (HSD) test, using a Minitab statistical program (version 17) to determine the influence of the acid type of chitosan dispersions on the properties of the CHI/PVA-based films.

Regression analyses were applied to evaluate the influence of NCC concentrations on the properties of the CHI/PVA-based films.

All analyses and measurements were performed three times, and the difference was determined, considering the confidence level of 95 %.

3. Results and Discussion

3.1 *Fourier transform infrared spectroscopy (FTIR)*

FTIR analysis is a qualitative spectroscopic method used to investigate and classify possible changes in the inter- and intramolecular interactions that occurs during polymer blending or modifications (Freitas et al., 2020; Kanatt & Makwana, 2020).

The FTIR spectra of the control nanocomposites films (APCONT and ALCONT - without EXTJ and CNC) and those added with different CNC concentrations (AL 0, 2, 4, 6, and 8%; AP 0, 2, 4, 6, and 8%), as described in Table 1, are reported in Fig. 1A and Fig. 1B, respectively. To complement the analysis and interpretation of the results, the spectra of chitosan powder, CNC, chitosan films manufactured with lactic acid, chitosan films manufactured with propionic acid, PVA films, Jussara extract and glycerol are reported in Supplementary material (SM1).

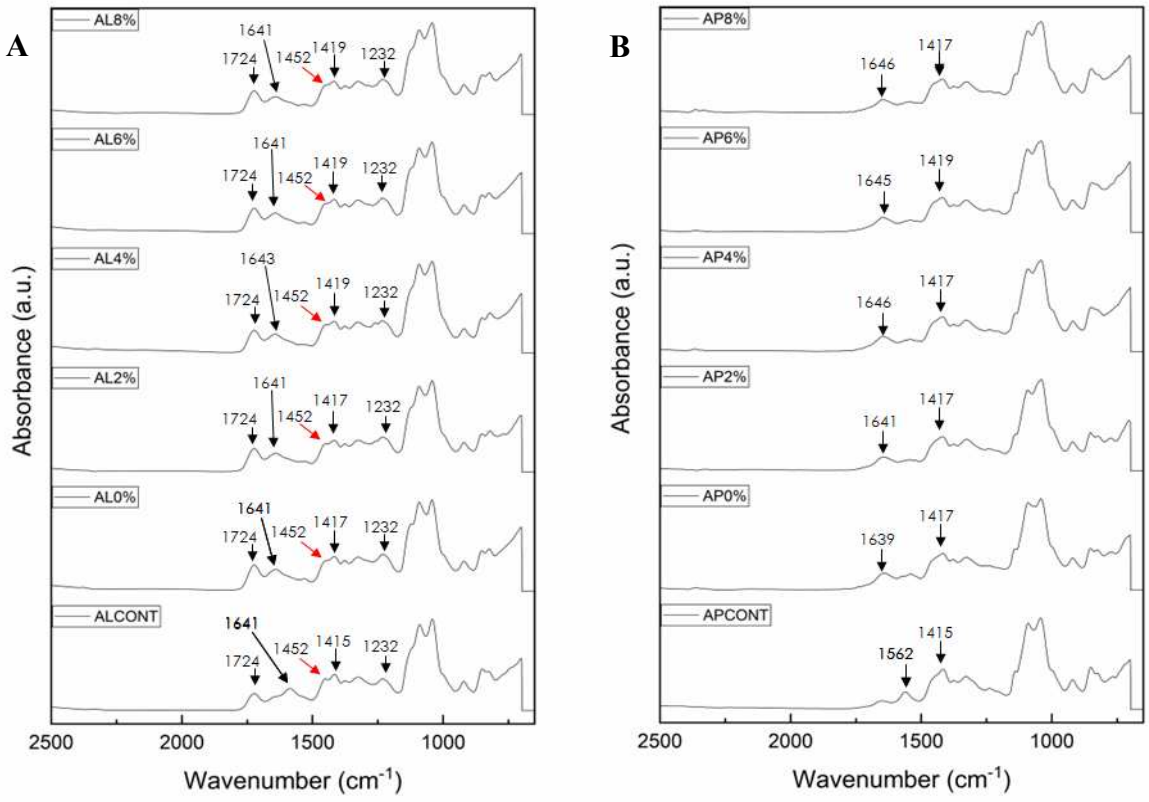

Fig. 1 – FTIR espectras (from 2500 cm^{-1} to 400 cm^{-1}) for A) nanocomposite CHI/PVA/JEXT-based films with lactic acid and B) nanocomposite CHI/PVA/JEXT-based films with propionic acid.

When evaluating the ALCONT and APCONT spectra, it can be seen that the region that showed the greatest changes was between 1820 cm^{-1} and 1150 cm^{-1}. In fact, this region is rich

in data sources, being considered a fingerprint region, as it serves to confirm the identity of certain compounds (Soares et al., 2019; Barbosa, 2007). For the blends without the addition of Jussara extract and CNC, it is evident the changes in some bands in this region when we take propionic and lactic acids into account.

The band 1415 cm^{-1} (-CH_2 and -CH_3 angular deformation) is more pronounced in films manufactured with propionic acid, showing that the type of acid may have influenced the interactions of PVA with chitosan, since this peak is very characteristic in the spectrum of PVA. This fact may have occurred because lactic acid promotes greater protonation of the amino groups of chitosan, causing the polymer chain to change its conformation to a more extended form, exposing even more the amino groups of chitosan, wich reduced the interactions by hydrogen bonds between the hydroxyls of chitosan and PVA, and increased the interactions between the polymers and the water, since these have a more hydrophilic characteristic. This explains the greater flexibility of films produced with lactic acid. It is also possible to note the appearance of a new peak at 1452 cm^{-1} in the films with lactic acid, which indicates a splitting of the peak and its shift to lower wavenumbers. The same was observed by Soares et al. (2019) when studying dispersions of chitosan in different types of organic acids, including lactic and propionic acids. The authors attributed the event to two possible situations, the first being attributed to the fact that the vibration energy of NH_3^+/lactate is higher than that of NH_3^+/propionate, causing a shift of these peaks toward lower wave numbers; and the second related to the fact that the contra-anions lactate and propionate have a different dipole moment.

In the spectra of films manufactured with lactic acid, one notices the presence of the band at 1724 cm^{-1} related to the stretching of the C=O bond of carboxylic acids (Barbosa, 2007) and 1234 cm^{-1}, also characteristic of this acid (Melro et al, 2020), showing that after drying the films, lactic acid residues are still present in the material.

As for the addition of Jussara extract into the films manufactured with propionic acid, one notices in the films with propionic acid the shift of the band from 1542 cm^{-1}, referring to the amine band, to 1562 cm^{-1}, and from the band 1658.7 cm^{-1} to 1643.2 cm^{-1} (C=O vibration of flavonoids), with a doubled increase in intensity. In the films manufactured with lactic acid, there was a shift in the band from 1587 cm^{-1}, to 1641 cm^{-1}. These observations show the interactions of EXTJ with chitosan and PVA, mainly through hydrogen bonding type interactions, and the presence of aromatic compounds of the flavonoid class in the films, such as anthocyanins and phenolic acids (Freitas et al., 2020).

Regarding the addition of CNC, it was not possible to notice differences between the spectra of films with both lactic and propionic acid with increasing concentration. However, for films manufactured with propionic acid, there was a subtle reduction of intensity in the band 1542.8 cm^{-1}, implying interactions of CNC with the amino groups of chitosan. The absence of characteristic peaks of CNC in the spectra shows the excellent compatibility of this loading agent with the other film components.

3.2 Color characteristics and visual appearence

Color is an important property that directly reflects on the appearance of the films. In Fig. 2 is possible to observe the visual color difference between the nanocomposite films produced with lactic and propionic acids. It can be noticed that the films manufactured with lactic acid exhibited a pink/reddish coloration (Fig. 2d), while those formulated with propionic acid exhibited a purplish coloration (Fig. 2c). The differences in color can be explained by the structural changes of the anthocyanin molecules due to the difference in pH of the filmogenic dispersions manufactured with each acid type. The pH of the filmogenic dispersions containing propionic acid was, on average, 3.87 ± 0.02 (visual appearance of the dispersions in Fig. 2a) and those containing lactic acid was 2.98 ± 0.05 (visual appearance in Fig. 2b).

At pH values ≤ 3 there is predominance of the flavilium cation, which presents intense red coloration. However, at 4 ≤ pH ≤ 6 values there are the coexistence of quinoidal base (purple/blue color) and pseudobase carbinol (colorless hemicetal form) structures, being less stable structures, causing them to be easily transformed into chalcones (Flores et al., 2022).

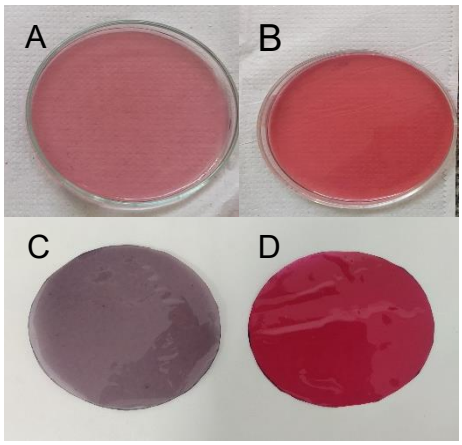

Fig. 2. Visual appearance of chitosan nanocomposite dispersions (A and B) and their respective films (C and D) incorporated with different acid types (A, C = propionic acid; B, C = lactic acid) and Jussara concentrated extract.

It can be observed that the dispersions exhibited differences in color, less rose for films prepared with propionic than those with lactic acid. During the drying of the films, water is evaporated and the interaction between the polymers and other constituents of the medium is modified, and some can be more intensified than others. Through FTIR analysis, it was not possible to identify a characteristic band of propionic acid after the addition of Jussara extract into polymeric matrices. This behavior indicates that the acid was evaporated during the drying process, remaining only those dissociated and established through interactions with the amino groups of the chitosan. Then, these acids contributed less to the pH maintenance of the medium. Regarding film produced with lactic acid, residues were identified in the spectra of the nanocomposite films, characteristic groups were identified in the spectra of the nano composite films, indicating the presence of free acids in the polymeric matrices, even after the drying process. Therefore, those acids contributed to the pH and the structure of the anthocyanins.

Colorimetric analysis was also conducted to verify the influence of CNC and acids on the colorimetric properties of the films. The results of the analyses are presented in Table 2.

Table 2 - Color coordinate values (L*, a*, b*) of chitosan/PVA/EXTJ nanocomposite films.

Treatment	**Lactic acid**			**Propionic acid**		
CNC (%)	**L***	**b***	**a***	**L***	**b***	**a***
0	22.81 ± 0.78 **a**	24.87 ± 0.62 **a**	6.52 ± 0.14 **a**	22.05 ± 1.19 **a**	5.95 ± 0.44 **a**	1.63 ± 0.07 **a**
2	22.03 ± 1.46 **a**	25.53 ± 0.37 **a**	6.36 ± 0.05 **a**	23.29 ± 1.39 **a**	5.44 ± 0.25 **a**	1.48 ± 0.08 **a**
4	19.86 ± 0.90 **b**	25.32 ± 0.15 **a**	6.34 ± 0.13 **a**	21.34 ± 0.64 **a**	5.53 ± 0.19 **a**	1.59 ± 0.04 **a**
6	18.63 ± 0.42 **b**	25.50 ± 0.12 **a**	6.48 ± 0.20 **a**	17.15 ± 0.56 **b**	5.80 ± 0.06 **a**	1.50 ± 0.01 **a**
8	17.92 ± 0.26 **b**	25.75 ± 0.13 **a**	6.55 ± 0.08 **a**	18.14 ± 0.50 **b**	5.48 ± 0.23 **a**	1.60 ± 0.07 **a**

L*: Luminosity; a* refers to the intensity of red (red to green); b* refers to the intensity of yellow (yellow to blue). Values are given as mean ± standard deviation. Different letters in the same column indicate significant differences ($p < 0.05$).

According to the results, for the films manufactured with lactic acid and propionic acid, there was no significant difference between the color coordinates a* and b*. As for the luminosity (L*) coordinate, the films manufactured with lactic acid, without CNC (AL0%) addition, differed significantly ($p < 0.05$) from those with 4%, 6% and 8% of CNC. As for the films prepared with propionic acid, lower values of the L* coordinate was observed for the

treatments with higher concentrations of CNC (6% and 8%) than the other treatments (0%, 2% and 4%), statistically different ($p < 0.05$).

It is possible to observe that with increasing nanocrystal concentration there was a reduction in the luminosity value regardless the acid used to produce the films. Increasing the CNC concentration, a film with denser structural characteristics and agglomerate presence can be formed, wich can lead to a reduction in the luminosity of the films (Pacheco et al., 2019). On the other hand, the formation of a percolation network due to these interactions contributes to the filling of the created network, and is a desirable factor within the polymer matrix (Oun et al., 2022).

A desirable characteristic of packaging is that it should have a high brightness and transparency so that the product has a quality visual presentation. However, many foods require protection from light, especially those susceptible to lipid oxidation. Thus, color is not a limiting factor (Sutharsan et al., 2022).

3.3 Moisture content (MC) and swelling degree (%)

The total water molecules which are present in the network microstructure of a composite film contribute to its MC (Kanatt & Makwana, 2020). The moisture content of the films is shown in Fig. 3. MC was significantly ($p>0.05$) higher for the films produced with lactic acid, with an average of 35.07 ± 1.48 %, while the films manufactured with propionic acid had an average of 14.08 ± 1.87 %. The difference associated with the type of acid can be explained by the fact that the counter-anion of lactic acid presents a greater contribution to the protonation of the amino groups of chitosan (Soares et al., 2019), allowing greater interactions to occur with the components present in the filmogenic dispersion, including EXTJ.

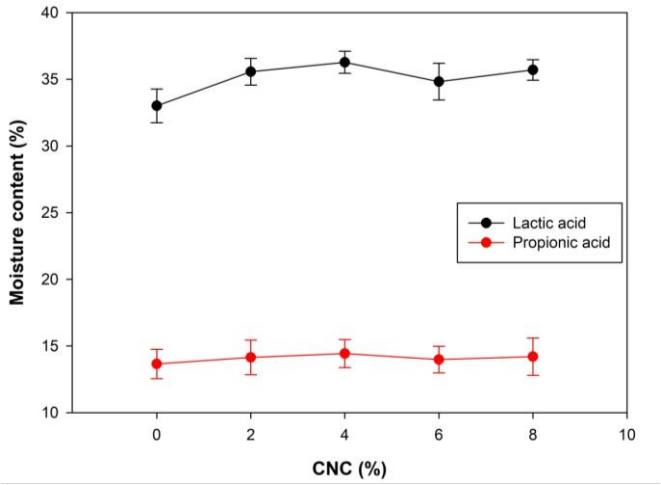

Fig. 3 – Moisture content of nanocomposite CHI/PVA/ EXTJ – based films.

Jussara extract is rich in anthocyanins and other phenolic compounds such as ferrulic acid, gallic acid, quercetin among others (Qian et al., 2017). Studies show that phenolic compounds can have a plasticizing effect when added to films, reducing the intensity of interaction between polymers and conferring greater flexibility (Freitas et al., 2020; Yong et al., 2019). Thus, with the addition of EXTJ concentrated into the filmogenic dispersions prepared with lactic acid, greater interactions between the components present in the extract may have occurred with the chitosan chains, promoting greater spacing between the polymer chains. Therefore, more water volume was maintained inside the polymeric chain interaction of water with the other components. Since the polymeric chains of films prepared with propionic acid, the same behavior can't be observed.

For the swelling degree, the interaction between the type of acid and the CNC concentrations also had a significant effect ($p<0.05$) on this variable. The model test was performed for the lactic acid data, where the F for the regression was significant ($p<0.05$) and the lack of fit was not significant ($p>0.05$), showing a determination coefficient (R2) of 90.62%. However, for propionic acid, it was not possible to fit a model.

The swelling degree was measured to determine the film hydration degree. It can be observed that the swelling degree decreased with increasing CNC concentration regardless of the acid type (Fig. 4). This behavior can be associated with the varying stability of molecular interactions, the CNC structure, and the films' surface morphology. This indicates that with the CNC addition, the interstices of the three-dimensional polymeric structure are filled, making it difficult for the passage of water and interaction with the film components, which difficult the film's hydration. The results obtained are also in agreement with the moisture of the films. Lactic acid also acts as a plasticizer in the films, promoting greater flexibility between the chains. This makes the addition of CNC to fill the interstitial spaces greater than in propionic acid films, as can be seen in Fig. 4 when 8% NCC is added to films. Their hydration capacity is greater than that of films with propionic acid.

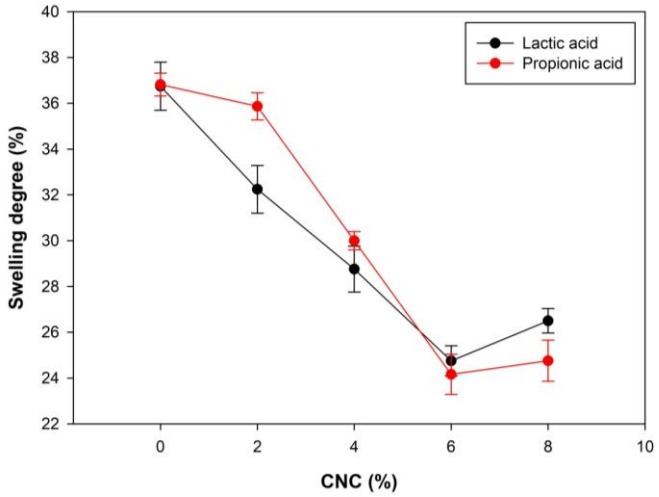

Fig. 4- Swelling degree (%) of nanocomposite CHI/PVA/ EXTJ – based films

3.4 Thickness and Mechanical properties

It was observed that the interaction between CNC and acid type showed a significant effect ($p < 0.05$) on the response variable thickness. Thus, the model test was performed for lactic ($\hat{y} = 0.07781 + 0.602$ CNC - 4.4 NCC*CNC) and propionic ($\hat{y} = 0.085571 + 0.0645$ CNC - 1.369 CNC*CNC) acids. According F test, the regression was significant ($p<0.05$) and the lack of fit was not significant ($p>0.05$) for both. It is concluded that the proposed models fit the data well. Moreover, high values of the adjusted coefficients of determination of 79.38% and 77.45% were obtained for lactic and propionic acid, respectively.

Film thickness is related to its homogeneity, which can interfere with the barrier and mechanical properties (De Oliveira et al., 2020). Films prepared with propionic acid varied less their thickness than those prepared with lactic acid (Fig.5), which indicates greater maintenance of film homogeneity. Propionic acid has fewer hydroxyl groups, which limits its interaction with other molecules to form new chains. This acid may have contributed to the formation of films with a more compact structure and uniform thickness (Wang et al., 2018). In addition, films with higher moisture content tend to be thicker, since they have more water molecules in their structure, as is the case with films produced with lactic acid.

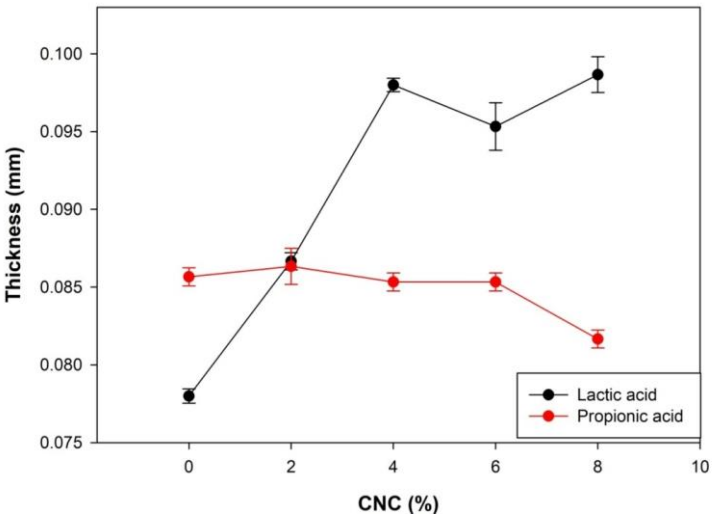

Fig. 5. Thickness (mm) of nanocomposite CHI/PVA/ EXTJ – based films.

As for the mechanical properties, it is of great relevance to evaluate them in films, because they indicate their durability and their ability to preserve the integrity of foods during handling, transport and storage. The elongation at break and tensile strength of films are generally attributed to their network microstructure and intermolecular forces between their components (Zareie et al., 2020). The results of the mechanical analysis of the nanocomposite films are presented in Fig.6. When evaluating the influence of the type of acid, there was a significant difference ($p \leq 0.05$) for all response variables (elongation at break, tensile strength and Young's modulus) studied. The films formulated in the presence of lactic acid were more flexible, showing greater elongation at break. The films formulated with propionic acid presented higher tensile strenght and Young's modulus.

Young's modulus is a mechanical property associated with the stiffness of the material and can be defined as the material's resistance to elastic deformation. This property presented an increase with the CNC addition, showing the ability of CNC to act as reinforcement material and its strong interaction with the other components of the film. These strong interactions may have hindered the flow between the polymeric chains, contributing to the reduction of film elongation. A subtle reduction in the tensile strength of the films was also observed, which may be related to the emergence of weaker interactions than those previously existing. Similar results were found in the literature and a possible explanation would be the lack of uniformity of the polymer blend when higher concentrations of cellulose nanocrystals are employed (Oliveira et al. 2020).

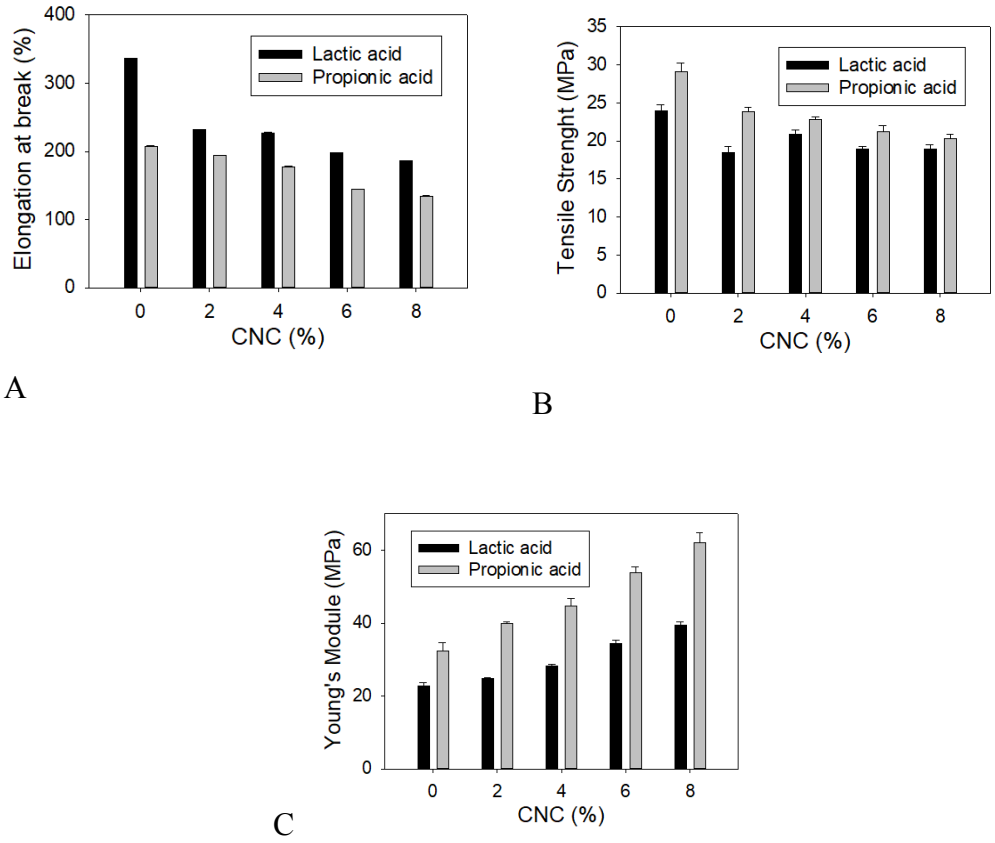

Fig. 6. Mechanical test results. A) Elongation at break (%); B) Tensile Strenght (MPa) and C) Young´s modulus (MPa).

It is known that the order of addition of the components in a dispersion influences the interaction between them. In the case of the films produced in this study, the order of mixing of the components was QUI - PVA - GLI - CNC - EXTJ. EXTJ had a pH=1.0 after the concentration step. When added to the filmogenic dispersion, the predominance of the flavilium cation in the medium may have led to a greater affinity of the sulfonate groups of the CNC with the extract rather than the polymeric blend, which led to the weakening of the three-dimensional network formed, resulting in less rigid and more fragile films, even with increasing concentration of CNC. Furthermore, the mixing time after the addition of CNC was 15 minutes, which may have been insufficient to promote interactions between the polymeric blend and the CNC. Thus, two factors must be taken into consideration when producing blends with anthocyanin source extracts and CNCs: mixing time after the addition of each component and order of addition of the components.

3.5 Water Vapour Permeability (WVP)

It was verified that the interaction CNC and acid type showed a significant effect ($p < 0.05$) on the response variable WVP. The model test was performed for lactic and propionic acids. in which F for the regression was significant ($p<0.05$) and for the lack of fit was not significant ($p>0.05$) for both and the coefficients of determination of 79.38% and 77.45% were obtained. respectively.

WVP indicates the ability of film to prevent moisture transfer between food and the environment (Yoshida et al., 2014). As shown in Fig. 7, the WVP values of the propionic acid films were lower than the lactic acid films. This indicates that possibly the lower amount of hydroxyl groups present in this acid might have contributed to reduced hydrophilic groups, thus reducing the affinity of the films for water vapor. In addition, this reduction can be due to dense compact structure formed through intermolecular interactions between the propionate contra-anion, the phenolics compounds and the chitosan chains (Wang, Dong, Men, Tong, & Zhou, 2013; Yoshida et al., 2014).

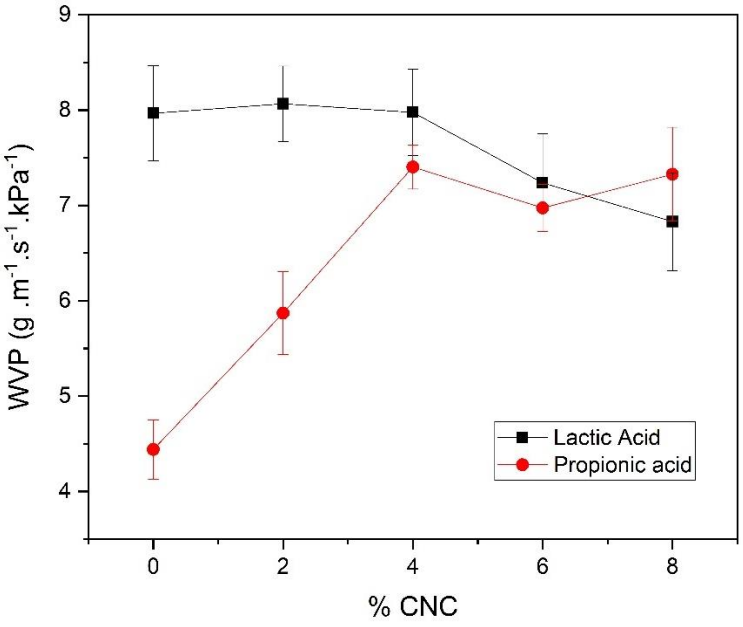

Fig. 7 – Water vapour permeability (WVP) OF nanocomposite CHI/PVA/ EXTJ – based films.

3.6 Determination of antioxidant capacity (DPPH)

The DPPH radical scavenging test was used to determinate the antioxidant capacity of different films. It was observed that interaction between concentration and acid type influenced significantly ($p<0.05$) in the antioxidant activity of the films by the DPPH radical scavenging

method. The control films showed no antioxidant activity, so the functional and active property of the films is due to the presence of the Jussara extract.

The effect of CNC addition was not significant, i.e., NCC addition up to 8% does not interfere with the antioxidant capacity of the film incorporated with extract. In addition, as shown at Fig. 8, the lactic acid film had the highest DPPH radical scavenging ability. This can be explained by the fact that lactic acid is a hydroxyacid, a mean, compared to propionic acid, lactic acid has one more hydroxyl group in their structure, attached to their C2 carbon. As consequence, the protons of this acid are more easily released into the medium, being able to protonate the amino groups of chitosan with greater efficiency (Soares et al., 2019). So, when lactic acid is used to disperse the chitosan, the polymer chains acquire a more extended conformation, forming a less dense and more flexible three-dimensional network, due to the larger space between the polymer chains. So, when Jussara extract is added, it can more easily diffuse out of the polymeric matrix and interact more efficiently with DPPH radical.

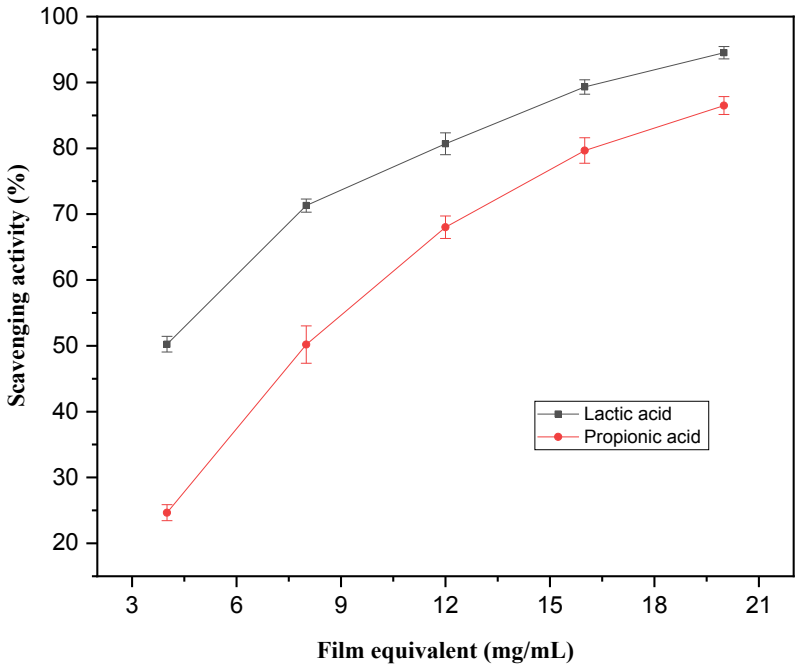

Fig. 8. DPPH radical scavenging activity of nanocomposite CHI/PVA/ EXTJ – based films.

4. Conclusion

The limitations of some films produced from biopolymers allow some strategies to be used to supply these needs. In addition, to achieve better performance of the materials, studying

the influence of factors that interfere in their physical-chemical properties and interactions with other components becomes crucial.

The nanocomposite polymer blends developed in this study were based on chitosan, PVA, glycerol and Jussara extract, being evaluated regarding the type of acid used (lactic and propionic) in the chitosan dispersion and the concentration of CNC added (0% - 8%). As for the effect of the type of acid, all the variables studied (moisture content, swelling degree, thickness, mechanical properties, color, WPV and antioxidant properties. More flexible and less rigid films were obtained with the use of lactic acid, while more fragile films, with rigid structures and less flexibility were obtained with the use of propionic acid, which pointed to two factors to be taken into consideration in the production of nanocomposite blends: mixing time after the addition of each component and the order of their addition. Films with propionic acid showed purplish coloration, indicating the presence of more unstable structures of anthocyanins (pseudobase carbinol and quinoidal base).

As for the concentration of CNC, it did not significantly influence the antioxidant activity of the films. Moreover, for the water vapor permeability of the films, CNC had a more pronounced effect on the films with propionic acid, increasing the WPV up to a concentration of 4%. From this concentration onwards, the WPV variation was not significant.

The films added with Jussara extract showed excellent antioxidant activity, especially those developed with lactic acid. However, other studies should be developed in order to study the application of the films in different food matrices and also as biosensors in the food area, since the anthocyanin molecules present in the Jussara extract have great potential as colorimetric indicators for pH alterations.

5. References

Abdul khalil. H. P. S.. Saurabh. C. K.. Adnan. A. S.. Fazita. M. N.. Syakir. M. I.. Davoudpour. Y.. ... & Dungani. R. (2016). A review on chitosan-cellulose blends and nanocellulose reinforced chitosan biocomposites: Properties and their applications. *Carbohydrate polymers*. *150*. 216-226.

Ali. A.. & Ahmed. S. (2018). A review on chitosan and its nanocomposites in drug delivery. *International journal of biological macromolecules*. *109*. 273-286.

Andrade. J.. González-Martínez. C.. & Chiralt. A. (2022). Physical and active properties of poly (vinyl alcohol) films with phenolic acids as affected by the processing method. Food Packaging and Shelf Life. 33. 100855.

Aranha. I. B.. & Lucas. E. F. (2001). Poli (álcool vinílico) modificado com cadeias hidrocarbônicas: avaliação do balanço hidrófilo/lipófilo. *Polímeros*. *11*. 174-181.

Barbosa. L. C. A. (2007). *Espectroscopia no infravermelho: na caracterização de compostos orgânicos*. Ed. UFV.

Bicudo. M. O. P.. Jó. J.. Oliveira. G. A. D.. Chaimsohn. F. P.. Sierakowski. M. R.. Freitas. R. A. D.. & Ribani. R. H. (2015). Microencapsulation of juçara (Euterpe edulis M.) pulp by spray drying using different carriers and drying temperatures. *Drying Technology*. *33*(2). 153-161.

Bonilla. J.. Fortunati. E. L. E. N. A.. Atarés. L.. Chiralt. A.. & Kenny. J. M. (2014). Physical. structural and antimicrobial properties of poly vinyl alcohol–chitosan biodegradable films. *Food Hydrocolloids*. *35*. 463-470.

Brand-Williams. W.. Cuvelier. M. E.. & Berset. C. L. W. T. (1995). Use of a free radical method to evaluate antioxidant activity. *LWT-Food science and Technology*. *28*(1). 25-30.

Cardoso. A. L.. de Liz. S.. Rieger. D. K.. Farah. A. C. A.. Vieira. F. G. K.. de Assis. M. A. A.. & Di Pietro. P. F. (2018). An update on the biological activities of Euterpe edulis (Juçara). *Planta Medica*. *50*(08). 487-499.

Chen. J. L.. & Zhao. Y. (2012). Effect of molecular weight. acid. and plasticizer on the physicochemical and antibacterial properties of β-chitosan based films. *Journal of Food Science*. *77*(5). E127-E136.

De Barros Freitas. R.. Melato. F. A.. de Oliveira. J. M.. Bastos. D. S. S.. Cardoso. R. M.. Leite. J. P. V.. & Lima. L. M. (2017). Euterpe edulis effects on cardiac and renal tissues of Wistar rats fed with cafeteria diet. *Nutrición Hospitalaria*. *34*(1). 186-192.

De Oliveira. T. V.. de Freitas. P. A. V.. Pola. C. C.. da Silva. J. O. R.. Diaz. L. D. A.. Ferreira. S. O.. & de FF Soares. N. (2020). Development and optimization of antimicrobial active films produced with a reinforced and compatibilized biodegradable polymers. *Food Packaging and Shelf Life*. *24*. 100459.

Soares. L.S., Perim. R. B., de Alvarenga. E. S., de Moura Guimarães. L., de Carvalho Teixeira. A. V. N., dos Reis Coimbra. J. S.. & de Oliveira. E. B. (2019). Insights on physicochemical aspects of chitosan dispersion in aqueous solutions of acetic, glycolic, propionic or lactic acid. *International journal of biological macromolecules*. *128*. 140-148.

El Miri. N.. Abdelouahdi. K.. Zahouily. M.. Fihri. A.. Barakat. A.. Solhy. A.. & El Achaby. M. (2015). Bio-nanocomposite films based on cellulose nanocrystals filled polyvinyl alcohol/chitosan polymer blend. *Journal of Applied Polymer Science*. *132*(22).

Flores. R. V.. Silva. R. R. A.. de Oliveira. T. V.. de Oliveira. E. B.. Stringheta. P. C.. & Soares. N. D. F. F. (2022). Recent advances and challenges on chitosan-based nanostructures by polyelectrolyte complexation and ionic gelation for anthocyanins stabilization. *Research. Society and Development*. *11*(10). e401111033092-e401111033092.

Freitas. P. A.. de Oliveira. T. V.. Silva. R. R.. e Moraes. A. R. F.. Pires. A. C. D. S.. Soares. R. R.. ... & Soares. N. F. (2020). Effect of pH on the intelligent film-forming solutions produced with red cabbage extract and hydroxypropylmethylcellulose. *Food Packaging and Shelf Life*. *26*. 100604.

Fuleki. T.. & Francis. F. J. (1968). Quantitative methods for anthocyanins. 2. Determination of total anthocyanin and degradation index for cranberry juice. *Journal of food science*. *33*(1). 78-83.

Larrauri, J. A., Rupérez, P., & Saura-Calixto, F. (1997). Effect of drying temperature on the stability of polyphenols and antioxidant activity of red grape pomace peels. *Journal of agricultural and food chemistry*, *45*(4), 1390-1393.

Lim. L. T. (2015). Enzymes for food-packaging applications. In *Improving and tailoring enzymes for food quality and functionality* (pp. 161-178). Woodhead Publishing.

Luzi. F.. Fortunati. E.. Giovanale. G.. Mazzaglia. A.. Torre. L.. & Balestra. G. M. (2017). Cellulose nanocrystals from Actinidia deliciosa pruning residues combined with carvacrol in PVA_CH films with antioxidant/antimicrobial properties for packaging applications. *International journal of biological macromolecules*. *104*. 43-55.

Kanatt. S. R.. & Makwana. S. H. (2020). Development of active. water-resistant carboxymethyl cellulose-poly vinyl alcohol-Aloe vera packaging film. Carbohydrate polymers. 227. 115303.

Kanatt. S. R.. Muppalla. S. R.. & Chawla. S. P. (2017). Eco-friendly polymers for food packaging. Handbook of Composites from Renewable Materials; Thakur. VK. Thakur. MK. Kessñer. MR. Eds. 309-352.

Kim. K. M.. Son. J. H.. Kim. S. K.. Weller. C. L.. & Hanna. M. A. (2006). Properties of chitosan films as a function of pH and solvent type. *Journal of food science*. *71*(3). E119-E124.

Mali. P.. & Sherje. A. P. (2022). Cellulose nanocrystals: Fundamentals and biomedical applications. *Carbohydrate Polymers*. *275*. 118668.

Melro. E., Antunes. F. E., da Silva. G. J., Cruz. I., Ramos. P. E., Carvalho. F., & Alves. L. (2020). Chitosan films in food applications. tuning film properties by changing acidic dissolution conditions. *Polymers*. *13*(1). 1.

Oun, A. A., Shin, G. H., & Kim, J. T. (2022). Antimicrobial, antioxidant, and pH-sensitive polyvinyl alcohol/chitosan-based composite films with aronia extract, cellulose nanocrystals, and grapefruit seed extract. *International Journal of Biological Macromolecules*.

Pacheco, N., Naal-Ek, M. G., Ayora-Talavera, T., Shirai, K., Román-Guerrero, A., Fabela-Morón, M. F., & Cuevas-Bernardino, J. C. (2019). Effect of bio-chemical chitosan and gallic acid into rheology and physicochemical properties of ternary edible films. International Journal of Biological Macromolecules, 125, 149–158.

Pavoni. J. M. F., Luchese. C. L., & Tessaro. I. C. (2019). Impact of acid type for chitosan dissolution on the characteristics and biodegradability of cornstarch/chitosan based films. *International journal of biological macromolecules*. *138*. 693-703.

Perumal. A. B., Sellamuthu. P. S., Nambiar. R. B., & Sadiku. E. R. (2018). Development of polyvinyl alcohol/chitosan bio-nanocomposite films reinforced with cellulose nanocrystals isolated from rice straw. *Applied Surface Science*. *449*. 591-602.

Qian, B. J., Liu, J. H., Zhao, S. J., Cai, J. X., & Jing, P. (2017). The effects of gallic/ferulic/caffeic acids on colour intensification and anthocyanin stability. *Food chemistry*, *228*, 526-532.

Rocha. J. D. C. G.. Procopio. F. R.. Mendonca. A. C.. Vieira. L. M.. Perrone. I. T.. Barros. F. A. R. D.. & Stringheta. P. C. (2017). Optimization of ultrasound-assisted extraction of phenolic

compounds from jussara (Euterpe edulis M.) and blueberry (Vaccinium myrtillus) fruits. *Food Science and Technology*. *38*. 45-53.

Silva. M. G. P. C.. Barretto. W. S.. Serôdio. M. H. Comparação nutricional da polpa dos frutos de juçara e de açaí. In: XVIII BRAZILIAN FRUIT CULTURE CONGRESS. Florianópolis. Santa Catarina. 22 a 26 de novembro de 2004..Anais...CD ROOM. Florianópolis. SC. 2004.

Singleton, V. L., & Rossi, J. A. (1965). Colorimetry of total phenolics with phosphomolybdic-phosphotungstic acid reagents. *American journal of Enology and Viticulture*, *16*(3), 144-158.

Sivashankari. P. R.. & Prabaharan. M. (2017). Deacetylation modification techniques of chitin and chitosan. In *Chitosan Based Biomaterials Volume 1* (pp. 117-133). Woodhead Publishing.

Sutharsan, J., Boyer, C. A., & Zhao, J. (2022). Physicochemical properties of chitosan edible films incorporated with different classes of flavonoids. *Carbohydrate Polymer Technologies and Applications*, *4*, 100232.

Wang, L., Dong, Y., Men, H., Tong, J., & Zhou, J. (2013). Preparation and characterization of active films based on chitosan incorporated tea polyphenols. *Food hydrocolloids*, *32*(1), 35-41.

Wang. X.. Yong. H.. Gao. L.. Li. L.. Jin. M.. & Liu. J. (2019). Preparation and characterization of antioxidant and pH-sensitive films based on chitosan and black soybean seed coat extract. *Food hydrocolloids*. *89*. 56-66.

Yong. H.. Wang. X.. Zhang. X.. Liu. Y.. Qin. Y.. & Liu. J. (2019). Effects of anthocyanin-rich purple and black eggplant extracts on the physical. antioxidant and pH-sensitive properties of chitosan film. *Food hydrocolloids*. *94*. 93-104.

Yoshida, C. M., Maciel, V. B. V., Mendonça, M. E. D., & Franco, T. T. (2014). Chitosan biobased and intelligent films: Monitoring pH variations. LWT-food science and technology, 55(1), 83-89.

Yun. D.. Cai. H.. Liu. Y.. Xiao. L.. Song. J.. & Liu. J. (2019). Development of active and intelligent films based on cassava starch and Chinese bayberry (Myrica rubra Sieb. et Zucc.) anthocyanins. *RSC advances*. *9*(53). 30905-30916.

Zhang. W.. Jiang. Q.. Shen. J.. Gao. P.. Yu. D.. Xu. Y.. & Xia. W. (2022). The role of organic acid structures in changes of physicochemical and antioxidant properties of crosslinked chitosan films. *Food Packaging and Shelf Life*. *31*. 100792.

Supplementary Material for "The influence of chitosan dispersions' type of acid and cellulose nanocrystal on chitosan/PVA-based blend films added of Jussara (Euterpe edulis M.) extract: Effect on mechanical, molecular and physico-chemical properties"

Rafaela Venancio Flores[a], Katia Silva Maciel[a], Kely de Paula Correa[b], Sukarno Olavo Ferreira [c], Paulo César Stringheta [a], Eduardo Basílio de Oliveira [a], Taíla Veloso de Oliveira [a], Nilda de Fátima Ferreira Soares [a]

[a] Food Technology Department, Viçosa University Federal, Universitary campus, s/n, 36570-900, Viçosa, MG, Brazil.

[b] Candido Tostes Dairy Institute – Agricultural Research Company of Minas Gerais, R. Tem. Luís de Freitas, 116 – Santa Terezinha, 36045-560, Juiz de Fora, MG, Brazil.

[c] Physics Department, Viçosa University Federal, Universitary campus, s/n, 36570-900, Viçosa, MG, Brazil.

∗Corresponding author: R. V. Flores.
E-mail address: rafavenacio2@gmail.com

I – FTIR spectrum of powder chitosan, PVA, cellulose nanocrystal, glycerol, Jussara extract, lactic acid chitosan dispersion and propionic acid chitosan dispersion

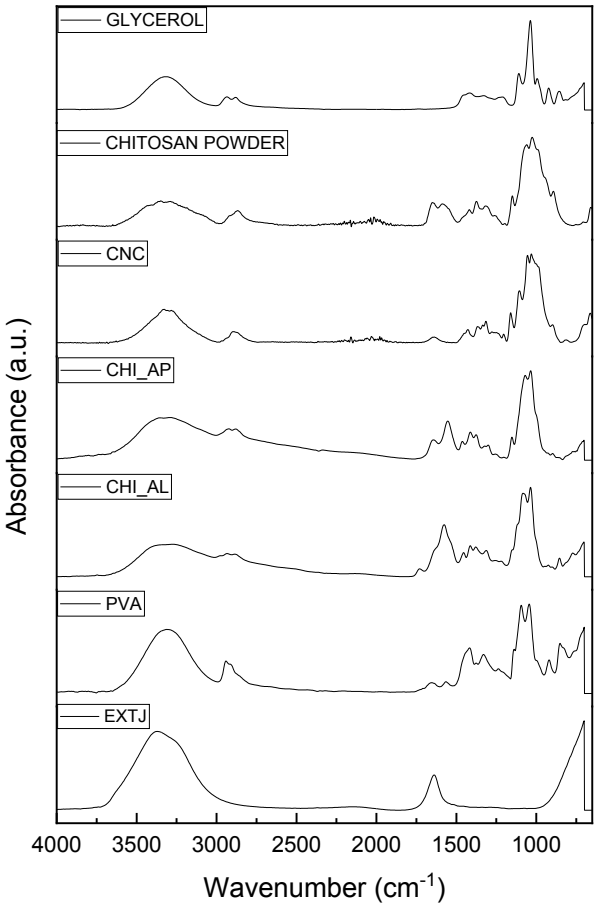

Figure SM1 - FTIR spectrum of powder chitosan, PVA, cellulose nanocrystal, glycerol, Jussara extract, lactic acid chitosan dispersion and propionic acid chitosan dispersion.

CONCLUSÃO GERAL

O estudo de materiais e fatores que afetam suas propriedades e funções é primordial para o desenvolvimento de novas estruturas na área de ciência dos materiais com aplicação em alimentos. Quitosana e nanocristal de celulose são influenciados por diversos fatores intrínsecos e extrínsecos, o que torna estritamente necessário o entendimento da influência de cada um deles para a realização de pesquisas.

No primeiro capítulo, duas metodologias amplamente empregadas no desenvolvimento de nanocomplexos foram discutidas: complexação polieletrolítica e gelatinização iônica. As principais limitações no desenvolvimento desses sistemas nanoparticulados foram discutidas e diversas estratégias foram apontadas para melhorar o nanoencapsulamento de antocianinas. Contudo, grande parte dessas estratégias podem ser aplicadas a diversos compostos bioativos.

No segundo capítulo, a fim de empregar parte das estratégias pontuadas, nanocomplexos de quitosana/CNC foram desenvolvidos e otimizados. Ao considerarmos os fatores corretos, excelentes resultados foram alcançados, obtendo-se partículas com diametro médio entre 151 e 195 nm, baixa polidispersidade ($0.25 \leq PDI \leq 0.3$), altos valores de potencial zeta (+44.57 a +51.30 mV) e altos valores de rendimento, sendo possivel alcançar valores até 9%. Os nanocomplexos apresentaram formato ovalado e maior resistência térmica. Com base nos resultados encontrados e no estudo de estabilidade durante 30 dias a 25ºC e 7ºC, o sistema com melhores propriedades foi aquele com proporção molar de quitosana:NCC = 3:1, pH = 5,0 e sem adição de NaCl.

No último capítulo, os filmes nanocompósitos desenvolvidos foram fortemente influenciados pelo tipo de ácido usado para dispersar a quitosana, mostrando mais uma vez a importancia da avaliação dos fatores que interferem nas propriedades estruturais e fisico-quimicas dos polimeros durante o desenvolvimento de materiais. Filmes mais flexíveis e menos rígidos foram obtidos com uso do ácido lático, enquanto que filmes mais frágeis, com estruturas rígidas e menor flexibilidade foram obtidos com uso de ácido propiônico, o que apontou para dois fatores a serem levados em consideração na produção das blendas nanocompositas: tempo de mistura após a adição de cada componente e ordem de adição dos mesmos. Além disos, filmes com ácido propiônico apresentaram coloração arroxeada, indicando a presença de estruturas mais instáveis das antocianinas (pseudobase carbinol e base quinoidal). Quanto a influência da concentração de nanocristal de celulose na permeabilidade ao vapor de água,

houve um efeito mais pronunciado nos filmes com ácido propiônico, com aumento da WPV até a concentração de 4%. A partir dessa concentração, a variação de WPV não foi significativa.

REFERÊNCIAS

ABDUL KHALIL H.P.S. et al. A review on chitosan-cellulose blends and nanocellulose reinforced chitosan biocomposites: Properties and their applications. **Carbohydrate polymers**, v. 150, p. 216-226, 2016.

ABO-ELSEOUD, W. S. et al. Chitosan nanoparticles/cellulose nanocrystals nanocomposites as a carrier system for the controlled release of repaglinide. **International journal of biological macromolecules**, v. 111, p. 604-613, 2018.

ALI, A.; AHMED, S. A review on chitosan and its nanocomposites in drug delivery. **International journal of biological macromolecules**, v. 109, p. 273-286, 2018.

AMORIM, M. L. et al. Physicochemical aspects of chitosan dispersibility in acidic aqueous media: effects of the food acid counter-anion. **Food Biophysics**, v. 11, n. 4, p. 388-399, 2016.

BICUDO, M. O. P. et al. Anthocyanins, phenolic acids and antioxidant properties of juçara fruits (Euterpe edulis M.) along the on-tree ripening process. **Plant Foods for Human Nutrition**, v. 69, n. 2, p. 142-147, 2014.

BONILLA, J. et al. Physical, structural and antimicrobial properties of poly vinyl alcohol–chitosan biodegradable films. **Food Hydrocolloids**, v. 35, p. 463-470, 2014.

CANER, C. E. N. G. İ. Z.; VERGANO, P. J.; WILES, J. L. Chitosan film mechanical and permeation properties as affected by acid, plasticizer, and storage. **Journal of food science**, v. 63, n. 6, p. 1049-1053, 1998

CHEN, F.; GÄLLSTEDT, M.; OLSSON, R. T.; GEDDE, U. W.; HEDENQVIST, M. S. Unusual effects of monocarboxylic acids on the structure and on the transport and mechanical properties of chitosan films. **Carbohydrate polymers**, v. 132, p. 419-429, 2015.

CHENG, S. Y.; WANG, B. J.; WENG, Y. M. Antioxidant and antimicrobial edible zein/chitosan composite films fabricated by incorporation of phenolic compounds and dicarboxylic acids. **LWT-Food science and technology**, v. 63, n.1, p. 115-121, 2015.

FERNANDES, S. C.; FREIRE, C. S.; SILVESTRE, A. J.; PASCOAL NETO, C.; GANDINI, A. Novel materials based on chitosan and cellulose. **Polymer International**, v. 60, n. 6, p. 875-882, 2011.

HEMBRAM, C. K.; PRABHA, S.; CHANDRA, R.; AHMED, B.; NIMESH, S. Advances in preparation and characterization of chitosan nanoparticles for therapeutics. **Artificial cells, nanomedicine, and biotechnology**, v. 44, n. 1, p. 305-314, 2016.

KIM, K. M.; SON, J. H.; KIM, S. K.; WELLER, C. L.; HANNA, M. A. Properties of chitosan films as a function of pH and solvent type. **Journal of food science**, v. 71, n. 3, p. E119-E124, 2006.

LUO, Y.; WANG, Q. Recent development of chitosan-based polyelectrolyte complexes with natural polysaccharides for drug delivery. **International journal of biological macromolecules**, v. 64, p. 353-367, 2014.

MA, Q.; LIANG, T.; CAO, L.; WANG, L. Intelligent poly (vinyl alcohol)-chitosan nanoparticles-mulberry extracts films capable of monitoring pH variations. **International Journal of Biological Macromolecules**, v. 108, p. 576-584, 2018.

MU, R. et al. Recent trends and applications of cellulose nanocrystals in food industry. **Trends in food science & technology**, v. 93, p. 136-144, 2019.

PAVONI, J. M. F.; LUCHESE, C. L.; TESSARO, I. C. Impact of acid type for chitosan dissolution on the characteristics and biodegradability of cornstarch/chitosan based films. **International journal of biological macromolecules**, v. 138, p. 693-703, 2019.

SANTOS-BUELGA, C.; GONZÁLEZ-PARAMÁS, A. M. Anthocyanins. **Reference Module in Food Science**, p. 1–12, 2018.

SOARES, L.S. et al. Insights on physicochemical aspects of chitosan dispersion in aqueous solutions of acetic, glycolic, propionic or lactic acid. **International journal of biological macromolecules**, v. 128, p. 140-148, 2019.

SUNASEE, R.; HEMRAZ, U. D.; CKLESS, K. Cellulose nanocrystals: a versatile nanoplatform for emerging biomedical applications. **Expert Opinion on Drug Delivery**, v. 13, n. 9, p. 1243-1256, 2016.

WANG, H.; ROMAN, M. Formation and properties of chitosan− cellulose nanocrystal polyelectrolyte− macroion complexes for drug delivery applications. **Biomacromolecules**, v. 12, n. 5, p. 1585-1593, 2011.

WANG, W.; JUNG, J.; ZHAO, Y. Chitosan-cellulose nanocrystal microencapsulation to improve encapsulation efficiency and stability of entrapped fruit anthocyanins. **Carbohydrate polymers**, v. 157, p. 1246-1253, 2017.

YOUSUF, B.; GUL, K.; WANI, A. A.; SINGH, P. Health benefits of anthocyanins and their encapsulation for potential use in food systems: a review. **Critical reviews in food science and nutrition**, v. 56, n. 13, p. 2223-2230, 2016.

ZHANG, W. et al. The role of organic acid structures in changes of physicochemical and antioxidant properties of crosslinked chitosan films. **Food Packaging and Shelf Life**, v. 31, p. 100792, 2022.